Nuclear Operating Company
South Texas Project Electric Generating Station P.O. Box 289 Wadsworth, Texas 77483

May 31, 2016
NOC-AE-16003378
10 CFR 54
File No. G25

U. S. Nuclear Regulatory Commission
Attention: Document Control Desk
Washington, DC 20555-0001

South Texas Project
Units 1 and 2
Docket Nos. STN 50-498, STN 50-499
Additional Information for the
Review of the South Texas Project, Units 1 and 2,
License Renewal Application – Aluminum Bronze AMP (TAC Nos. ME4936 and ME4937)

References:

1. Letter; G. T. Powell to the NRC Document Control Desk; "License Renewal Application", NOC-AE-10002607; dated October 25, 2010. (ML103010257)
2. Letter from NRC, Lois James to STP G.T. Powell, "Plan for the 2016 Selective Leaching of Aluminum-Bronze Aging Management Program Regulatory Audit Regarding the South Texas Project, Units 1 and 2, License Renewal Application Review", dated March 18, 2016. (ML16076A118)

By Reference 1, STP Nuclear Operating Company (STPNOC) submitted a License Renewal Application (LRA). In Reference 2, the NRC initiated a follow-up regulatory audit of STPNOC's Selective Leaching of the Aluminum Bronze Program. Enclosure 1 to this letter provides the basis for STPNOC's Selective Leaching of the Aluminum Bronze Program. Enclosure 2 provides a technical report regarding this topic.

There are no commitments in this letter.

A147
NRR

STI: 34316871

If there are any questions regarding this submittal, please contact Arden Aldridge, STP License Renewal Project Lead, at (361) 972-8243 or Rafael Gonzales, STP License Renewal Project regulatory point-of-contact, at (361) 972-4779.

I declare under penalty of perjury that the foregoing is true and correct.

Executed on May 31, 2016
Date

James Connolly
Site Vice President

rjg

Enclosures:

1. STPNOC LRA Aluminum Bronze Basis Document
2. Intertek Report

cc:
(paper copy)

Regional Administrator, Region IV
U.S. Nuclear Regulatory Commission
1600 East Lamar Boulevard
Arlington, TX 76011-4511

Lisa M. Regner
Senior Project Manager
U.S. Nuclear Regulatory Commission
One White Flint North (MS 8 G9A)
11555 Rockville Pike
Rockville, MD 20852

NRC Resident Inspector
U. S. Nuclear Regulatory Commission
P. O. Box 289, Mail Code: MN116
Wadsworth, TX 77483

Lois James
License Renewal Project Manager (Safety)
One White Flint North (MS O11-F1)
U.S. Nuclear Regulatory Commission
Washington, DC 20555-0001

Tam Tran
License Renewal Project Manager
(Environmental)
One White Flint North (MS O11F01)
U. S. Nuclear Regulatory Commission
Washington, DC 20555-0001

(electronic copy)

Morgan, Lewis & Bockius LLP
Steve Frantz

U.S. Nuclear Regulatory Commission
Lisa M. Regner
Lois James

NRG South Texas LP
Chris O'Hara
Jim von Suskil
Skip Zahn

CPS Energy
Kevin Pollo
Cris Eugster
L. D. Blaylock

Crain Caton & James, P.C.
Peter Nemeth

City of Austin
Elaina Ball
John Wester

Texas Dept. of State Health Services
Helen Watkins
Robert Free

Enclosure 1

STPNOC LRA Aluminum Bronze Basis Document

STP Nuclear Operating Company
Overview and Bases for License Renewal Aging Management Program Outlined in License Renewal Application Appendix A1.37, B2.1.37, and PSALBZ "Selective Leaching of Aluminum Bronze"

CR-12-29261-109

1.0 AGING MANAGEMENT PROGRAM OVERVIEW:

The STP Aging Management Program, B2.1.37, Selective Leaching of Aluminum Bronze is a station specific existing program with the following aging management enhancement and activities to manage the aging effects of weld cracking associated with Aluminum Bronze welds.

- Inspections and Walkdowns
- Replacements prior to Period of Extended Operation
- One-Time Volumetric Examination
- Periodic Volumetric Examination
- Acceptance Criteria
- Additional Testing elements

Aluminum Bronze Welds in the Essential Cooling Water (ECW) system are not susceptible to general through wall (TW) dealloying due to basic material properties (Aluminum content) and installation methods (welding processes). The root pass provides most resistance to dealloying but additional weld passes have resistance also. Welds with pre-existing flaws have conditions that can lead to weld failures. This is due to residual stresses and environmental conditions especially installations with backing rings and potential for surface dealloying. These conditions can lead to crack propagation resulting in through wall weld failure. There is no evidence of general weld dealloying or weld failures since 1994. Any failures of below ground pipes can be detected prior to reaching critical crack size.

Aging Management Program Elements and Bases

Based on metallurgical properties, historical evidence and on-going tests and inspections, STP has developed a robust Aluminum Bronze Aging Management Program ensuring that plant safety is maintained. Below is an overview of the aging management activities and description of the bases for their expected effectiveness.

1.1 Inspections and Walkdowns:

- Visual inspections are performed every six months (not to exceed nine months) of the external surfaces of the above ground welds for evidence of through wall leakage.
- Yard walkdowns are performed every six months (not to exceed nine months) in areas above the buried piping with aluminum bronze welds to look for changes in ground conditions that would indicate leakage.

Bases:

- Operating experience utilizing visual inspections has demonstrated that they provide early detection of any through-wall indications. Identification of dealloying includes discoloration with residue and minor weeping from a suspected dealloyed location. Dealloying to the point of creating a through-wall leak is slow and the visual inspection will provide early detection to assure the leakage is repaired or replaced prior to any loss of intended function. Once the susceptible components are replaced the only potential area for through-wall leakage will be from the welds.
- The last leaking weld was discovered in 1994. The leaking welds contained pre-existing defects which propagate by a combination of progressive local dealloying and crack growth through aluminum bronze material. Any degradation of the welds to the point of creating a TW leak is slow and the visual inspection will provide

early detection to assure the leakage is repaired or replaced prior to any loss of intended function. Section 6.0 provides the discussion pertaining the stress analysis and structural integrity evaluations performed that show the cracked pipe welds maintain adequate margins for design conditions. In addition, one time and periodic volumetric examinations, discussed below, are performed to assure any weld degradation is understood.

- The visual inspections performed every six months provides reasonable assurance that a weld exhibiting through wall leakage will be repaired or replaced prior to any loss of intended function.
- Yard walkdowns are performed to detect leaks in buried piping with aluminum bronze welds to look for changes in ground conditions that would indicate leakage. Leak detection is used to support identification of through-wall weld flaws in buried piping welds before pipe integrity is challenged. For the buried portions of the ECW piping, the minimum leak rate detectable at the surface is 10 gpm.

1.2 Replacements prior to Period of Extended Operation:

- Replace all aluminum bronze castings susceptible to selective leaching, including attachment welds related to the castings with material that is not susceptible to selective leaching.
- Replace aluminum bronze root valve with adapter socket welds with material that is not susceptible to selective leaching.
- Replace extruded piping tees with aluminum bronze weld repairs where the existing repair size is such that postulated failure of the repair would affect the structural integrity of the component.

Bases:

- Replacing all aluminum bronze castings susceptible to selective leaching including attachment welds related to the castings with material that is not susceptible to selective leaching will eliminate the potential of selective leaching causing through wall leakage that could challenge ECW system intended function. The replacement of these susceptible aluminum bronze castings provides reasonable assurance that ECW system will not experience a loss of intended function during the period of extended operation (PEO).
- Replace aluminum bronze root valve with adapter socket welds with material that is not susceptible to selective leaching will eliminate the potential of selective leaching of susceptible weld material. The replacement of these welds provides reasonable assurance that the ECW system will not experience a loss of intended function during the PEO.
- Replace extruded piping tees with aluminum bronze weld repairs where the repair size is such that postulated failure of the repair would affect the structural integrity of the component will eliminate the potential of an extruded piping tee failure due to selective leaching that could challenge ECW system intended function. The replacement of these extruded piping tees provides reasonable assurance that ECW system will not experience a loss of intended function during the PEO.

1.3 One-Time Volumetric Examination:

- Verify the weld integrity of the above ground weld population with no backing rings by performing a one-time volumetric examination on 3 percent with a maximum of 10 welds prior to the period of extended operation. If rejectable weld flaws (weld defects) per ASME Section IX requirements are found during the one-time inspection of weld with no backing rings, periodic volumetric examinations of 20 percent with a maximum of 25 welds will be performed every 10 years thereafter.

- Discovery of weld defects requires expansion of the volumetric examination sample population. Each weld found with a defect requires five additional volumetric examinations to be performed until no additional weld defects are found.

Bases:

- The one-time inspection method of a sample population is a proven method used to verify that an aging effect is either not occurring or is occurring at a rate that will not challenge the systems, structures, or components (SSC) intended functions during the PEO. STP has no plant-specific operating experience of selective leaching of welds with no backing rings. The revised XI.M33, Selective Leaching program for subsequent license renewal (SLR) specifies a sample size of 3 percent of the population or a maximum of 10 components per population for one-time inspections. Using the one-time volumetric examination on 3 percent with a maximum of 10 welds prior to the period of extended operation provides reasonable assurance that selective leaching of welds with no backing rings is not occurring. If rejectable weld flaws (weld defects) per ASME Section IX requirements are found during the one-time inspection of weld with no backing rings the program required periodic volumetric examinations of 20 percent with a maximum of 25 welds will be performed every 10 years thereafter. Additionally discovery of weld defects requires expansion of the volumetric examination sample population. Each weld found with a defect requires five additional volumetric examinations to be performed until no additional weld defects are found.

- The expansion of the inspection sample size is based on the guidance provided in Generic Letter 90-05. Generic Letter 90-05 states that at least five additional locations are inspected. Additionally Generic Letter 90-05 states the additional sample of the same size should be performed until no flaw are detected in the additional inspection sample. Use of the Generic Letter 90-05 sample expansion criteria provides reasonable assurance that the ECW piping systems will be aged managed and that the ECW system will not experience a loss of intended function during the PEO. This is similar to the revised expansion criteria provided in XI.M33 for SLR which states the number of additional inspections is equal to the number of failed inspections for each material and environment population with a minimum of five additional visual and mechanical inspections when visual and mechanical inspections(s) did not meet acceptance criteria.

1.4 Periodic Volumetric Examination:

- Verify the weld integrity of the above ground weld population with backing rings by performing periodic volumetric examinations on 20 percent with a maximum of 25 welds prior to the period of extended operation and every 10 years thereafter. If no weld defects are found during the inspection performed prior to the period of extended operation of weld with backing rings, the follow up volumetric examinations will be reduced to 3 percent with a maximum of 10 welds.

- Discovery of weld defects requires expansion of the volumetric examination sample population. Each weld found with a defect requires five additional volumetric examinations to be performed until no additional weld defects are found.

Bases:

- The periodic inspection method of a sample population is a proven method used to verify that an aging effect that has occurred or is occurring at a rate that will not challenge the SSC's intended functions during the PEO. Since STPNOC has plant-specific operating experience of selective leaching of welds with backing rings a periodic inspection of a sample population will be used to detect selective leaching of welds with backing rings prior to challenging the ECW system intended function. The periodic volumetric examinations on 20 percent with a maximum of 25 welds prior to the period of extended operation and every 10 years thereafter provides reasonable assurance that defective welds will be found and the ECW system will not experience a loss of intended function during the PEO.

- The expansion of the inspection sample size is based on the guidance provided in Generic Letter 90-05. Generic Letter 90-05 states that at least five additional locations are inspected. Additionally Generic Letter 90-05 states the additional sample of the same size should be performed until no flaw are detected in the additional inspection sample. Use of the Generic Letter 90-05 sample expansion criteria provides reasonable assurance that the ECW piping systems are managed and that the ECW system will not experience a loss of intended function during the PEO. This is similar to the expansion criteria provided in XI.M33 for SLR which states: "The number of additional inspections is equal to the number of failed inspections for each material and environment population with a minimum of five additional visual and mechanical inspections when visual and mechanical inspections(s) did not meet acceptance criteria."

1.5 Acceptance Criteria

- The acceptance criterion for volumetric examination of aluminum bronze welds is no defects.

- The acceptance criterion for visual inspection of the aluminum bronze welds and adjacent copper alloy piping during the walkdowns is no indication of through wall leakage.

- If an acceptance criterion is not met, the condition is documented in the corrective action program and a structural integrity analysis is performed to confirm that the load carrying capacity of the tested material remains adequate to support the intended function of the ECW system through the period of extended operation

- Discovery of weld defects requires expansion of the volumetric examination sample population. Five additional volumetric examination will be performed for each weld found with a defect until no additional weld defects are found.
- When acceptance criteria are not met a determination of operability and an assessment of the extent of condition is performed

Bases:

- The acceptance criterion for volumetric examination of aluminum bronze welds is no defects. STP has no plant-specific operating experience of selective leaching of welds without backing rings. All defective welds experienced local dealloying and crack growth through the dealloyed material because the welds contained defects. Setting the acceptance criterion for volumetric examination of aluminum bronze welds to no defects provides reasonable assurance that ECW system will not experience a loss of intended function during the PEO.
- The acceptance criterion for visual inspection of the aluminum bronze welds and adjacent copper alloy piping during the walkdowns is no indication of through wall leakage provides reasonable assurance that that the aluminum bronze welds and adjacent copper alloy piping is not experiencing selective leaching that could cause a loss of intended function during the PEO.

1.6 Additional Testing elements:

- Two welds with backing rings will be destructively examined prior to the period of extended operation to verify the absence of selective leaching.
- Aluminum bronze welds found to have defects or through wall leakage are removed and destructively examined to determine extent of cracks or selective leaching. The condition is documented in the corrective action program and a structural integrity analysis is performed to confirm that the load carrying capacity of the installed welds remain adequate to support the intended function of the ECW system through the period of extended operation.
- If a leak from a buried pipe weld is discovered by surface water monitoring or during a buried ECW piping inspection, a section of each leaking piping weld will be removed for destructive examination.

Bases:

- The performance of destructive examinations will confirm that selective leaching is not occurring. Additionally destructive examinations are used to determine extent of cracks or selective leaching to verify that the structural integrity of the ECW system remains adequate to support the intended function of the ECW system through the period of extended operation. The use of destructive examinations has proven to be an effective method in evaluating the extent of selective leaching within the base or weld material and its relationship to any existing defects.

2.0 ALUMINUM BRONZE OVERVIEW (HISTORY)

Below is a historical review and general information of how the dealloying events at STP have evolved over time. This history outlines the progression of cast dealloying and weld cracking .

The dealloying phenomenon was observed first in small bore cast fittings. Later, it was seen in large bore cast fittings and in welds with backing rings. The first discovery of "weeping type leaks" occurred in small bore valves and fittings, on April 1, 1988. By May of 1988, 90 of 800 small bore valves and fittings were observed to exhibit weeping. Similar information was presented more formally by letter, dated November 1, 1988 (ST-HL-AE-2748). Subsequently, leaks were observed in large bore piping.

Calculation RC-9890, "Stress Summary for Large Bore ECW Piping" was initially issued in June of 1989 and revisited all of the stress calculations to demonstrate the acceptability of the entire system, including the underground portion.

On March 12, 1991, Station Problem Report (SPR) 910099 was written to document discovery of a through-wall leak accompanied by significant dealloying of a 6" welded cast flange. Calculation RC-9890 was revised in May 1991, specifically to address this SPR. The revised calculation reconfirmed the conclusion that dealloying could not cause loss of structural integrity in large bore ECW piping. On July 13, 1991 another through-wall leak was observed in ECW piping. A subsequent extent-of-condition inspection discovered several additional pipe flaws by November of 1991. These findings are documented in SPR 910273. A Relief Request was submitted to the NRC on January 17, 1992 (ST-HL-AE-3984/ML16098A352). In response to an RAI, STP updated the analysis results that reduced the critical crack sizes from 34 to 30.3" for typical pipe and from 21 to 18.8" for peak stress. The Relief Request was approved by letter from the NRC dated April 12, 1993 (ST-AE-HL-93369/ ML16098A353).

In 1992 STP developed a formal calculation, CC-5089,"Detection of Seepage from ECW Pipes", establishing the leak rate that could be detected at the surface through surface wetness. The STP calculation confirmed an earlier Bechtel study calculation, and concluded that an underground leak of 10 gpm would be seen at the surface during monthly inspections.

Engineering Report 95-3235-1, "Evaluation of Ability to Detect Leakage from Underground ECW Piping", dated May 22, 1995, confirmed the conclusion of the previous calculation (CC-5089), that a 10 gpm underground leak could be detected at the surface.

Responses to License Renewal request for additional information in Request for Additional Information Supplement - AMR Set 2 (NOC-AE-11002766/ ML11354A087), December 8, 2011, tabulated the through wall leakage history on Tables 1 and 2, labeled as ECW Dealloying Data and ECW Weld Cracking Data respectively. Clarifying questions on the tables were presented in Request for Additional Information on Aging Management Program, Set 16 (NOC-AE-12002853/ML12163A333), May 31, 2012. Table 1 was updated to add four additional leaking components that occurred since July 28, 2011 through July 31, 2014 by Request for Additional Information on Aging Management Program, Set 26 (NOC-AE-14003135/ML14224A151), July 31, 2014. Since July 31, 2014 there has been one additional through wall leaks attributed to dealloying.

Table 1 and 2 have been updated to include all through wall leaks to date and was reorganized to more clearly present the history of dealloying and weld cracking.

2.1 Table 1 - ECW De-alloying Data

This table tabulates the history of through wall leaks attributed to dealloying.
The population includes:

- Castings (Flanges, Pumps, valves, tees) manufactured using CA-952 and CA-954 material.
- Cast Tee to pipe weld using CA-952 and ERCuAl-A2 weld filler material. The components that are included are based on an increased in Aluminum content of the weld, thus making this component and weld more susceptible to dealloying.
- Extruded Tees made from CA-614 material with susceptible weld repairs using ERCuAl-A2 weld filler material affected by the repair process making the weld material susceptible to dealloying.
- Root Valve Socket Adapters made from CA-614 material and ERCuAl-A2 Shop welds.

Dealloyed Root Valve Socket Adapter Shop welds and Extruded Tees with weld repairs represent dealloying of susceptible weld material resulting in through-wall leakage.

TABLE 1 – ECW DE-ALLOYING DATA						
No	**Date**	**Component Type**	**Metallurgical Exam Information**	**Location**	**Information without Metallurgical Exam**	**References Comments**
1	7-6-87	U1 Cast Flange 6 inch	None	Essential Chiller 11C condenser outlet	Two pinhole leaks on cast flange at butt weld. Flange had cold spring and weld fusion line indications.	Non-Conformance Report (NCR) 87-77
2	12-11-88	U1 Cast Flange 6 inch	Fracto-graphic features of the crack did not provide definitive information concerning cracking mechanism due to the corroded condition of the crack surface. Crack located adjacent to the weld heat affected zone (HAZ) and oriented parallel to edge of the HAZ. Flange was sectioned (8 sections) to determine extent of de-alloying. In leak section, a through-wall crack present at leak location and through-wall de-alloying on both sides of the crack. In 5 sections, attack ranged up to 0.11 inch deep. In the two sections opposite the leak, de-alloying was minimal. Supplemental Report: Flange was sectioned (8 sections) to determine extent of de-alloying. In all but 1 section, de-alloying at isolated spots along the bore with maximum depth 0.13 inch. At one location, continuous de-alloying along the bore and along face of the bore/face intersection with maximum depth of 0.16 inch. In 3 sections, isolated de-alloying along the flange face. In the other 5, continuous attack along the face for distances up to 0.7 inch from bore.	Essential Chiller 11C outlet valve	LP showed ½ inch long indication on outside diameter (OD) and 1.5 inch on the inside diameter (ID). Crack located adjacent to a butt weld to 6 inch pipe.	NCR 88-282, Southwest Research Institute Metallurgical Investigation of Leak in Aluminum Bronze Fitting No.17-2520-520 dated 1-6-89 and Supplemental Report 6-21-89

TABLE 1 – ECW DE-ALLOYING DATA						
No	**Date**	**Component Type**	**Metallurgical Exam Information**	**Location**	**Information without Metallurgical Exam**	**References Comments**
3	5-20-90	U1 Cast Flange 6 inch	Flange was sectioned in 8 pieces and examined. Maximum depth of de-alloying was 100 percent and average depth was 64.8 percent. De-alloying occurred in the HAZ and in the base metal in the vicinity of the backing ring and not in the weld. Crack in flange is related to original installation where shop weld was cutout and re-welded.	Essential Chiller 11C supply valve	3.5 inch circumferential crack under the backing ring.	RFA 90-1219, SPR 910099, MT3047-2
4	10-30-90	U2 Cast Flange 6 inch	A second flange from U2 was also examined (MT 3047-1) and leakage was attributed to a through-wall crack and not to de-alloying. Maximum depth of de-alloying in the U2 Flange was 15.2 percent and average was 8.3 percent. Crack in flange is related to original installation where shop weld was cutout and re-welded.	Essential Chiller 21C condenser outlet	Through-wall leakage at a crack in the weld fusion line of a cast weld neck flange.	RFA 90-2108A SPR 910099, MT 3047-1 (for U2)
5	3-28-91	U2 Cast Flange 6 inch	Leakage due to through-wall de-alloying without cracks. Flange cut into 10 sections to determine de-alloying depth. Average depth of de-alloying was 0.226 inch with maximum thru wall (0.281 inch wall thickness).	Essential Chiller 21B supply valve	Through-wall leakage at 3 locations (4th thru wall site found in the lab that was not yet leaking).	RFA 91-684, MT-3383
6	6-25-91	U2 Cast Flange 8 inch	Rings cut out in two locations (one away from the weld) were sectioned into 8 pieces and examined to determine crack and de-alloying extent. Average de-alloying was 0.07 inch up to 0.19 inch at the location away from the weld. Average de-alloying at the weld root location was 0.10 inch. Average de-alloying at the flange face (gasket crevice) was 0.07 inch. The leak was the result of de-alloying at the tip of the crack.	Large Chiller 22C inlet supply valve	Circumferential crack length at the ID was 2 inch and initiated at the root of the weld. It terminated in the weld metal near the crown of the weld.	RFA 91-1005, MT-3727

TABLE 1 – ECW DE-ALLOYING DATA						
No	**Date**	**Component Type**	**Metallurgical Exam Information**	**Location**	**Information without Metallurgical Exam**	**References Comments**
7	8-7-91	U1 Cast Flange 6 inch	None	Diesel Generator (DG) 11 Intercooler Expansion Bellows inlet	3½-inch long hairline crack in neck of cast flange parallel to the butt weld.	RFA 91-1246
8	01-92	U2 Cast Flange 6 inch	Flange de-alloyed in area of the backing ring. No crack found in this flange. Sectioned into 8 parts at two locations to determine de-alloying depths. De-alloying at the weld root location was insignificant and average de-alloying at the backing ring was 0.19 inch with maximum through-wall. De-alloying at the flange face was 0.26 inch at all the sections (flange thickness 1.41 inch).	Essential Chiller 21B outlet	None	RFA 92-0020, RR-ENG-10, MT-3840
9	01-92	U2 Cast Flange 6 inch	Flange de-alloyed in areas of the weld root and at the end of the backing ring. Through-wall crack found at the weld root. Sectioned into 8 parts at two locations to determine de-alloying and crack depths. Average de-alloying at the crack location was 0.09 inch (Wall 0.34 inch) and average de-alloying away from the crack was 0.05 inch with maximum 0.16 inch. De-alloying at the flange face was 0.03 inch at all the sections (flange thickness 1.41 inch).	Essential Chiller 21B inlet	Through-wall crack with 8 degrees at the OD and 21 degrees at the ID.	RFA 92-0021, RR-ENG-10, MT-3840

TABLE 1 – ECW DE-ALLOYING DATA						
No	**Date**	**Component Type**	**Metallurgical Exam Information**	**Location**	**Information without Metallurgical Exam**	**References Comments**
10	02-92	U2 Cast Flange 6 inch	The flange was de-alloyed at the weld root and at the end of the backing ring. No cracking was found. Flange sectioned into 8 parts and at two transverse planes to determine de-alloying depths. At the first location at the end of the backing ring the average de-alloying depth was 0.18 inch with a maximum depth through-wall (wall thickness 0.28 inch) at 2 locations. At the second location, the average de-alloying was 0.10 with a maximum depth through wall at 1 location through the root of the weld. Average de-alloying at the flange face was 0.16 inch with maximum 0.23 inch (flange thickness 1.41inch).	Essential Chiller 21C outlet	None	RFA 92-0216, RR-ENG-10, MT-3923
11	3-23-92	U1 Extruded Tee (weld repair region in the Tee) 30x30x14	Leak result of de-alloying which initiated in repair weld metal contained within the Tee. The area of through-wall de-alloying initiation was confined to the repair metal in the HAZ of the pipe-to-tee butt weld. The repair weld metal was susceptible due to the presence of a continuous second phase network that may have contained gamma 2 phase. Review of fabrication documents shows cracking ¾ inch long was found at the edge of the 14 inch tee outlet during the outlet extrusion process.	Train 1B supply line to Essential Chiller 11B/12B	None	RFA 92-0359, SPR 92-742, RR-ENG-10 Supplement 2, MT-4102

TABLE 1 – ECW DE-ALLOYING DATA						
No	**Date**	**Component Type**	**Metallurgical Exam Information**	**Location**	**Information without Metallurgical Exam**	**References Comments**
12	4-92	U2 Cast Blind Flange 6 inch	Flange leak was due to a crack extending from the end of the backing ring to the weld root. At the end of the backing ring the crack went through-wall. Flange was sectioned into 8 segments and the sectors on either side of the leak were further sectioned into 5 equal parts to determine de-alloying and crack profile. Flange examined at 2 transverse planes with respect to pipe axis, location 1 at end of backing ring and location 2 the weld root. Average depth of de-alloying at location 1 was 0.045 inch with maximum depth through-wall (wall thickness 0.28 inch). At location 2, the average depth was 0.37 inch with maximum depth of 0.25 inch (wall thickness 0.37 inch).	DG 21 Supply Line End Flange	None	RFA 92-427, RR-ENG-10, MT-4046
13	10-01-92	U1 Cast Flanges 6 inch	Both flanges were sectioned into 8 segments to determine de-alloying profile. Extent of de-alloying was determined at 3 locations on all 8 segments: at the backing ring, weld root, and flange face. Average depth of de-alloying for the first flange was 0.05 inch, 0.08 inch, and 0.04 inch for the backing ring, weld root, and flange face, respectively. The greatest amount of de-alloying was 0.22 inch at the 225° position at the weld root. Average depth of de-alloying for the second flange was 0.03inch, 0.03 inch, and 0.02 inch for the backing ring, weld root, and flange face, respectively. The greatest amount of de-alloying was 0.07 inch at the 90° position at the end of the backing ring	Essential Chiller 12B Inlet Flange and Outlet Flange	Preemptive removal of cast flanges (neither flange had any surface indications).	EW-160727, EW-160729, MT-4089

TABLE 1 – ECW DE-ALLOYING DATA						
No	**Date**	**Component Type**	**Metallurgical Exam Information**	**Location**	**Information without Metallurgical Exam**	**References Comments**
14	10-22-92	U1 Cast Flanges 6 inch	Each flange was sectioned into 8 segments to determine de-alloying profile. Extent of de-alloying was determined at 3 locations on all 8 segments: at the backing ring, weld root, and flange face. Average depth of de-alloying for the first flange was 0.10 inch, 0.18 inch, and 0.17 inch for the backing ring, weld root, and flange face, respectively. The greatest amount of de-alloying was 0.33 inch at the 0° position on the flange face. Average depth of de-alloying for the second flange was 0.01 inch, 0", and 0.01 inch for the backing ring, weld root, and flange face, respectively. The greatest amount of de-alloying was 0.03 inch at the 90° and 180° positions at the end of the backing ring. Average depth of de-alloying for the third flange was 0.02 inch, 0.04 inch, and 0.07 inch for the backing ring, weld root, and flange face, respectively. The greatest amount of de-alloying was 0.14 inch at the 135° position on the flange face. Average depth of de-alloying for the fourth flange was 0.02 inch, 0.005 inch, and 0.04 inch for the backing ring, weld root, and flange face, respectively. The greatest amount of de-alloying was 0.06 inch at the 315° position on the flange face.	Essential Chiller 11B Inlet Valve Upstream Flange, Essential Chiller 11A Inlet and Outlet Flanges and Inlet Valve Downstream Flange	Preemptive removal of cast flanges (none of the flanges had any surface indications).	EW-160728, EW-160730, EW-160732, EW-160733 MT-4141

TABLE 1 – ECW DE-ALLOYING DATA						
No	**Date**	**Component Type**	**Metallurgical Exam Information**	**Location**	**Information without Metallurgical Exam**	**References Comments**
15	12-18-92	U1 Cast Tee 10x10x6	Defect originated in a weld repair in the Tee casting and crack propagated into the butt weld. A 1 inch diameter plug sample was removed from the cracked butt weld and sent to lab for analysis. Lab confirmed the crack originated in the tee adjacent to the weld prior to service. Crack promoted de-alloying in the cast tee by progressive extension of the crack through de-alloyed material. The maximum depth of de-alloying from the inside diameter surface was 0.1 inch in the plug specimen. The crack did not extend through-wall. This area was ground out and weld repaired during fabrication of the tee. Note this Tee was subsequently replaced after another through-wall indication developed in the bulk portion of the Tee (see Table item 44)	DG13 Intercooler 10 inch Return Tee	None	Weld Repaired Service Request 161574, MT-4303, SPR 92-1575
16	2-1-93	U2 Cast Flange	De-alloyed flange weld with pre-existing cracks subjected to Bend Test to Failure. On the fracture surface, 2 pre-existing cracks (one through-wall) were noted. The de-alloying and crack profiles were mapped. In the area of the through-wall crack, de-alloying depth ranged from 50 percent to 100 percent. In the area of the partial through-wall crack, de-alloying depth ranged from 35 percent to 94 percent. Mapping results provided in the lab report.	DG21 Intercooler Supply	None	MT-4907

TABLE 1 – ECW DE-ALLOYING DATA						
No	**Date**	**Component Type**	**Metallurgical Exam Information**	**Location**	**Information without Metallurgical Exam**	**References Comments**
17	3-17-93	U2 Root Valve Socket Adapter 1 inch	Both sides of the valve were sectioned into approximately 45 degree sectors. The leak was the result of localized de-alloying in the socket weld between the valve body and the adapter. Through-wall dealloying was confined to the leak location where a two phase microstructure extended from the socket crevice through the weld.	2-EW-0287, Supplemental Cooler return root valve	Leak at the inlet end of a ½-inch ball valve with a vendor supplied socket welded adapter.	MT-4629
18	12-8-93	U2 Cast Flange 6 inch	De-alloying observed at small area on the OD surface of the weld as a result of a through-wall crack. Crack appears to have initiated prior to service. Outside the HAZ, the base metal was de-alloyed to a depth of approximately 0.01 inch along the crack faces on either side of the crack and along the crevice between Flange and Backing Ring. In the HAZ de-alloying of crack faces was most severe just before the crack penetrated into the weld. De-alloying to greater than 0.05 inch was found in one location approximately. 180 degrees removed from the crack location. No de-alloying at the flange face.	DG 22 Supply Line End Flange	Crack initiated .09 inch from the weld root. Extend circumferentially was 9 degrees on OD and 60 degrees on ID.	MT-5369
19	1-4-94	U2 Cast Tee 10 inch 10x10x6 (with backing ring)	Pre-existing 10 inch weld crack allowed de-alloying to initiate in the susceptible weld metal microstructure and progress through-wall. 8 segments removed from ring in two locations (second location away from the weld). Sections were ground and etched to reveal crack and de-alloying extent. At the crack location, crack depth up to 0.31 inch (wall 0.44 inch) with de-alloying at average 14 percent. In the section location away from the crack, de-alloying averaged 10 percent.	DG 23 supply line weld at Cast 10x10x6 Intercooler supply Tee	Moisture and residue buildup at weld between pipe and cast Tee.	EW-212847, MT-5050

TABLE 1 – ECW DE-ALLOYING DATA						
No	**Date**	**Component Type**	**Metallurgical Exam Information**	**Location**	**Information without Metallurgical Exam**	**References Comments**
20	1-11-94	U2 6-inch supply line weld between pipe and elbow (with backing ring)	No evidence of a leak through-wall was found in the pipe to elbow weld. 8 segments removed from ring in two locations (second location away from the weld). Sections were ground and etched to reveal crack and de-alloying extent. Crack depth up to 0.07 inch with a de-alloyed depth up to 0.08 inch (wall thickness 0.34 to 0.41 inch) at the same section.	DG 23 Intercooler 6-inch supply line weld between pipe and elbow	A possible second indication was discovered at a shop weld between a downstream elbow and 6-inch pipe.	EW-212847, MT-5050
21	3-30-94	U2 Root Valve Socket Adapter 1 inch	Leaks on the inlet end of both valves resulted from de-alloying of the weld metal in the socket weld made in the shop between the valve body and adaptor. Through-wall de-alloying confined to HAZ where the morphology of the second phase was changed when the pipe to adaptor field weld was made. Aluminum bronze has a susceptible microstructure when a continuous second phase network exists. On both valves, no de-alloying in the field welds between the adaptor and pipe.	2-EW-0373B, Screen Wash 2B Flow Indicator root valve	Multiple residue deposits on a vendor socket weld between the valve body and a ½-inch adaptor.	MT-5368
22	3-30-94	U2 Root Valve Socket Adapter 1 inch	See above (item 21)	2-EW-0374B, Screen Wash 2B Flow Indicator root valve	Multiple residue deposits on a vendor socket weld between the valve body and a ½-inch adaptor.	MT-5368

TABLE 1 – ECW DE-ALLOYING DATA						
No	**Date**	**Component Type**	**Metallurgical Exam Information**	**Location**	**Information without Metallurgical Exam**	**References Comments**
23	7-26-95	U1 Cast Fitting with Socket Weld	None	Half coupling for vent stub in DG13 Lube Oil Cooler supply line	Residue buildup in a cast fitting at the socket weld to the vent pipe stub.	Condition Report (CR) CR 95-9332, CR 97-16442, CR 97-17172, CR 97-17425 This small bore socket welded cast fitting was missed in the original small bore replacement program probably since it was only shown on a Large Bore isometric drawing.
24	4-23-96	U2 Cast Flange 8 inch	None	Chiller 22A 8-inch return flange downstream of 2-EW-1002	1¾-inch long crack in neck of cast flange parallel to butt weld. Radiographic inspection indicated 3 and 1/16-inch subsurface crack length.	CR 96-4612, RR-ENG-14

TABLE 1 – ECW DE-ALLOYING DATA						
No	**Date**	**Component Type**	**Metallurgical Exam Information**	**Location**	**Information without Metallurgical Exam**	**References Comments**
25	4-24-96	U1 Cast Flange 8 inch	Crack that caused the leak was result of inter-granular de-alloying at the edge of the HAZ of the weld attaching pipe to flange. Three sections A, B & C were taken through the pipe and the extent of de-alloying was determined on the face of each section. The average depth of de-alloying in section A was 14.5 percent, B was 31 percent and C (away from the crack) was very small.	Chiller 12A 8-inch return flange downstream of 1-EW-1002	1⅜-inch long crack in neck of cast flange parallel to butt weld. Radiographic inspection indicated 4 and 1/16-inch subsurface crack length.	CR 96-4652, RR-ENG-14, TR-11078
26	5-22-96	U2 Cast Tee 6x6x6	None	Self cleaning strainer 2B backwash	Two residue spots on a cast Tee at a butt weld to a cast flange.	CR 96-5918, RR-ENG-14
27	2-03-97	U2 Cast Tee 10x10x6	Tee sectioned into 37 sections with etching of each section to show de-alloyed area. Plots made at 3 locations showing de-alloying depth versus axial and circumferential locations. De-alloying depths varied significantly over the surface area of the tee from zero to 100 percent through-wall.	DG 23 Jacket Water Cooler Supply line	Residue buildup at one spot within the bulk of the 10-inch portion of the cast Tee.	CR 97-1775, RR-ENG-17, CREE 05-1919-4
28	10-6-97	U2 Cast Tee 10x10x6	None	Essential Chiller 2A supply line cross connect Tee	Residue buildup at several pinpoints on a cast Tee near the 10-inch inlet butt weld.	CR 98-3106, RR-ENG-19, CR 97-16160, (originally classified as blemish)
29	10-7-97	U2 Cast Flange 3 inch	None	ECW Pump 2C discharge vent line 2-FO-6956 upstream flange	Moisture buildup on cast flange neck near the butt weld.	CR 97-16264, RR-ENG-18,

TABLE 1 – ECW DE-ALLOYING DATA						
No	**Date**	**Component Type**	**Metallurgical Exam Information**	**Location**	**Information without Metallurgical Exam**	**References Comments**
30	7-1-98	U2 Cast Pump 3 inch	None	Screen Wash Booster Pump 2C outlet flange	Residue buildup on the flange directly below the drilled connection for the pump mechanical seal flush tubing connection.	CR 98-10849, RR-ENG-27
31	11-22-99	U2 Cast Flange 10 inch	None	Chiller 2C to 2B cross tie isolation valve 2-EW-0275 cross-tie side flange	Residue buildup in several spots on the neck of cast flange near the butt weld. Two areas of residue buildup had spots forming along a line on the flange neck near and parallel to the butt weld.	CR 99-16610, RR-ENG-35
32	7-18-00	U2 Cast Valve 6 inch	None	2-EW-0277 Self- Cleaning Strainer 2A Emergency Backwash valve	Drop of water next to the gasket and multiple pinpoint residue buildup spots on the valve body. Leakage could be a combination of gasket seepage and valve body de-alloying.	CR 00-11814,

TABLE 1 – ECW DE-ALLOYING DATA						
No	**Date**	**Component Type**	**Metallurgical Exam Information**	**Location**	**Information without Metallurgical Exam**	**References Comments**
33	7-24-00	U1 Extruded Tee (Weld repair region in the Tee) 30x30x14	Leak result of de-alloying which initiated in repair weld metal contained within the Tee. The area of through-wall de-alloying initiation was confined to the repair metal in the HAZ of the pipe-to-tee butt weld. The repair weld metal was susceptible due to the presence of a continuous second phase network that may have contained gamma 2 phase.	Train 1A supply line to Essential Chiller 11A/12A	Residue buildup at a spot on the bottom of 14-inch portion of 30-inch by 30- inch by 14-inch extruded Tee.	CR 00-12050, RR-ENG-2-24, Similar to de-alloyed condition in Train 1B extruded tee where weld repair was performed during fabrication of the tee. Lab report MT 4102 investigated the region in the Train 1B Tee.
34	1-17-01	U1 Cast Flange 3 inch	None	Screen Wash Booster Pump 1B flow element 1-FE-6958 upstream flange	Residue buildup at several spots forming along a line on the flange neck near the butt weld. Line of spots is parallel to the butt weld and about ½-inch long. .	CR 01-912, RR-ENG-2-25

TABLE 1 – ECW DE-ALLOYING DATA						
No	**Date**	**Component Type**	**Metallurgical Exam Information**	**Location**	**Information without Metallurgical Exam**	**References Comments**
35	1-17-01	U1 Cast Valve Seat Retainer 6 inch	None	1-EW-0093, Essential Chiller 11C Inlet Valve	Seepage at two locations at the joint between the cast seat retainer and the cast valve body. Seepage could be due to poor gasket seal combined with possible de-alloying in the seat retainer.	CR 01-914 Essential Chiller 11C was abandoned and this valve was removed from the system.
36	2-1-01	U2 Cast Valve Bonnet 1 inch	None	2-EW-PSV-6865, DG 22 Relief Valve	Residue buildup spot on the cast bonnet near the outlet flange.	CR 01-1888 The bonnet is not pressurized but retains the spring on this PSV and directs flow to the floor drain when the PSV lifts.
37	11-26-01	U1 Cast Flange 3 inch	None	Screen Wash Pump 1C suction flow orifice Flange 1-EW-FE-6959	Residue buildup at several spots on the flange neck near the butt weld.	RR-ENG-2-26, CR 01-19152
38	11-28-01	U2 Root Valve Socket Adapter 1 inch	None	2-EW-0284 Supplemental Cooler 2A transmitter/flow indicator, FT/FI-6856 low side root valve	Residue buildup at a spot on the vendor valve to ½-inch adapter socket weld.	CR 01-19319 Similar to de-alloyed condition in the other adapter socket welds. Lab report MT 5368

TABLE 1 – ECW DE-ALLOYING DATA						
No	**Date**	**Component Type**	**Metallurgical Exam Information**	**Location**	**Information without Metallurgical Exam**	**References Comments**
39	11-04-02	U2 Cast Flange 3 inch	None	Pump 2B discharge vent line check valve 2-EW-0370B upstream flange	Water drop forms on top of cast flange at one spot near the flange neck butt weld.	CR 02-16257, found and fixed in the outage
40	11-6-02	U1 Cast Tee 10x10x6	None	DG13 Intercooler Return Tee	⅛-inch residue deposit in about a ½-inch round circle of secondary located near the middle of the 10-inch run of the cast Tee.	CR 02-16395, This Tee was originally repaired by plug welding in 1992. . This tee was replaced when the second through-wall leak was found in 2002.
41	10-15-03	U2 Cast Flange 8 inch	None	Essential Chiller 12B ECW Return Valve 1-EW-1004 downstream flange	Residue buildup at several spots along a line on the flange neck near the butt weld. Line of spots is parallel to the butt weld and about ¾-inch long.	CR 03-15710
42	10-15-03	U2 Cast Flange 6 inch	None	Self-cleaning Strainer 2B Emergency Backwash Valve 2-EW-0278 Inlet Flange	1½ inch long area of pinpoint residue buildup parallel to butt weld in neck of cast flange.	CR 03-15730

TABLE 1 – ECW DE-ALLOYING DATA						
No	**Date**	**Component Type**	**Metallurgical Exam Information**	**Location**	**Information without Metallurgical Exam**	**References Comments**
43	7-27-05	U1 Cast Blind Flange 6 inch	None	Return line flange from abandoned 150-Ton Chiller 11B	Residue buildup at several spots forming along a line on the flange neck near the butt weld. Line of spots is parallel to the butt weld and about ½-inch long.	CR 05-9622 Although the 150-ton Essential Chillers have been abandoned, this flange is downstream of the blind and is pressurized by ECW Train 1B.
44	1-9-06	U1 Cast Flange 10 inch	None	Cross-tie valve upstream of Essential Chillers 11C/12C to 11A/12A 1-EW-0276 Upstream Flange	Through-wall indications are several small spots with residue buildup at the flange neck near the butt weld.	CR 06-360
45	1-16-06	U2 Cast Valve Bonnet 1 inch	None	2-EW-PSV-6866, Supplemental Cooler 2B thermal relief valve	Residue buildup spot on the cast bonnet.	CR 06-696, The bonnet is not pressurized but retains the spring on this PSV and directs flow to the floor drain when the PSV lifts.

TABLE 1 – ECW DE-ALLOYING DATA						
No	**Date**	**Component Type**	**Metallurgical Exam Information**	**Location**	**Information without Metallurgical Exam**	**References Comments**
46	7-6-06	U2 Cast Tee 10x10x4	None	10-inch DG 21 supply header and Lube Oil Cooler supply Tee	Residue buildup at one spot on the cast Tee at the inlet butt weld fusion line.	CR 06-8594
47	6-6-07	U2 Cast Valve Seat Retainer	None	2-EW-0204, DG 23 Engine Cooler Return Flow Balance Throttle Valve	Residue buildup on the valve seat retainer near the flange gasket. Could be a combination of gasket leakage and dealloying.	CR 07-9166
48	12-2-08	U2 Cast Flange 8 inch	None	Essential Chiller 22B ECW return throttle valve 2-EW-1004 flange	Residue buildup about one half inch long in a line parallel to the butt weld for the downstream flange.	CR 08-18477
49	8-19-10	U1 Cast Flange 6 inch	None	Piping flange downstream of abandoned 150-Ton Essential Chiller 11A	Linear through-wall indication with residue buildup. The indication is in the neck of the cast flange, about ¼ inch away and roughly parallel to the flange to pipe shop weld.	CR 10-17899, This portion of piping has been isolated from ECW but is still part of the pipe support structure for the 300-ton Essential Chiller 12A ECW piping.

TABLE 1 – ECW DE-ALLOYING DATA						
No	**Date**	**Component Type**	**Metallurgical Exam Information**	**Location**	**Information without Metallurgical Exam**	**References Comments**
50	8-19-10	U1 Cast Valve Bonnet 1 inch	None	1-EW-PSV-6855, DG 11, thermal relief valve	Residue buildup spot on the cast bonnet near the outlet flange.	CR 10-17957, The bonnet is not pressurized but retains the spring on this PSV and directs flow to the floor drain when the PSV lifts.
51	7-28-11	U2 Cast Valve Body 4 inch	None	1-EW-FV 6936 ECW 2B Return Header Blowdown Valve	Residue buildup at several discrete spots on the valve body at the machined inlet portion near the flange.	CR 11-12309
52	1-9-12	U2 Cast Valve body 4 inch	None	2-EW-FV 6937 Return Header Blowdown Valve	Residue buildup indicative of through-wall dealloying at Valve Body.	CR 12-1044
53	6-12-12	U2 Cast flange 10 inch	None	3R282TEW0274 Chiller ECW Cross-Tie valve flange	Residue buildup indicative of through-wall dealloying on the cross-tie side flange.	CR 12-22876

TABLE 1 – ECW DE-ALLOYING DATA						
No	**Date**	**Component Type**	**Metallurgical Exam Information**	**Location**	**Information without Metallurgical Exam**	**References Comments**
54	3-4-14	U1 Root Valve Socket Adapter 1 inch	None	3R281TEW0283 CCW Pump Supplemental Cooler 11A FI/FT high side root valve	Discoloration spots at 9 o'clock and 2 o'clock on shop weld.	CR 14-4206
55	8-27-15	U2 Cast flange 8 inch	None	EW2185WT3 Essential Chiller 22A ECW outlet line	Residue buildup indicative of through-wall dealloying.	CR 15-20365

Clarifications to Table 1

- Items 4, 6, 7, 12, 16, 18, and 20 are dealloying and cracks associated with castings and connection welds.
- Item 7 is for a crack in a cast flange. The crack was in the casting, running parallel to the flange to pipe weld but did not involve dealloying of the weld metal. Table 1 Item 7 is not related to Table 2 Item 5.
- Items 11 and 33 are associated with weld metal dealloying in the weld repair of extruded Tees. Extruded Tees are a special case of weld metal dealloying that is not associated with linear indications or cracks.
- Items 19 and 20 are captured as part of Table 1 because Lab report MT-5050 concluded these items weld were associated with a pipe to Cast Tee. Further details are provided in section 3.0 conclusions.
- Items 17, 21, 22, 38, and 54 are associated with weld metal dealloying in the socket weld done by the valve manufacturer to add an adapter. This is another special case of weld metal dealloying not associated with linear indications or cracks.
- Item 24 and 25 are associated with a crack indication in a cast flange. The cracks were in the casting, running parallel to the flange to pipe weld but did not involve dealloying of the weld metal. The Unit 1 flange was sent out for failure analysis (TR-11078). The report notes that the crack that caused the leak was the result of inter-granular dealloying in the casting at the edge of the heat affected zone of the butt weld. The crack was entirely within the metal of the casting.
- Item 49 is for a crack indication in a cast flange. The crack was in the casting, running parallel to the flange to pipe weld but did not involve dealloying of the weld metal. Crack indication and residue deposits in the metal of the casting.

The below graph provides a graphical representation of the through wall trends over time.

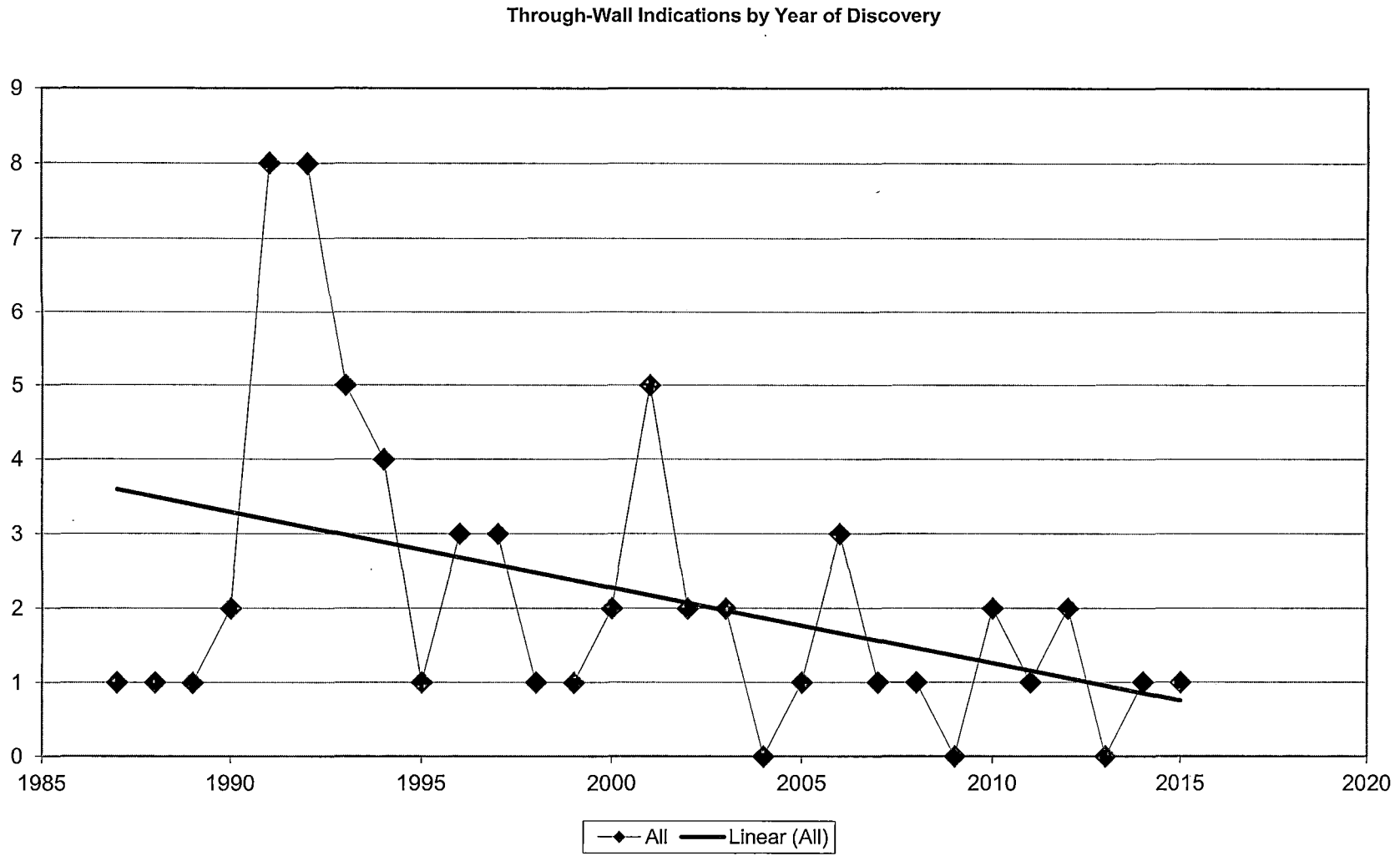

2.2 Table 2 – ECW Weld Crack Data

This table tabulates the history of through wall leaks attributed to Weld Cracking of susceptible weld material. This population is made up of ASME SB-315, CA-614 pipe to pipe material welded utilizing ERCuAl-A2 filler material associated with backing ring configurations. There have been no leaks identified from this same material and welds where backing rings were not utilized.

The first two entries are special case Stainless steel to aluminum bronze welds which have been removed from the system.

TABLE 2 - ECW WELD CRACK DATA

No	Date	Weld Location	Metallurgical Exam Information	Information without Metallurgical Exam	Reference/ Comments
1	1-30-89	U1 stainless steel (SS) thermo-wells welded to aluminum bronze socko-let fittings (2)	Crack was in the 316 SS and no de-alloying was found in the aluminum bronze socko-let fitting. Source of weepage were tiny fissures (liquation cracks) which can occur when copper alloys are welded to SS. Lab analysis indicated cracking caused by liquid embrittlement of the SS and crevice corrosion. **All SS thermo-wells were replaced in both units with Aluminum Bronze thermo-wells or non-welded thermo-wells.**	2 thermo-wells in ECW piping	Cracking not associated with de-alloying of aluminum bronze
2	1-30-89	U2 SS thermo-well welded to aluminum bronze socko-let fitting	See above **All SS thermo-wells were replaced in both units with Aluminum Bronze thermo-wells or non-welded thermo-wells.**	1 thermo-well in ECW piping	Cracking not associated with de-alloying of aluminum bronze
3	5-6-89	U2 Train 2C, 24 inch ECW Strainer Bypass Line (with backing ring)	None	Pinhole leak in 24-inch butt weld. Grinding revealed 3-inch long linear indication. No evidence of de-alloying by silver nitrate checks during defect excavation.	NCR 89-2-112, EW-80837

TABLE 2 - ECW WELD CRACK DATA					
No	**Date**	**Weld Location**	**Metallurgical Exam Information**	**Information without Metallurgical Exam**	**Reference/ Comments**
4	7-13-91	U2 Train 2B, 30 inch CCW Heat Exchanger line (with backing ring)	In-service 5-¾ inch crack initiated at tip of pre-existing lack of fusion defect and propagated by combination of progressive, local de-alloying and crack growth through de-alloyed material. Other areas showed only slight de-alloying with no crack propagation.	Crack location had been subject to major repair during construction with a weld width double a normal weld.	MT-3512B (Repaired Failure Analyzed)
5	8-6-91	U1 Train 1B, 30 inch line between elbow and CCW Heat Exchanger (with backing ring)	In-service 4 inch crack initiated at tip of pre-existing cracks and/or lack of fusion defect and propagated by combination of progressive, local de-alloying and crack growth through de-alloyed material. Crack propagation was confined to the deepest portion of the pre-existing defect. Other areas showed only slight de-alloying with no crack propagation.	Weld was cut out and re-welded during original installation	RFA 91-1241, RR-ENG-10, SPR-910273, MT-3512A (Repair cracked and repair failure analyzed)
6	12-13-91	U1 re-crack of weld above	Lab analysis showed part of a crack occurred during welding and the balance progressed by the mechanism of de-alloying and cracking that is identified in earlier failure analyses	Re-crack at repair location	RFA 91-2056, EW-154081, MT-3800
7	11-5-91	U1 Weld Train 1C, 30 inch Line ECW Intake Structure (with backing ring)	Crack occurred subsequent to an earlier weld repair. No de-alloying noted on the ID and only minimal de-alloying observed along the fracture surface. Average through-wall crack widths of 0.029 inch (20.4 degrees) and 0.049 inch (31 degrees).	Crack on OD 5.3 inch and ID 13.6 inch.	RFA 91-1803, RR-NNG-10, MT-5623
8	6-11-93	Same weld as above	None	Re-crack at repair location	EW-179340

TABLE 2 - ECW WELD CRACK DATA					
No	**Date**	**Weld Location**	**Metallurgical Exam Information**	**Information without Metallurgical Exam**	**Reference/ Comments**
9	11-7-91	U1 Train 1A, 30 inch Supply Line in Mechanical Auxiliary Building (with backing ring)	Microscopy of the microstructure from a boat sample showed de-alloying in the vicinity of a crack was mechanism responsible for the leak. De-alloying was predominately located around the cracked region and not in area away from the crack.	Seepage from a fine hair line crack about 1¼-inch long on the surface and about 3⅝-ich long on the pipe internal diameter.	RFA 91-1835, EW-103016, RR-ENG-10, MT-4181
10	12-6-93	U2 Essential Chiller 11C, 6 inch Elbow (vendor weld with backing ring)	Presence of pre-existing welding cracks at the juncture between the piping and backing ring. Crack dimensions were obtained by examining cross sections at various locations around the pipe. Section of material containing a portion of the through-wall crack was broken open to view the fracture surface. Crack is semi-elliptical with a length approximately twice the maximum radial crack depth at the failure location.	Moisture and residue on a shop weld with a backing ring between a wrought elbow and pipe.	EW-212839, MT-5487

Clarifications to Table 2

- Items 1 and 2 are associated with cracking and leakage at aluminum bronze to stainless steel welds. This leakage, however, is not associated with aluminum bronze dealloying and all these stainless welds were replaced in both units with Aluminum Bronze thermo-wells or non-welded thermo-wells.

3.0 WELD BACKGROUND

Pipe welds with backing rings were found to have through-wall leaks in 1989. The weld flaws originated on the inner diameter of the pipe near backing rings. Root cause lab reports MT-3512A and MT-3512B indicated the crack propagation occurred by a process of de-alloying in the weld in a narrow band along the crack front. Cracks initiated under the backing ring from pre-existing weld flaws at the root of the weld. Once initiated, cracks are driven by operating and residual weld stresses combined with the effects of de alloying at the crack tip.

The last leak identified from a pipe weld was from a weld with backing ring and it was discovered in 1994.

3.1 Weld Cracks, Failure Reports, and Summary Results

The below Table 3 documents the identified weld crack locations with the evaluation and evaluation results summaries. The evaluations support the premise that flaw propagation is predominately accompanied with dealloying within the flaw/crack tip material. There is no evidence of general dealloying in the weld root or filler material or associated base material.

Table 3 - Identified Weld Crack Locations

Weld Crack Location	Date	Evaluation Report	Results Summary
U2 "C", 24 inch line EW2302/FS3469	5/6/89	NCR 89-2-112, EW-80837	None
U2 "B", 30 inch line EW 2205/FW3099:	7/13/91	MT-3512B	The Unit 2 crack initiated at pre-existing weld defects (cracks and/or lack of fusion).
U1 "B", 30 inch line CCW HX	8/6/91& 12/13/91	MT-3512A & MT-3800	-The in-service crack initiated at the tip of the pre-existing defect and propagated by a combination of progressive, local dealloying and crack growth through the dealloyed material. -The crack initiated at the root of the weld on the nozzle side early in the repair .process. The crack was formed as a result of weld shrinkage stresses combined with poor weld geometry. Attempts to get a proper fit up of the backing ring on the inside diameter surface were unsuccessful due to the taper on the inside diameter surface of both the elbow and the nozzle and the fit up of the elbow to the nozzle. A gap between the backing ring and the nozzle ultimately created a notch at the weld root suitable for crack initiation under the applied shrinkage stresses. The mechanism responsible for in-service crack propagation is identical to that found in the original crack at this location (see

Weld Crack Location	Date	Evaluation Report	Results Summary
			Materials Technology Report MT-3512A) and in a pipe-to-pipe weld from Unit 2 (see Materials Technology Report MT-3512B).
U1 "B", 30 inch line EW1205, FW0043	11/5/91& 6/11/93	MT-5623	The weld on aluminum bronze pipe had cracked subsequent to a repair performed on this weld joint. No dealloying was noted on the ID surface of the pipe only minimal dealloying was observed along the fracture surface.
U1 "A", 30 inch line EW1102, FW0032	1/7/91	MT-4181	Boat sample revealed that dealloying of the two-phase weld-metal in the vicinity of a crack was the mechanism responsible for the leak in the weldment. Boat sample did not penetrate through the weld to the backing ring, it did not contain any portion of the weld- root
U2 "C", 6 inch line Chiller elbow:	12/6/93	MT-5487	The leak in this pipe to elbow weld was due to the presence of small pre-existing welding defects (cracks) at the juncture between the pipe/elbow and backing ring.
U2 "C", 10 inch line DG intercooler supply	1/4/94	MT-5050	The leak in this pipe to cast tee weld was due to the presence of small pre-existing welding defects (cracks) at the juncture between the pipe/elbow and backing ring.
2 "C", 6 inch line DG intercooler supply	1/11/94	MT-5050	The indication was in the pipe to elbow weld was due to the presence of small pre-existing welding defects (cracks) at the juncture between the pipe/elbow and backing ring.

Conclusions:

Lab reports MT-3512A, MT-3512B, MT-3800, MT-5623, MT-4181, and MT-5487 support the conclusion that pre-existing defects at the root of the weld lead to in-service crack initiation at the tip of the pre-existing defect and propagated by a combination of progressive, local dealloying and crack growth. A consistent postulated failure mechanism would be as follows: The pre-existing defect acted as a stress concentrator. Operating stresses, weld residual stresses, and possibly cyclic stresses were intensified at the tip of the defect. A volume of weld metal at the tip of the defect dealloyed. The crack then initiated and propagated through the dealloyed region of material until it was arrested by the surrounding, unaffected weld material. The process of local dealloying at the crack tip and subsequent local crack growth continued until the crack propagated through wall.

Lab report MT-5050 concluded this weld was associated with a pipe to Cast Tee. The failed weld was not a true pipe-to-pipe weld, but instead was a pipe-to-tee (casting) weld with a backing ring. A pre-existing partial crack in the pipe-to-tee weld allowed dealloying to initiate in the susceptible weld microstructure. This evidence supports the fact that all of the weld failures did occur early in plant life (1991-1994) and that no evidence of other leaks have

occurred since. If a weld flaw(s) were to be present during fabrication, significant enough such that the weld root pass was breached, then the weld could lead to dealloying thus causing early crack growth. If no weld flaws existed or if the weld flaw was insignificant enough as to not breach the protective weld root pass, then the weld would not experience dealloying. (CREE 12-29261-108)

3.2 Weld Categories and Groupings Being Managed

The Selective Leaching of Aluminum Bronze program manages loss of material and cracking due to selective leaching for aluminum bronze (copper alloy with greater than eight percent aluminum) components and welds exposed to raw water within the scope of license renewal. Between Units 1 and 2, there are approximately 3300 circumferential welds in the ECW piping. Of this total, 1100 welds have backing rings and 2200 without backing rings.

Welds requiring Aging Management were grouped into two categories and all combinations of similar welds were included as part of these categories. Below is a breakdown of the two categories and included weld types under each category.

3.2.1 Welds without backing rings:

- Shop or Field welds without backing rings using either original ERCuAl-A2 material or replacement ERCuNiAl material.
- Pipe seam welds without backing rings using ERCuAl-A2 material.
- ECW/CCW heat exchanger shop welds in the Seam, Nozzle, and Head Flange, using ERCuAl-A2 material.
- Socket Welds (small bore) using ERCuAl-A2 material.

3.2.2 Welds with backing rings:

- Shop or Field Welds with backing rings using ERCuAl-A2 material.

3.3 Weld Categories Being Replaced

Three additional weld categories are being replaced or evaluated as commitments outlined in the Aging Management Program.

3.3.1 Welds that are part of the susceptible casting component replacement commitment:

- Attachment welds related to the castings, with backing rings and ERCuAl-A2 material. (Will be replaced during casting replacement)
- Attachment welds related to the castings, without backing rings with either original ERCUAl-A2 material or replacement ERCuNiAl material. (Will be replaced during casting replacement.)

3.3.2 Root valve socket adapter welds:

- Root valve socket with adaptor shop welds (small bore) with ERCuAl-A2 material. These socket adapter and root valves will be replaced and are tracked by the dealloying component change-out scope.

3.3.3 Weld Repairs on Extruded Tees:

- Extruded Tee weld repairs using ERCuAl-A2 material where structural integrity margin cannot be assured. A structural integrity evaluation will be performed on the extruded tees with weld repairs that do not demonstrate margin will be replaced and are tracked by the dealloying component change-out scope.

4.0 WELD AUDIT TOPICS

4.1 Table 4 - Topics, Summary, and References

The below table provides a matrix of common topics discussed in audits with related summary response discussion and applicable references.

Table 4 - Topics, Summary, and References

		Summary or location within this report	References
1	a. Validation to be performed through a One Time Inspection: to demonstrate no active aging on low susceptible welds. b. Periodic Inspection to monitor for crack tip dealloying of population of welds with operating experience of weld cracking. c. Destructive examination of any identified leaking welds. d. Periodic Visual External inspections. e. Opportunistic examination if buried pipe is exposed.	a. one-time examination of 3 percent with a maximum of 10 welds of the above ground weld population with no backing rings are examined one-time volumetrically to validate weld integrity. If rejectable weld flaws (weld defects) per ASME Section IX requirements are found during the one-time inspection of welds with no backing rings, periodic volumetric examinations of 20 percent with a maximum of 25 welds will be performed every 10 years thereafter. b. 20 percent with a maximum of 25 welds of the above ground weld population with backing rings are examined volumetrically prior to the period of operation and every 10 years thereafter. If no weld defects are found during the inspection performed prior to the period of extended operation of welds with backing rings, the 10 year follow-up volumetric examinations scope will be reduced to 3 percent with a maximum of 10 welds. c. Aluminum bronze welds found to have defects or through wall leakage are removed and destructively examined to determine the extent of cracks or selective leaching.	a-e B2.1.37 Selective Leaching of Aluminum Bronze Section 1.0 of this report

		Summary or location within this report	References
		d. The Selective Leaching of Aluminum Bronze program includes visual inspections every six months (not to exceed nine months) of the external surfaces of the above ground components and welds for selective leaching and cracking. e. Whenever aluminum bronze materials are exposed during inspection of the buried ECW piping, the components are examined for indications of selective leaching. If leaking below-grade welds are discovered during a buried ECW piping inspection, a section of each leaking weld will be removed for destructive examination.	
2	Review basic weld material information: a. Alloys that the pipes, backing rings, and welds are fabricated from. b. Specifications for the alloys were produced/procured to c. Certified Material Test Report and material certification data, to the extent that it is useful/available	a/b. ECW Piping <10 Inches • Pipe SB-315 (Conforms to SB-169 CA-614 Annealed Seamless) • Fittings SB-150 CA-614 or SB-169 CA-614 or Castings SB148 (CA952) • Plugs SB-150 CA-614 or SB-169 CA-614 • Flanges SB-169 CA-614 or Castings SB-271 CA-952 or Slip-on Carbon Steel • Valves Socket Welded Aluminum Bronze CA-614 for small bore, flanged castings(CA952) or (CA954) or 316 stainless steel ECW Piping > 14 Inches • Pipe Welded SB-169 CA-614 (6% to 8% Aluminum) • Fittings SB-169 CA-614 • Flanges Slip-on Carbon Steel • Valves Aluminum Bronze	a. Intertek report "Metallurgical Analysis of Al-Brz Pipe-to-Pipe Welds in the ECW System," AIM 130784455-2Q-7, May 2016. Section 5.1 of this report b. 5L019PS004, Specification for Criteria for Piping Design and Installation c. Intertek report "Metallurgical Analysis of Al-Brz Pipe-to-Pipe Welds in the ECW System," AIM 130784455-2Q-7, May 2016.

		Summary or location within this report	References
		• Weld joints CA 614 aluminum bronze pipe material with ERCuAl-A2 filler material;(current practice uses ERCuNiAl for root passes, followed by ERCuAl-A2) • Cast fittings (CA954/CA952) are not installed for buried ECW 30" and 10" piping(extruded/forged elbows/tees used as components) c. Certified Materials Test Reports (CMTR) data was reviewed and compared to tested material properties to validate finding that tested material property values aligned with CMTR data.	
3	Welding process information to ensure that the staff understands the details of how the pipes were prepared prior to welding (e.g.; weld joint and edge peroration/configuration) and how the welds were performed.	Referenced Weld procedure guidance documents outline the weld preparations, fit-up, weld material, and weld process requirements. These documents have specific controls on interpass temperatures to assure proper penetration and minimize adverse weld grain boundary formation due to elevated temperatures vs time.	- MR 540: Welding of Aluminum Bronze ECW Piping System - MR 643: Welding of Aluminum Bronze ECW Piping System - MR 644: Repair Methods for EWC System Underground Welds (65552825) Need Copy) - WPS_P35-T-ArHe Weld Procedure - Estimated Cooling Rates for the Root Pass of Aluminum Bronze Pipe Welds
4	Grouping of weld population: a. Review historical and general information of how the dealloying events have evolved over time and if there is	a-e Details provided in this report include: - Only failures have been identified as welds with backing rings and last occurred in 1994. - No history of non-backing ring weld cracking or dealloying	a. Section 2.1 and 2.2 of this report b. Section 3.2 and 3.3 of this report c. Section 3.1 d. Section 2.0 e. Section 2.0

		Summary or location within this report	References
	a difference in the populations (welds vs. casting). b. Population size of potentially susceptible welds c. Failure analysis reports and root cause evaluations for dealloyed welds d. Number of occurrences of dealloyed components over time, broken into populations of casting and welds e. Number of dealloyed welds that were accompanied by nonstandard/nontypical features (e.g., crack, pit, fabrication defect, fit up defect, weld defect, weld rework)	- Weld failures are bias toward the large diameter pipe (>14-inch) which limits the at-risk weld population.	Additional information: - 1992 RR-ENG-10 - 1992 RR-ENG-10 NRC RAI 7-9-92 - 1992 RR-ENG-10 amended response to NRC - 1992 RR-ENG-10 NRC Response - NOC-AE-11002766 (RAI Supplement - AMR Set 2) Attachment B to Enclosure 1 - NOC-AE-12002853 (Set 16) - Buried Piping Welds Aptech
5	Microstructure and material property information including the following: a. Resolutions and experimental uncertainty of measurement techniques b. References/sources of data used to substantiate positions (e.g., Phase diagrams, Time-temperature-transformation diagrams, continuous cooling	Wrought CA614 pipe is single phase alloy (primary alpha phase with no transformed material) and is immune from dealloying. The susceptibility of the weld metal (ERCuA1-A2) of wrought CA614 pipe are not susceptible to general dealloying beyond the ID due to a more resistant microstructure to dealloying compare to the cast grades (transformed material is dispersed and not a continuous network from weld root to weld crown). The details are discussed in the Intertek report. a. Chemical composition measurements of the welds including uncertainties are discussed in Section 4 of the Intertek report.	a-f: Intertek report "Metallurgical Analysis of Al-Brz Pipe-to-Pipe Welds in the ECW System," AIM 130784455-2Q-7, May 2016. MT-3512A, MT-3512B (Failure Reports)

		Summary or location within this report	References
	transformation diagrams), as applicable c. Key difference between the susceptible microstructure of the cast material and the weld material. d. Key variables/features of the weld material microstructure that impact its degree of susceptibility e. Procedures associated with stereology and/or quantitative metallography being used to determine the special distribution or connectivity of phases, as applicable f. Procedures used to correlate processing parameters, microstructure, and susceptibility (e.g., cooling rates, dilution of weld material), including computer modeling	Weld metal dilution is observed in the as-welded condition such that Al content in the root pass will be lower that the bulk content of the welding wire. This promotes a less susceptible microstructure to dealloying as compared with cast structure b. Phase and time-temperature transformation diagrams and sources are given in Sections 5 and 6 of the Intertek report. c. The key difference between welds and castings is that the welds have a discontinuous network of transformed material and less likely to have gamma-2 phase whereas the castings show a continuous network of transformed material with gamma-2 present. The comparison of the microstructure of welds and castings is given in Section 6 of the Intertek report. d. Weld microstructural constituents were composed primarily of alpha grains with transformed phase forming a semi-continuous or discontinuous network. Formation of gamma-2 in the welds is not likely due to rapid cooling, which is supported by the formation of isolated or semi-continuous transformed phase (likely beta). Aluminum dilution was measured in root pass and resulted in lower volume fraction of transformed phases. All of these features for the weld metal contribute to it being more resistant to general dealloying. Sections 5 and 7 of the Intertek report discuss these findings.	

		Summary or location within this report	References
		A feature of welds that can result in local dealloying are the presence of weld flaws at backing rings Dealloying in welds is local and restricted to the presence of weld flaws. Weld flaws create crevices and aggressive environmental conditions. Dealloying has been observed lateral to the crack face and at the crack tip. e. Standard metallurgical procedures were used to establish the microstructure and phase identification of the weld metal. Light microscopy and scanning microscope were used to characterize the nature and connectivity on 6 weld samples. These samples were removed from actual pipe welds, either removed from the ECW system of created by field mockups using the welding procedures used at the time of construction. EDS was used to identify the composition of the welds and XRD was used to identify the phases within the eutectoid. f. Published time-temperature transformation (TTT) diagrams for Al-Brz were used to determine the nature of the transformed phase as a function of Al content and cooling rate. The Al dilution in the weld metal was measured by EDS. The cooling rate in the first (root) pass was conservatively calculated by finite element heat transfer analysis of the weld root geometry. The combine experimental/measured results and numerical calculations were used in the TTT correlation to conclude that the microstructure resulting from the interactions of the key variables (i.e., Al content, weld geometry, and cooling rate would predict the	

		Summary or location within this report	References
		microstructure that was observed in all 6 sample welds.).	
6	Plant-specific engineering documents that address the magnitude of emergency cooling water system loads (e.g., pressure, deadweight, seismic).	Essential Cooling Water Stress Calculations, and sections 5.0 and 6.0 of this document.	- 5R289MB1006 ECW DBD, - 3L049RS007 ECW Piping Spec, - Essential Cooling Water Pipe Stress Calculations
7	Configuration of buried piping components that supports the position that 360 degree circumferential through-wall cracks will not result in piping segment lateral offset.	30" pipes are buried in trenches excavated in natural clay soils or category 1 backfill. The trenches have a minimum 4 inch thick lean concrete seal mats covering the bottom. Category 1 structural backfill was used to fill the trenches. The centerline of the pipes range from 10 to 18 feet below the ground surface. Each pipe is continuously supported on a concrete cradle with a concrete embedment of 8.5 inches.	- 5Y57-OY10001 Yard-Civil Essential Cooling Water Pipe Installation Details - 5Y57-OY10002 Yard-Civil Essential Cooling Water Pipe Installation-Plan Sections & Details
8	Structural integrity evaluations of welds with postulated or actual flaws.	- Structural integrity evaluations of weld leaks indicate large margins against failure are inherent of in the design and Code flaw acceptance requirements are met - Large leakage can be accommodated without impacting the ability of the ECW system to perform its safety function	- 1992 RR-Eng-10 - AES-C-1630-1 "Bounding Stress Analysis of Buried ECW Piping". - AES-C-1630-2 "Calculation of Critical Bending Stress for Flawed Pipe Welds in the ECW System - AES-C-1964-7 "Leak Rate Analysis for a Circumferential Crack in 10-inch and 30-inch Underground ECW Piping - CREE 12-29261-106 Critical Bending Stress for Above Ground

5.0 WELD SUSCEPTIBILITY: (Intertek report)

The following section provides the material condition and properties that outline the susceptibility of the welded material to experience dealloying due to susceptible phase formation. This information is based on data presented in Enclosure 2 (Intertek Report). The phase formation and geometry of the grain boundaries are dependent on aluminum concentration and cooling rates.

Aluminum Bronze Welds in the ECW system are not susceptible to general through wall dealloying due to basic material properties (Aluminum content) and installation methods (welding processes). The root pass provides the most resistance to dealloying but additional weld passes have resistance as well.

Any welds with pre-existing flaws provide increased susceptibility for flaw propagation. This is due to residual stresses, environmental conditions, and installations with backing rings providing conditions that can lead to crack propagation resulting in through wall weld failure.

The welds with significant flaws have been found, the latest in 1994. There is no evidence of general weld dealloying or weld failures since 1994.

Welds without backing rings have a low probability of failure due to the following reasons:

a. All failures of welds above ground have occurred in welds with backing rings.

b. Field welds without backing rings were routinely subject to an initial volumetric examination, so pre-existing flaws do not exist. Shop welds on larger pipes were assessed at the shop from both sides.

c. ID of weld not subjected to attack by concentrated chemistry due to backing ring to pipe fit up and crevices.

5.1 Material Properties

Table 5 – Material Properties

Property	Wrought Pipe SP-315 CA614	Weld Metal SFA 5.7 ERCuAl-A2	Casting SB-148 CA952	Casting SB-148 CA954
Aluminum	6%-8%	9%-11%		
Yield, 0.5% EUL, (min)	32 ksi	-	25 ksi	30 ksi
Ultimate Strength, (min)	72 ksi	60 ksi *	65 ksi	75 ksi
Elongation,% (min)	30	-	20	12
Brinell, HB	-	130 - 150	110	150

*Actual minimum σ_{UTS} established through purchase requisition requirements (72,000 psi).

Pipe Welded SB-315 CA-614 (6% to 8% Aluminum) Fracture toughness (K_{IC}) ranged from 150 to 200 ksi $\sqrt{in}$. For calculation purposes 120 ksi $\sqrt{in}$ is used. (AES C-1630-2)

5.2 Microstructure

Light microscopy and Scanning Electron Microscope (SEM) examinations were performed on areas of interest to identify the microstructure and constituents within the transformed phase.
X-ray diffraction (XRD) was used for phase identification.

- Microstructural constituents in welds consisted of primary alpha grains with transformed phase forming a semi-continuous or discontinuous network.
- Aluminum dilution was measured in root pass.
  - Lower volume fraction of transformed phase.
  - Transformed phase showed discontinuous morphology.
- Localized dealloying was observed in weld region near a crevice. Dealloying restricted to the transformed phase in the region adjacent to the crevice at the weld.
- Unlike cast Al-Brz, the transformed phase is segregated and not continuous. A continuous network from the weld root to crown was not observed.
- The weld metal, specifically the root pass, shows a more resistant microstructure to dealloying.
- Formation of gamma 2 in the welds is not likely due to rapid cooling.
- Local dealloying at wetted crevices, if it occurs, is expected to be contained and non-propagating
- The welds are less susceptible to general dealloying than the castings due to the significantly different microstructures (isolated and lesser volume fractions of the transformed phase in the weld metal)

5.3 Chemical Analysis

Surface scans using Scanning Electron Microscope (SEM) configured with an Energy Dispersive X-ray Spectroscopy (EDS) were completed on three field-fabricated Al-Brz pipe welds to determine the chemical composition and distribution of Al and Fe in the weldment.

CMTR data on as-installed pipe and welds were reviewed and used to benchmark observations and show reasonable assurance the results were representative to the total population of welds.

Statistical analysis of the Al and Fe content was performed on a sample of CA614 pipe. The data included approximately 20 supplied heat lots. The variability in the Al and Fe compositions were within specification with little scatter and easily represented by Table 6 and falls within a normal distribution curve.

Table 6 - Calculated Statistical Parameters for Supplied Material (CMTR DATA)

Parameter	Base Pipe		Weld Wire	
	Aluminum (Al)	Iron (Fe)	Aluminum (Al)	Iron (Fe)
Mean, μ (Wt%)	6.81	2.47	9.48	0.907
Standard Deviation, σ (Wt%)	0.291	0.213	0.106	0.0790
Min/Max, (Wt%)	6.26/7.60	2.15/2.94	9.24/9.82	0.69/1.1
Lower 5th Percentile, (Wt%)	6.33	2.12	9.30	0.78
Upper 95th Percentile, (Wt%)	7.29	2.82	9.65	1.04
Specification Range, (Wt%)	6 .0- 8.0	1.5 – 3.5	8.5 – 11.0	0.5 - 1.5
Number of Heats	20		63	

The following is a summary of the surface measurements for weld metal chemistry in as-deposited condition:

1) Weld metal dilution of Al is observed resulting from the melting process involving the higher Al weld metal with the lower Al content of the wrought pipe.
2) Weld root pass shows more dilution in Al content than the subsequent filler passes (less weld metal deposited in the root pass). Al content varies roughly linearly from the root pass to the crown.
3) Fe content in the weld increases due to higher Fe present in the base pipe. Fe level is also observed to vary systematically from the root to the crown.
4) EDS results for the root pass indicates the Al content is less than ~9 wt% at the weld inside surface.

The composition of the weld metal in the root pass, having generally lower Al content, will contribute to a less susceptible microstructure for dealloying.

5.4 Cooling rates of weld process

Estimated cooling rates were calculated for the root pass weld in Al-Brz pipe welds (30 inch and 10 inch sizes) to estimate the character of the microstructure at the weld root when comparing a cooling rate to the time/temperature/transition diagram on Al-Brz.

A Finite Element Analysis was developed to estimate the cooling rate during solidification which was used to predict the character of the microstructure at the weld root from the cooling rate and the time/temperature/ transformation curves show discontinuous grain structure (AIM-13078445-2Q-7 Appendix A "Weld Root Pass Cooling Rate). This study concluded:

- The cooling rate was relatively fast: time to go from 900°C to 400°C (1650°F to 750°F) was on the order of 0.6 minutes.

- The transformed phase in the weld root consists of alpha & beta (α + β). Gamma$_2$ (γ_2) does not have time to form even for high Al content (~9.5 wt%)

The cooling rates for Al-Brz pipe welds will be much faster than the normal cooling rates expected for the cast components. The faster cooling rate of the weld, especially the root pass, will not promote conditions to form continuous transformed phase of (alpha and beta).

These results support the microstructure observations of examined welds.

5.5 Weld Comparisions

A semi-continuous network of transformed phase is observed in the welds at the root and crown. Semi-continuous morphology is characterized by lack of long range connectivity of the transformed phase. Locally the transformed phase may be connected but a long range continuous network is disrupted by alpha rich regions that formed at previous beta grain boundaries. Furthermore, networks of alpha phase boundaries are observed between filler passes in the multi-pass welds. The semi-continuous morphology is most prevalent in the filler and crown passes of the pipe welds. Typical transformed phase volume fractions are between 10% and 23% at the root of the weld or 6% and 32% at the crown. Under some conditions or rapid cooling and low aluminum content, the volume fraction of the transformed phase is discontinuous and discrete. Discontinuous transformed phase is present in volume fractions ranging from 5% to 22%. Continuous networks of transformed phase were not evident in the multi-pass welds.

Although conclusive phase identification was not possible due to measurement uncertainties, the XRD pattern revealed qualitative structural differences between the casting and weld samples.

The morphology of the welds shows stark contrast to the casting morphology. A continuous and long range network of transformed phase is observed in both casting alloys (CA952 and CA954). Volume fraction measurements for CA952 determined that 10% of the material consists of transformed phase and iron rich precipitates. Microstructure morphology and phase composition for CA952 shows isolated alpha phase surrounded by transformed phase and the volume fraction was measured at 41% therefore, the alloy shows the highest susceptibility to dealloying.

6.0 LEAKAGE RATE ANALYSIS AND STRUCTURAL INTEGRITY:

6.1 Above Ground Leak Rate Analysis

Engineering Calculation 14-EW-003 "Flood and Leak Rate Analysis for a Circumferential Crack in Above Ground ECW Piping" was developed to evaluate the leakage rate behavior of through wall leakage in the ECW system. The purpose of this calculation was to determine the crack lengths for various above ground component/pipe sizes that would produce leak rates equivalent to one-half the design basis internal flooding level for the Mechanical Auxiliary Building (MAB), Essential Cooling Water Intake Structure (ECWIS), and the Diesel Generator Building (DGB). In addition, this calculation determined the leak rate safety factors available should the pipe develop leakages without adversely impacting intended design basis functions of the safety related equipment.

The Appendix 9A to STPEGS UFSAR discusses the potential effects of through-wall cracks in the Essential Cooling Water System (ECWS) piping. The leaks are considered non-conforming to the ASME Code, Section XI Code compliance (i.e. temporary non-code condition requiring operability evaluations).

STP has administrative leakage limits of 8 GPM, 0.3375 GPM, and 2.3 GPM for the Mechanical Auxiliary Building (MAB), Standby Diesel Generator Building (SBDG), and the Essential Cooling Water Intake Structure (ECWIS) respectively. Therefore, the maximum total leakage at any time is controlled at approximately 10.5 GPM assuming each of the supplied buildings has at least one actively leaking component. The below evaluation tables (Tables 7 and 8) "Flow requirements for the supplied safety related equipment and Unit 1 Train A (Typical)" and "Summary of Acceptable Leak Rates and Critical Crack Sizes" are from Attachment E of NOC-AE-14003135/ML14224A151 "Request for additional Information-Set 26".

Table 7 - Flow requirements for the supplied safety related equipment. Unit 1 Train A (Typical)

Safety-Related Equipment	TAG/TPNS [1]	Design Specified Flow Requirement GPM[3]	ECW piping Flow Capacity To Equipment Inlet GPM	Flow Safety factor (Flow Capacity – Flow Requirement)	Comments
Standby Diesel Generator Inter-coolers	3Q151MDG0134	560 GPM	572 GPM 6"EW1125WT3 @ 6.35 Ft per Second (FPS)	12 GPM	Total ECW flow requirement 1350 GPM @ 70' TDH 10"EW1106WT3

Safety-Related Equipment	TAG/TPNS [1]	Design Specified Flow Requirement GPM[3]	ECW piping Flow Capacity To Equipment Inlet GPM	Flow Safety factor (Flow Capacity – Flow Requirement)	Comments
Standby Diesel Generator Auxiliary Equipment Skid Coolers	3Q151MSA0134	628 GPM for Jacket Water Cooler 298 GPM for Lube Oil Cooler	628 GPM 6"EW1127WT3 @6.97 FPS 298 GPM 4"EW1129WT3 @ 7.51 FPS	0 GPM[4] 0 GPM[4]	CAPABLE SUPPLYING 1,498 GPM
Essential HVAC Chillers (300 Ton)	3V111VCH004	1,100 GPM	1,100 GPM @ 7.05 FPS	0 GPM[4]	Tube Side HX
Component Cooling Water Heat Exchanger	3R201NHX101A	15,000 GPM	15,000 GPM 30"EW1102WT3 @ 7.04 FPS	0 GPM[4]	Tube Side of HX
Component Cooling Water Pump Supplementary Coolers	3V101VAH001	36 GPM[2] 40 to 50 GPM per procedure 0POP02-EW-0001	75 GPM 3"EW1113WT3 @7.17 FPS	39 GPM per Design 25 GPM per procedure 0POP02-EW-0001	Tube Side HX

(1) All TAG TPNS numbers are referenced from Piping and Instrumentation Diagram (P&ID) Drawing 5R289F05038, Sht. 1, Rev. 15.
(2) Specification for Safety Class Air Handling Units 3V259VS0005 for the HL&P STPEGS, Page 19, Item C7 for CCW Pumps. Note that normal operating procedure (0POP02-EW-0001, Rev. 67, page 37 of 67), requires operation to set initial flow 40 to 50 GPM
(3) Design Flows are referenced from respective DBD and/or from respective equipment specification documents.
(4) The network flow analysis suggests potential leakages could impact Standby Diesel Generator Auxiliary equipment (Jacket water and lube oil cooler) in the SBDG building, and the Essential HVAC Chiller (300T) and CCWHX in the MAB because estimated flow requirements equals flow capacity (Flow Capacity – Flow requirement = 0 GPM).

Table 8 - Summary of Acceptable Leak Rates and Critical Crack Sizes[1]

Building ID	Administrative Limits[2]	Flooding Limits	Leak Rates through Crack GPM (Dealloyed Material)	Crack Size (inches) Limiting to Leakage Rate below Administrative Limit (Dealloyed material)	Pipe Size Evaluated Diameter in Inches
Mechanical Auxiliary Building	8 GPM over 7 days	8 GPM over 15 days	8 GPM over 7 days	7.9 Inch 6.4 Inch 7.24 inch 8.1 Inch 7.72 Inch 6.0 Inch	30 14 10 8 6 3
Stand-By-Diesel Generator Building	0.3375 GPM over 7 days	0.1575 GPM over 30 days	0.3375 GPM over 7 days	3.1239 Inch	8
ECW Intake Structure	2.3 GPM over 7 days	545 GPM over 1.44 hours	2.3 GPM over 7 days	3.018 Inch	24

(1) These crack sizes are not intended to demonstrate structural integrity of the component and shall not be used for that purpose. It is to be used for estimating safety factor available for the observed leakage rate to potential leak rate through the crack size. (For example, 6" long crack is required to attain leak rate of 8 gpm for a 3 inch pipe. The critical crack size at which pipe may collapse is also approximately 6", therefore, to secure a safety factor of 2 one must not allow physical crack longer than 3 inches.)
Flooding and Administrative limits are defined in:
- NC-9703, Rev. 2, Flooding Calculation, Mechanical Auxiliary Building.
- CC-5038, Rev. 0, Leakage through Knockout Panels
- MC-5216, Rev. 2, Flooding Calculation, Essential Cooling Water Intake Structure
- CN-3091: UFSAR Appendix 9A – Assessment of Potential Effects of Through Wall Cracks in ECWS Piping

(2) Thirty days is assumed to restore make-up capability to the EC Pond after Design Basis Accident, while 7 days is assumed as sufficient time required establishing temporary pump facility to drain leakages out of MAB, ECWIS, and DGB buildings. Administrative limits are determined to maintain safety factors greater than 2 to flood limit.

Conclusion: The allowed loss of essential cooling water supply to the safety related equipment has adequate flow margins assuring the design bases functions are met. Also the leakage rate and crack lengths will be monitored further assuring structural integrity of the ECWS components.

6.2 Below Ground Leak Rate Analysis

AES-C-1964-7 "Leak Rate Analysis for a Circumferential Crack in 10-inch and 30-inch Underground ECW Piping" Since above ground pipe welds had experienced through wall cracking and leakage due to service induced degradation associated with localized dealloying of the weld metal at backing rings. Stress analysis and structural integrity evaluations were performed showing the cracked pipe welds maintain adequate margins for design conditions prior to discovery of leakage. Leakage flaw lengths for 10 and 20 gallon per minute were compared with the critical flaw lengths for upset and faulted conditions to establish the available leakage margins for buried piping. This calculation utilized AES-C-1630-1 "Bounding Stress Analysis of Buried ECW Piping", and calculated the bounding stresses in the buried ECW piping and AES-C-1630-2 "Calculation of Critical Bending Stress for Flawed Pipe Welds in the ECW System", performed the fracture mechanics analysis in order to determine the critical bending stress for a circumferential through wall crack. NOC-AE-11002766/ ML11354A087 (Request for Additional Information Supplement - AMR Set 2), December 8, 2011, address clarifying questions related to calculation methodology.

The below tables (Table 9 and 10) provide a summary of the below ground leakage margins for both upset and faulted loads.

Table 9 - Summary of Leakage Margins for Upset Loads

Leak Rate	Pipe Size	Line	Critical Length (in)	Leakage Length (in)	Leakage Margin for Upset Loads
10GPM	10 inch	Supply	21.4	11.8	1.81
		Discharge	21.4	13.8	1.55
	30 inch	Supply	32.6	14.9	2.19
		Discharge	32.6	21.2	1.54
20GPM	10 inch	Supply	21.4	13.9	1.54
		Discharge	21.4	16.3	1.31
	30 inch	Supply	32.6	18.7	1.74
		Discharge	32.6	26.7	1.22

Table 10 - Summary of Leakage Margins for Faulted Loads

Leak Rate	Pipe Size	Line	Critical Length (in)	Leakage Length (in)	Leakage Margin for Faulted Loads
10GPM	10 inch	Supply	20.4	11.4	1.76
		Discharge	20.4	13.5	1.51
	30 inch	Supply	30.1	14.9	2.02
		Discharge	30.1	21.2	1.42
20GPM	10 inch	Supply	20.4	13.5	1.51
		Discharge	20.4	15.8	1.29
	30 inch	Supply	30.1	18.7	1.61
		Discharge	30.1	26.7	1.13

6.3 Above Ground Structural Integrity Analysis

Above ground Structural Integrity Analysis CREE 12-29261-106 provides an evaluation addressing the adequacy of ECW pipe weld structural integrity (with stress margins, if applicable) based on the above ground critical crack sizes previously determined for meeting the administrative leak rate limits (Calculation 14-EW-003, Rev. 0. This includes nominal pipe size of 30", 24", 14", 10", 8", 6", and 3." The weld structural integrity evaluation was performed using the maximum un-intensified bending stresses calculated based on the "Stress Summary for Large Bore ECW Piping 2.5" above," Table A-3 of Calculation RC09890, Rev. 1.

The following Table 11 summarizes the acceptance of structural integrity for the administrative leak rate critical circumferential crack size for the listed above ground flawed pipe welds. Margin of Safety is calculated based on Maximum Un-Intensified Bending Stress and Governing Critical Bending Stress as shown in the footnote of the table.

Table 11 - Acceptance of structural integrity for administrative leak rate critical circumferential crack size

Nominal Pipe Size (in)	Critical Crack Size (Per Administrative Leak Rate Limit) (in)	Maximum Un-Intensified Bending Stress (ksi)	Governing Critical Bending Stress (ksi)	Critical Bending Stress Governing Process	Structural Integrity Acceptable per Specified Critical Crack Size? (Y/N)	Margin of Safety
30	7.9	15.049	22.86	LEFM	Y	34%
24	3.018	13.69	48.692	LEFM	Y	72%
14	6.4	11.179	24.93	LEFM	Y	55%
10	7.24	15.068	22.276	LEFM	Y	32%
8	8.1	15.08	18.076	LEFM	Y	17%
6	7.72	15.459	16.402	LEFM	Y	6%
4	1.699	5.352	45.494	Limit Load	Y	88%
3	6	2.613	8.412	Limit Load	Y	69%

Margin of Safety = 1 – (Maximum Un-intensified Bending Stress/ Governing Critical Bending Stress

LEFM – Linear Elastic Fracture Mechanics

6.4 Below ground Structural Integrity Analysis

Leak detection is used to support identification of through-wall weld flaws in buried piping before pipe integrity is challenged. For the buried portions of the ECW piping, the minimum leak rate detectable at the surface is 10 gpm. The purpose of the discussion is to present the information from the background documents regarding the bounding underground pipe stresses, calculated allowable through-wall (TW) flaw sizes, and leak rate evaluation that shows the ASME Section XI pipe flaw acceptance criteria will be satisfied at the time of leak detection.

Below ground piping was design by Bechtel and includes 10-inch and 30-inch straight pipe assemblies, 10-inch and 30-inch elbows, and 30x30x10-inch tees ("Stress Calculation/EW Piping Analysis," Document RC-6600) Forces and moments calculated by Bechtel were used to calculate the code stresses (Code Equations 8, 9B, 9D, and 10).

The highest enveloping (bounding) stresses for the underground piping were developed from the review of the Bechtel Calculation RC6600. The bounding stresses for each code equation were identified and the unconcentrated stresses with the SIF factor removed were used in calculating the allowable flaw sizes per ASME Section XI Appendix H procedures.

The results of the allowable flaw lengths under faulted conditions with the TW flaw lengths calculated to give a leak rate of 10 gpm are compared in Table 12. The allowable flaw lengths exceed the leak lengths for detection under the conservative condition of maximum operating internal pressure.

Table 12 - Summary of Leakage Rates and Margins for Faulted Loads

Size	Line	Weld	Allowable Length L_{Allow}, (in.)	Leak Length L_{Leak}, (in.)	Ratio L_{allow}/L_{leak}
10-inch	Intake	Pipe	21.0	11.8	1.78
		Elbow			
		Tee	18.3		1.55
	Discharge	Pipe	21.0	13.8	1.52
		Elbow			
		Tee	18.3		1.33
30-inch	Intake	Pipe	35.5	14.9	2.38
		Elbow	24.3	<14.9	>1.63
		Tee	17.3	14.9	1.16
	Discharge	Pipe	34.1	21.2	1.81
		Elbow	24.3	<21.2	>1.15
		Tee	21.5*	21.2	1.01

*Note: The pressure for the 30-inch discharge-side tee is assumed to be the normal internal operating pressure of 20 psig. Also even with a large leak on the discharge-side, the ECW system will perform its design function since the intake side of the system will maintain integrity due to the larger leak rate margin.

In summary, the above results indicate there are margins on leak detection over and above the flaw acceptance requirements in ASME Section XI. Given the conservative assumptions in both the structural and the leak rate analyses, namely,

1) Bounding (enveloping) bending stresses for all loading conditions were used in the calculation of allowable TW flaw size,
2) Use of lower bound fracture toughness for the weld metal in the fracture analysis in a linear elastic fracture mechanics assessment is conservative,
3) Max operating pressure is used in the determination of allowable flaw size, where the normal operating pressure is used in the leak rate analysis, and
4) The assumptions are stacked to give a worst case condition in each of the calculations (i.e., allowable flaw size and leak rate).

7.0 STP MANAGEMENT OF SUSCEPTIBLE CAST COMPONENTS, ROOT VALVES WITH ADAPTOR SOCKET WELDS, and EXTRUDED TEES WITH WELD REPAIRS

There are three categories of components susceptible to dealloying. They are the Cast components constructed of CA952 and CA954, aluminum bronze adaptor socket welds where the ERCuAl-A2 material shop weld is experiencing dealloying, and Extruded Tees with susceptible weld repairs.

7.1 Aluminum bronze castings susceptible to selective leaching

Aluminum bronze castings susceptible to selective leaching, including attachment welds related to the castings will be replaced prior to the period of extended operation with material that is not susceptible to selective leaching (enclosure 1 to NOC-AE-14003135/ ML14224A151, July 31, 2014 provides a tabulated list of the quantity and sizes of the susceptible cast components and root valve socket adapter welds). An updated listing reflecting the current population and scope is provided below in Tables 13 and 14:

Table 13 - Unit 1 List of the susceptible components, broken down by size

Size	Unit 1 Cast Flange	Unit 1 Cast Tee	Unit 1 Cast Pump Casing	Unit 1 Cast Booster Pump Casing	Unit 1 Cast Valve	Total Unit 1 Casts	Unit 1 Root Valve Socket Adapter1	Unit 1 Ext Tee [2]
½							28	
1								
3	25			3	18	46		
4	15				12	27		
6	31	2			12	45		
8	33				10	43		
10	11				6	17		
14					3	3		
24					3	3		
30			3		12	15		
6x6		2				2		
10X4		3				3		
10X6		6				6		
14X10								1
30X4								1
30X10								5
30X14								3
30X24								2
	115	13	3	3	76	**210**	**28**	**12**

[1] One inch manual valves with susceptible 1 to ½ inch socket adaptor welds not included in total weld number

[2] Extruded Tees susceptible to plug dealloying at the weld repairs

Table 14 - Unit 2 List of the susceptible components, broken down by size

Size	Unit 2 Cast Flange	Unit 2 Cast Tee	Unit 2 Cast reducer	Unit 2 Cast Pump Casing	Unit 2 Cast Booster Pump Casing	Unit 2 Cast Elbow	Unit 2 Cast Cap	Unit 2 Cast Valve	Total Unit 2 Casts	Unit 2 Root Valve Socket Adapter[1]	Unit 2 Extruded Tee[2]
½										17	
1											
3	38				3	1		18	60		
4	34							10	44		
6	31	1						13	45		
8	24							10	34		
10	6						1	6	13		
14								3	3		
24								3	3		
30				3				12	15		
6x6		1							1		
10X4		3	1						4		
10X6		4							4		
10x10		1							1		
14X10											1
30X4											2
30X10											2
30X14											0
30X24											3
	133	10	1	3	3	1	1	75	**227**	**17**	**8**

[1] One inch manual valves with susceptible 1 inch to ½ inch socket adaptor welds not included in total weld number

[2] Extruded Tees susceptible to plug dealloying at the weld repairs

7.1.1 Discussion:

Selective leaching is monitored through external visual observation of evidence of inside diameter to outside diameter (ID-OD) leakage due to dealloying. Calculation RC-9890, "Stress Summary for Large Bore ECW Piping" was initially issued in June of 1989 and it revisited the stress calculations for ECW piping using reduced allowable material properties and demonstrated the acceptability of the entire system, including the underground portion.

7.2 Aluminum bronze root valves with adapter socket welds

Aluminum bronze root valves with adapter socket welds will be replaced prior to the period of extended operation with material that is not susceptible to selective leaching (enclosure 1 to NOC-AE-14003135/ML14224A151, July 31, 2014 provides a tabulated list of the quantity and sizes of the susceptible cast components and root valve socket adapter welds).

7.2.1 Discussion:

Aluminum bronze root valves with adapter socket welds have experienced dealloying at the shop socket weld. Material Technology Division of Houston Lighting & Power Company performed a failure analysis documented in Lab Report MT 5368, December 1, 1994. The report concluded the leaks were the result of dealloying of the weld metal in the socket weld made in the shop and dealloying was confined to the heat affected zone between the field weld and the shop weld, where the morphology of the weld phase was changed when the pipe to adaptor field weld was made.

In 2016 STP performed analysis on another leaking root valve (1-EW-0283) with adapter socket weld. AES-13078445-2Q-5)Bronze Removed from the Essential Cooling Water System (Phase 3)", testing and analysis demonstrated the required flaw acceptance margins of 2.77 for service level B and 1.39 for Service Level D we exceeded.

Microstructure examination of the dealloyed section of the shop weld showed crevice between the weld metal and fitting and low heat input resulting in no dilution of the weld region. Other locations observed at root of the shop weld had higher heat input, better fusion and dealloying did not propagate through the root. Microstructure examination of the field weld showed dealloyed section of the shop weld showed higher heat input, better fusion and dealloying did not propagate through the root. There was no obvious interaction between the field weld and the shop weld.

7.3 Extruded piping tees with aluminum bronze weld repairs

Extruded piping tees with aluminum bronze weld repairs, where the repair size is be replaced prior to the period of extended operation.

Below (Table 15) is a listing of extruded tees with repairs and the description of the flaws:

Table 15 - Extruded Tees with repair welds

Train	Building	Tee	Size	Function	Record of Non-conforming (RoN) Remarks	MT-4701 Finding
1B	ECWIS	T7002	30x30x24	Strainer Bypass	Cracked on both sides of throat	None
1C	ECWIS	T7038	30x30x24	Strainer Bypass	Cracked on one side of the throat	None
1B	Yard (UG)	T7047	30x30x10	DG Supply	Four ½-inch long cracks but the extrusion was about ½-inch long	None

Train	Building	Tee	Size	Function	Record of Non-conforming (RoN) Remarks	MT-4701 Finding
1C	Yard (UG)	T7040	30x30x10	DG Supply	Extrusion outlet was 1/8 inch short and thickness was 0.160 inch vs. min wall 0.319 inch Pup piece welded to 10-inch outlet and weld buildup for min wall	None
1A	MAB	T4012	30x30x14	Chiller Supply	RoN is 4 inch deep split on one side and 8 inch deep split on other side	None
1A	MAB	T4011	30x30x10	Chiller Return	2 inch deep cracks both throat sides	None
1B	MAB	T4013	30x30x14	Chiller Supply	RoN 911 for more tears as extrusion continued RoN 903 two 3/4 inch long splits	6.5" (from 135° to 190°) 3" long and 7.5" (from 330° to 030°) 2 7/8" long
1B	MAB	T7025	30x30x4	Supplemental Cooler Supply	Cracked on both throat sides	
1B	MAB	T4010	30x30x10	Chiller Return	splits at the outlet extend about 4 inches	3 3/8" (from 150° to 190°) 2" long and 4" (from 337° to 023°) 2" long
1C	MAB	T4014	30x30x14	Chiller Supply	None	None
1C	MAB	T4009	30x30x10	Chiller Return	Split 2.5 inches down and 10 inches long	12.25" (from 215° to 355°) 2" long, 7/8" (from 175° to 185°) 2.5" long, and 3/4" (from 005° to 014°) 2" long
1C	MAB	T4008	14x14x10	Chiller X-Conn	Two splits on each side of throat	
2A	ECWIS	T7041	30x30x24	Strainer Bypass	cracks on both sides in an area 12 inches long and 1.5 inches down	Weld repair not identified
2B	ECWIS	T7048	30x30x24	Strainer Bypass	cracked on one side of throat, RoN 606 short on one end	Weld repair not identified
2C	ECWIS	T7037	30x30x24	Strainer Bypass	split open at throat about 1 inch	None

Train	Building	Tee	Size	Function	Record of Non-conforming (RoN) Remarks	MT-4701 Finding
2A	Yard (UG)	T7017	30x30x10	DG Supply	cracked on one side of throat	None
2C	Yard (UG)	T7008	30x30x10	DG Supply	cracked on one side of throat	None
2A	MAB	T7033	30x30x4	Supplemental Cooler Supply	cracked on both sides of the throat	None
2A	MAB	T4007	14x14x10	Chiller cross-connect	several splits on each side of the outlet (Tee from SW Fab as spare RIP 10860)	None

7.3.1 Discussion:

Station Problem Report (SPR) 92-0742 identified a through-wall indication in the 14-inch branch part of the tee just at the field weld. HL&P lab report MT-4102 (HSHS-22420) concluded the leak resulted from de-alloying in repair weld metal contained within the tee. HL&P later performed onsite evaluations of five tees to help determine extent of condition (lab report MT-4701).

Action 11 of SPR 92-0742 completed a random sampling of 5 repaired tees and examined the repaired locations. The repair lengths ranged from 0 to 12.25 inches and from 0% to 38% of the circumference. The action concluded structural Integrity would be maintained in all repaired tees assuming the worst case repair size.

In July 2000, a similar through-wall indication was discovered in the 30x30x14 tee supplying Chiller 11A/12A (CR 00-12050).

Code data packages for spools with tees larger than 10x10x10 were reviewed to identify the scope of extruded tees with significant weld repairs. Southwest fabricating documented major repairs (when the cavity exceeds the lesser of 3/8-inch or 10% of the section thickness) with a report of nonconformance. The preceding table details the results of this review and summarizes extruded tees with major repairs and southwest fabricating reports of nonconformance.

The extruded tees are manufactured from CA-614 aluminum bronze material resulting in the only potential susceptibility to dealloying is the weld repair regions.

Walkdowns of the above ground ECW piping system is performed every six months and is effective in the early detection of any through wall weepage from the tee weld repaired areas.

The repaired areas of the below ground repaired tees are less than the most limiting calculated Allowable Length (L_{Allow}, (in.)) of 17.3 inches discussed in section 6.4 and Table 10 - Summary of Leakage Rates and Margins for Faulted Loads.

Enclosure 2
Intertek Report

Intertek

AIM 13078445-2Q-7
Controlled Document I-16
May 2016
Revision 0

Metallurgical Analysis of Aluminum-Bronze Pipe-to-Pipe Welds in the Essential Cooling Water System

Prepared By

Rita Kirchhofer
Henry Vaillancourt
Russell C. Cipolla

Intertek AIM
3510 Bassett Street
Santa Clara, California 95054

Prepared For

South Texas Project Electric Generating Station
FM 521 Approximately 8 Miles West of Wadsworth
Wadsworth, TX 77483

Attention: Mr. Arden Aldridge

VERIFICATION RECORD SHEET

Report No.: AIM 13078445-2Q-7 Rev.: 0 Date: May 2016
Report Title: "Metallurgical Analysis of Aluminum-Bronze Pipe-to-Pipe Welds in the Essential Cooling Water System"

Originated By:		Project Engineer	5/23/2016 Date
Verified By::		Verifier	23 MAY 2016 Date
Approved By:		Project Manager	5/23/2016 Date
QA Approved By:		QA Manager	5/23/2016 Date

TABLE OF CONTENTS

EXECUTIVE SUMMARY

Dealloying of aluminum-bronze (Al-Brz) is an active degradation mechanism in selected large-bore castings in the essential cooling water system (ECW) at the South Texas Project Electric Generating Station (STP). Dealloying is a corrosion process where the aluminum in the transformed phase, beta (β) and gamma-2 ($\gamma 2$) can selectively leach out under certain conditions at wetted surfaces. This process leaves micro-voids in the microstructure along the grain boundaries. Leakage (weepage) will occur once dealloying has extended through the wall thickness via a continuous grain boundary network that has fully dealloyed.

Unlike cast components, the pipe welds (joining of wrought piping) have not exhibited general dealloying in either the base material or in the weld metal. A detailed metallurgical evaluation and analytical assessment of the welding process has been completed to establish a fundamental understanding of the resistance of the pipe welds to dealloying that explains the better performance of the welds versus the castings as demonstrated by the operating experience at STP.

The investigation, which included chemistry measurements within the weldment, calculations for the cooling rate during the time of phase formation, and comparative study of the weld and casting microstructures, concluded that the pipe-to-pipe welds are less susceptible to general dealloying than the castings. This was contributed to the significantly different microstructures owing to the different thermal conditions and alloy content during solidification. The transformed phases in the weld are isolated and exhibit smaller volume fractions of the eutectoid compared with the more susceptible castings. The castings, due to the much slower cooling rate during fabrication, form a continuous network of transformed material containing the more susceptible $\beta + \gamma 2$ phases, which has a greater propensity to dealloy in service and to form a leakage path through the wall. Formation of $\gamma 2$ in the welds is not likely due to rapid cooling during phase transformation.

Therefore, dealloying through the pressure boundary is not expected in the pipe-to-pipe welds. Local dealloying at wetted crevices, if it occurs, is expected to be contained within the dendrites and non-propagating

Section 1
INTRODUCTION

Dealloying of aluminum-bronze (Al-Brz) is an active degradation mechanism in selected large-bore castings in the essential cooling water system (ECW) at the South Texas Project Electric Generating Station (STP). Dealloying is a corrosion process where the aluminum in the transformed phase, beta (β) and gamma-2 (γ_2) can selectively leach out under certain conditions at wetted surfaces. This process leaves micro-voids in the microstructure within the eutectoid. Leakage (weepage) will occur once dealloying has extended through the wall thickness via a network of porous transformed phase. The dealloying process causes a reduction in mechanical strength and toughness properties.

Unlike cast components, the pipe welds (joining of wrought piping or fittings) have not exhibited general dealloying in either the base material or in the weldment. Early through-wall leaks in piping in the mid 1990s were observed in welded connections (Ref. 1). These early leaking failures were attributed to:

1) Use of backing rings in large diameter pipe to improve fit-up during field installation.
2) The presence of large weld fabrication flaws (i.e., lack of penetration/fusion) that were near through-wall at the start of service
3) The existence of a deep crevice due to these fabrication flaws to promote a corrosive environment beyond the root pass. In some cases, the initial fabrication flaw was beyond the mid-wall of the pipe weld.
4) Localized dealloying at the deepest flaw location causing the flaw to propagate through the wall by repetitive action of fracture of the dealloyed region to expose new Al-Brz weld metal, followed by initiation of dealloying within the crevice to further extend the flaw.

There have not been any pipe weld failures due to this local dealloying process since these early occurrences. This service experience is consistent with original construction flaws that propagate to a leaking condition early in service life.

Metallurgical evaluation and chemical composition analyses have been performed on exemplar pipe-to-pipe welds. The objective of this investigation is to obtain a fundamental understanding of the physical structure of the pipe welds and determine why the welds are less susceptible to general dealloying compared with the service history observed in the large bore castings. The important attributes to susceptibility to dealloying, namely the aluminum and iron content in the alloy, cooling rates during the solidification process, and the resulting microstructural differences between weldments and the cast products were studied and evaluated. The amount (volume fraction) and nature (continuous or not continuous network) of the transformed phases within the overall microstructure are dependent on these attributes which directly relate to the susceptibility of Al-Brz to dealloying corrosion.

This report describes the chemical composition and microstructure evaluation of field welds performed on pre-service weld conditions. Samples of field welds were obtained from original field fabricated pipe welds or from field mockups made in the mid-1980s. Surface chemistry analyses were performed with Scanning Electron Microscope (SEM) configured with an Energy Dispersive X-ray Spectroscopy (EDS) unit to conduct semi-quantitative measurements on 10-inch and 30-inch pipe weld cross-sections (without backing rings). In addition, a 3-inch pipe-to-flange weld (with backing ring) that was removed from service was sectioned and analyzed for chemical composition and microstructural variation across the weld for comparison with the large bore pipe welds.

Section 2
SAMPLE MATERIALS

2.1 TEST MATERIAL

Aluminum-bronze welded piping material was obtained from specimen material used in a fracture toughness testing program performed in 1983 (Ref. 2). This testing program was in support in the utility commitment to re-examine all Brown & Root field welds (100% RT and 100% PT) and to repair or replace welds as required. The specimens were full-thickness bend bars for measuring fracture toughness using the crack-tip opening displacement (CTOD) test method. The specimens were fabricated from welded pipe where coupons were removed by machining axial full-thickness strips from the pipe that contains the complete weld and segments from both mating pipe segments.

Figure 2-1 shows the testing material and CTOD specimens available from that effort for testing in this investigation. The specimens included 6-inch, 10-inch, and 30-inch pipe-to-pipe welds from field mockups, and original 30-inch field welds that were removed during the repair effort. These welds were all generated prior to service and used the same field welding procedures at the time of construction. Therefore, these specimens are exemplar samples of the field welding practice and represent original weld pre-service conditions (without backing rings).

In addition to these samples, a 3-inch flange-to-pipe weld was included in the investigation. The flange is a casting component (SB-148 CA952). This weld, which contains a backing ring, had been removed from service after ~26 years of operation and used in the analysis confirmation testing (ACT) evaluation (Ref. 3) and dealloying profile examination (PE) studies (Ref. 4). This sample was selected to provide a weld with a backing ring and that has seen ECW environment for comparison with the pipe-to-pipe welds.

The chemical composition specification of the pipe and weld metal is given in Table 2-1 (Refs. 5 and 6). The pipe is wrought Al-Brz, Grade CA614. The weld wire was supplied to SFA 5.7 ERCuAl-A2. For comparison, the chemical composition for the castings used in the ECW

system is also given Table 2-1 (Ref. 7). The CA954 alloy has a higher aluminum content and lower copper content than CA952.

2.2 SAMPLES EVALUATED

Chemical composition and microstructural evaluations performed on selected material samples are described in various sections in this report. A listing of the samples and source references is given in Table 2-2.

Chemical analysis and characterization of the microstructure were achieved by various test methods. The surface chemical analysis was performed with a scanning electron microscope (SEM). The measurement of the surface composition was obtained by the Energy Dispersive X-ray Spectroscopy (EDS) method. The EDS unit is contained within the SEM and designed to identify surface elements at precise locations on the test sample. The X-ray diffraction (XRD) test method was used for partial phase identification, mainly to identify the phases within the eutectoid (β and γ_2). This method was used on Sample 1 and CA954 cast material removed from a 4-inch valve (Ref. 8).

2.3 SUPPLIED MATERIAL

The certified material test reports and other procurement and service history information were provided by STP for the pipe and weld material supplied to the plant (Refs. 9 and 10). This information was reviewed to determine how well the test specimen chemistries represented the population of the material heats for pipe and weld metal that were used during construction. In particular, the variability of the supplied material in terms of Al and Fe content was quantified by a statistical analysis of the available CMTR data.

Data on 20 heats of pipe material were obtained as a sample of the pipe population chemistries. This is a reasonably large sample to assess the chemical composition of the samples used in this investigation compared to the larger population of pipe welds. Figure 2-2 shows the cumulative distribution of the Al and Fe content. The data were well represented by a normal distribution. The variability is not large with the extreme content values falling within the specification limits.

Figure 2-3 shows the cumulative distribution of Al and Fe content for the weld wire. These data represent about 60 heats from the mid-1980s (~9400 lbs) for weld wire sizes ranging in diameter from 0.045 inch to 0.125 inch.

Similar to the pipe CMTR data, the Al and Fe can be represented by a normal distribution. The statistical distributions were analyzed on a per heat basis and on a per lot basis. The evaluation on a per lot basis took into account the size of each lot supplied to each heat base on the weight of each lot. There was no significant difference on the distribution of Al and Fe content in the weld wire population whether it was calculated by per heat or by per lot method. As seen in Figure 2-2, the variability in alloy content in the supplied heats for ERCuAl-A2 weld wire, especially the Al content, is small.

The parameters for the cumulative normal distribution in Figures 2-2 and 2-3 are given in Table 2-3.

Table 2-1

MATERIAL CHEMICAL SPECIFICATIONS FOR PIPE AND WELDS

Element	Wrought Pipe SB-315 CA614	Weld Metal SFA 5.7 ERCuAl-A2	Casting SB-148 CA952	Casting SB-148 CA954
Copper, min (Cu)	Remainder	Remainder	86.0	83.0
Aluminum, (Al)	6.0 – 8.0	8.5 – 11.0	8.5 – 9.5	10.0 – 11.5
Iron, (Fe)	1.5 – 3.5	0.5 - 1.5	2.5 – 4.0	3.0 – 5.0
Silicon, (Si)	-	0.10 max	-	-
Manganese, (Mn)	1.0	-	-	0.5 max
Nickel, (Ni)	-	-	-	2.5 max
Zinc, (Zn)	0.20 max	0.20 max	-	-
Lead, (Pb)	0.01 max	0.02 max	-	-
Phosphorous, P	0.015 max	-	-	-

Note: Chemical composition of the backing rings used during fabricating of some pipe welds is reported to be the same as the pipe material.

Table 2-2

WELD SAMPLE IDENTIFICATION

Sample ID	Pipe Weld	Description	Source
1	30-inch	Weld cross-section from 30-inch field removed/repair pipe	Ref. 2
2	10-inch	Weld cross-section from 10-inch field fabricated pipe	
3	3-inch	PE ring from 3-inch flange-to-pipe weld	Ref. 4
A	6-inch	Weld cross-section from 6-inch field fabricated pipe	Ref. 2
B2	10-inch	CTOD test specimen removed from 10-inch field mockup weld	
C1	30-inch	CTOD test specimen removed from 30-inch field mockup weld	

Table 2-3

CALCULATED STATISTICAL PARAMETERS FOR SUPPLIED MATERIAL (CMTR DATA)

Parameter	Base Pipe		Weld Wire	
	Aluminum (Al)	Iron (Fe)	Aluminum (Al)	Iron (Fe)
Mean, μ (Wt%)	6.81	2.47	9.48	0.907
Standard Deviation, σ (Wt%)	0.291	0.213	0.106	0.0790
Min/Max, (Wt%)	6.26/7.60	2.15/2.94	9.24/9.82	0.69/1.1
Lower 5th Percentile, (Wt%)	6.33	2.12	9.30	0.78
Upper 95th Percentile, (Wt%)	7.29	2.82	9.65	1.04
Specification Range, (Wt%)	6 .0- 8.0	1.5 – 3.5	8.5 – 11.0	0.5 - 1.5
Number of Heats	20		63	

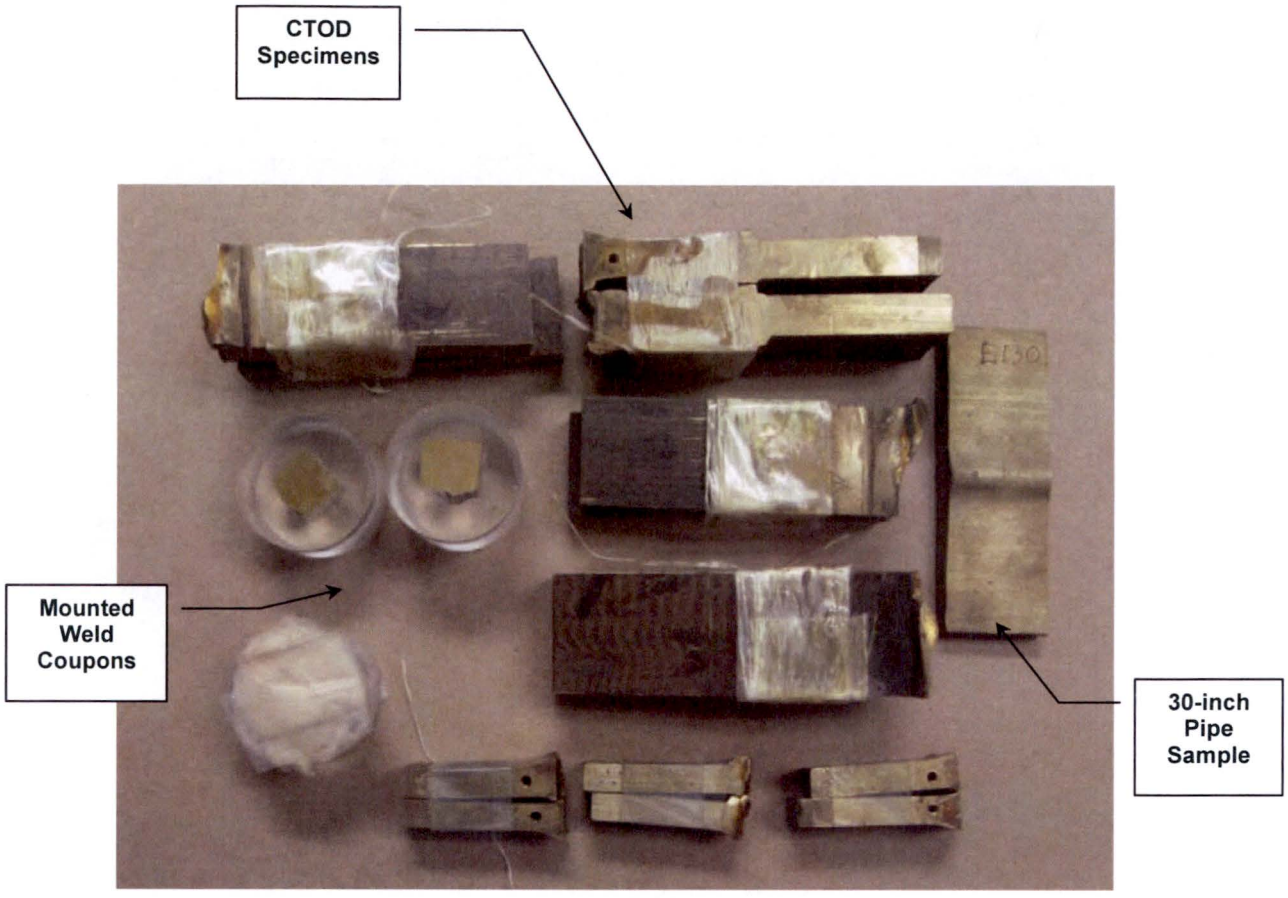

Figure 2-1 – Al-Brz Weld Samples and Test Specimens from the 1983 Testing Program

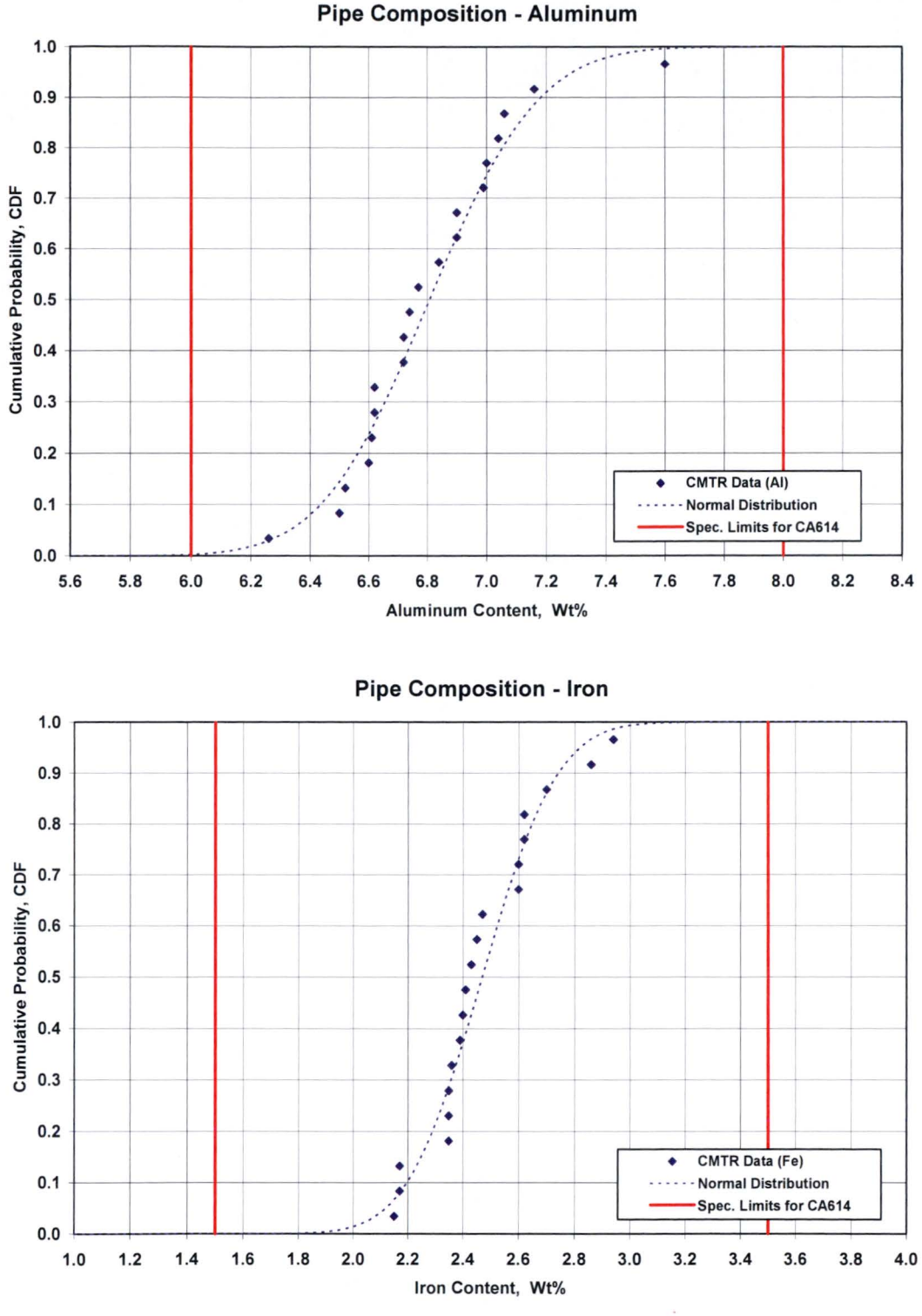

Figure 2-2 – Distribution of Aluminum and Iron Content in Supplied SB-315 CA614 Pipe (CMTR Data)

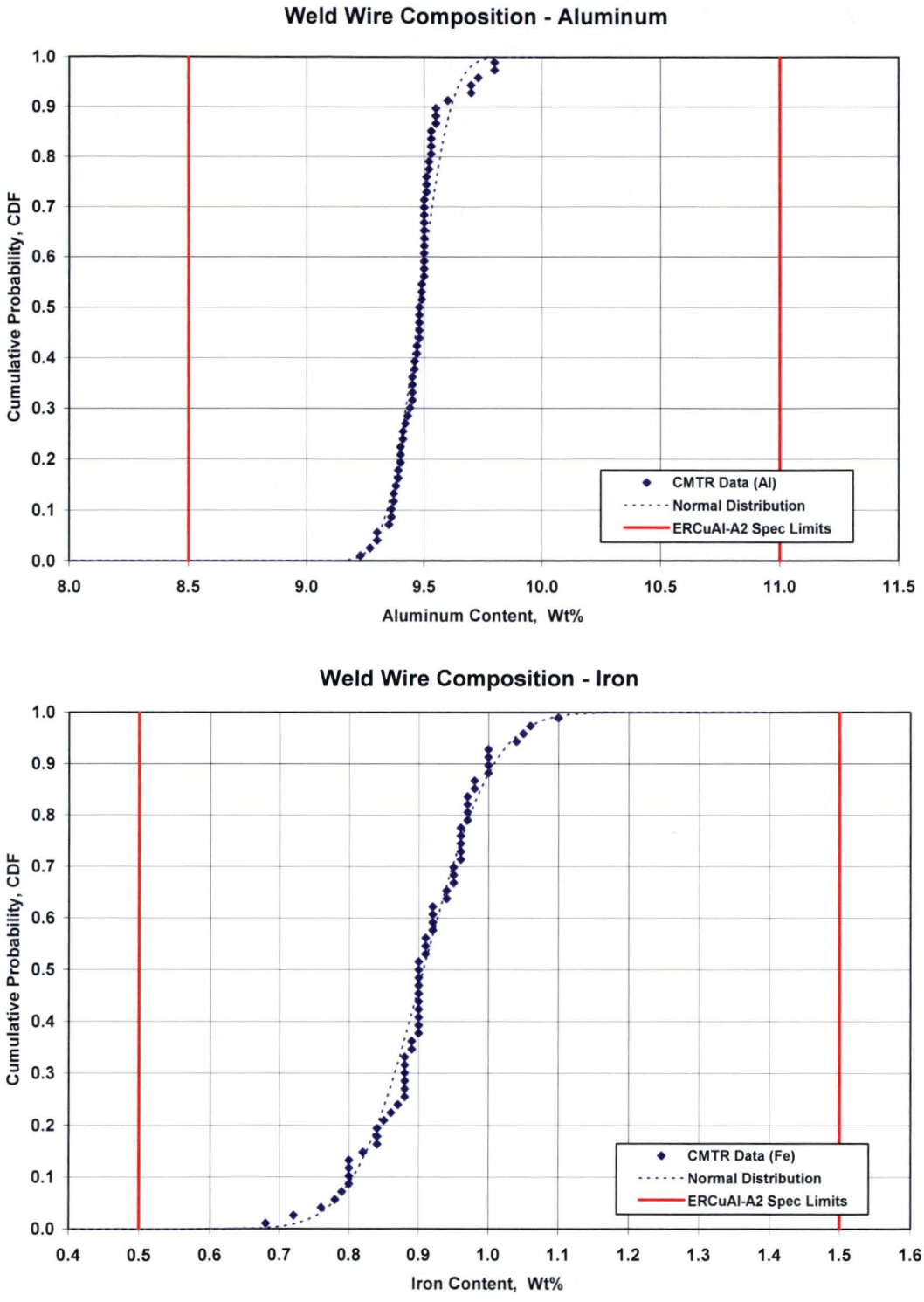

Figure 2-3 – Distribution of Aluminum and Iron Content in Supplied ERCuAl-A2 Weld Wire - CMTR Data

Section 3
TEST PLAN

3.1 SCOPE AND OBJECTIVES

The test plan contained specific objectives to characterize the microstructure of the pipe welds. The first objective was to determine the chemical composition of as-welded butt welds, both transverse to the weld centerline and through the wall thickness. The second objective was to characterize the microstructure and morphology of the transformed phases through the weld thickness from the weld root to the crown. The main focus is to establish whether the transformed phases are isolated within the weld metal or are linked, and whether the boundaries had formed a continuous network from the root pass to the weld crown.

There are six weld samples in the test plan as described in this section. These are described below:

1) Sample 1 – 30-inch pipe-to-pipe weld cross-section reported to be from a field removed ECW piping prior to service (no backing ring). This sample was selected because it is representative of a field weld in a large diameter pipe used in both under ground and above ground systems.

2) Sample 2 – 10-inch pipe-to-pipe weld reported to be produce by field mockup (no backing ring). This sample was selected for the same reason for Sample 1. Only the 30-inch and 10-inch sizes are used below ground.

3) Sample 3 – 3-inch flange-to-pipe weld (with backing ring) removed from service after approximately 26 years. This cast flange had been bend-tested for ACT as well as profiled for dealloying identification by PE. Although this is not a pipe-to-pipe weld, it was selected to represent smaller butt weld configurations and has a backing ring. Examination of the pipe-side will allow for examination of the weld root for possible dealloying within the backing ring crevice.

4) Sample 4 – 6-inch pipe-to-pipe weld reported to be produce by field mockup (no backing ring). This sample was selected to provide results for another pipe size when comparing volume fracture of the major material phases between welds and castings.

5) Sample B2 – CTOD fracture toughness test specimen that was removed from the 10-inch field mockup pipe and tested to failure. This sample provides another location in a 10-inch pipe weld primarily to examine the microstructure at the weld root and crown to study grain boundary morphology at these locations.

6) Sample C1 – CTOD fracture toughness test specimen that was removed from the 30-inch field mockup pipe and tested to failure. This sample was selected for the same reason as Sample B2.

Additional samples from the metallurgical investigation on the castings were used in the comparison of the microstructure between the pipe welds and the castings. The prior metallurgical work on the microstructure is given in Ref. 8.

3.2 PROCEDURE

3.2.1 Chemical Composition

Samples 1 through 3 were used in the measurement of the chemical composition of the weldment. The samples and survey map are shown in Figures 3-1 through 3-3. These samples were selected because they are representative of field welds over a range of pipe sizes and root geometry conditions. Four line scans per sample were performed with the approximate locations shown in Figures 3-1 through 3-3. These are

1) Traverse 1 - Line scan within the root pass in the axial direction across the weld section from pipe

2) Traverse 2 - Line scan within a filler pass close to the crown in the axial direction across the weld section from pipe

3) Traverse 3 – Line scan through the thickness at the weld centerline from the root to the crown (ID to OD of pipe)

4) Traverse 4 – Line scan through the thickness offset to the weld centerline near the fusion line from the root to the crown (ID to OD of pipe)

For Sample 3 (3-inch flange-to-pipe weld), Traverses 1, 3 and 4 include the heat-affected zone (HAZ) region in the backing ring. Two separate samples were removed from the pipe weld and are labeled as Section A and Section B in Figure 3-4. These two locations were selected because dealloying was observed at these circumferential locations on the flange-side of the weld. The dealloying penetration was about 20% of the wall thickness of the casting.

The area scan and patterns are illustrated in Figure 3-5. Area scans of ~0.25 mm^2 (0.5 mm by 0.5 mm squares) were made with uniform spacing along each traverse. The chemical composition within each area square was analyzed by SEM using the EDS method following the linear traverse lines across the sample. The specific procedure for the SEM setup and sample preparation is given in Ref. 11.

A single reference point defined the starting point for each traverse. The first 0.25 mm^2 square begins at the respective starting surface. The next square is placed approximately adjacent to the first and following along the line with subsequent areas incremented to complete the traverse. This indexing process is done automatically or manually depending on the area to be scanned. Each area scan within the 0.25 mm^2 boxes performs many multiple individual measurements over the surface area that is averaged by the scan processing system to give a single value for that area location.

Surface measurements and microanalyses of individual phases, precipitates and inclusions were performed using standard SEM techniques. A Hitachi-3700N Tungsten Filament Scanning Electron Microscope, which is fitted with an Oxford Instruments X-act Energy Dispersive X-ray detector was used. This system was running the Aztec 2.2 SP2 software. Detectability for EDS is about 0.5 wt% for the heavier elements (Al and greater), while it is about 1 wt% for anything lighter than Al. The theoretical measurement uncertainty is 1% of the value measured for each element present in quantities greater than the detection limit. The suitable measure of uncertainty in a single measurement is defined by the 2σ value and is a result of statistical analysis from peak fitting methods, background subtraction, experimental errors, etc (Ref. 12). The general rule is to approximate the error at +/-2% for each element to account for other potential factors. The uncertainty for the content of Al will be different than for Cu and Fe, where Fe would have the greatest uncertainty in the measurement because is present at lower concentrations.

3.2.2 Microstructure Evaluation

Light microscopy and SEM examinations were performed on areas of interest to identify the microstructure and constituents within the transformed phase. Magnifications to permit resolution in the photomicrographs between 50 and 500 μm were used for comparative study among the sample locations. Magnifications down to 4 μm were used in SEM evaluations. Details on polishing and etching of samples and specific locations are discussed in Section 5.

X-ray diffraction (XRD) was used for phase identification study on Sample 1 and a sample removed from CA954 cast valve body. Details of XRD scope and results are given in Section 6.

3.3 REPORTING OF RESULTS

The chemical composition results are plotted as a function of distance across the sample relative to the weld centerline or inside surface of the weld. The primary alloying elements (Cu, Al, and Fe) plus any residual elements detected on the surface are recorded. The wt% for each identified element is computed. A distribution of wt% is computed for just Cu, Al, and Fe. This second set of composition results eliminates any elements that may be present as surface contaminants and not an alloy constituent. The weight percents for this second set are normalized to include only Cu, Al, and Fe.

The magnitude of the amounts (wt%) of Cu, Al and Fe are plotted individually and compared with the reported CMTR data for the material. Results on chemical composition are given in Section 4. Microstructural features are documented as part of the metallurgical evaluation as described in Section 5 and 6.

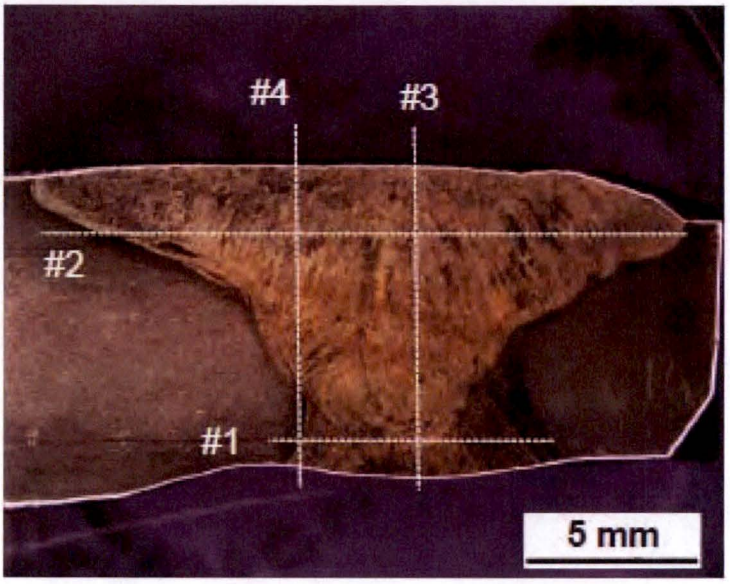

Figure 3-1 – Sample 1 – 30-inch Weld Cross-Section

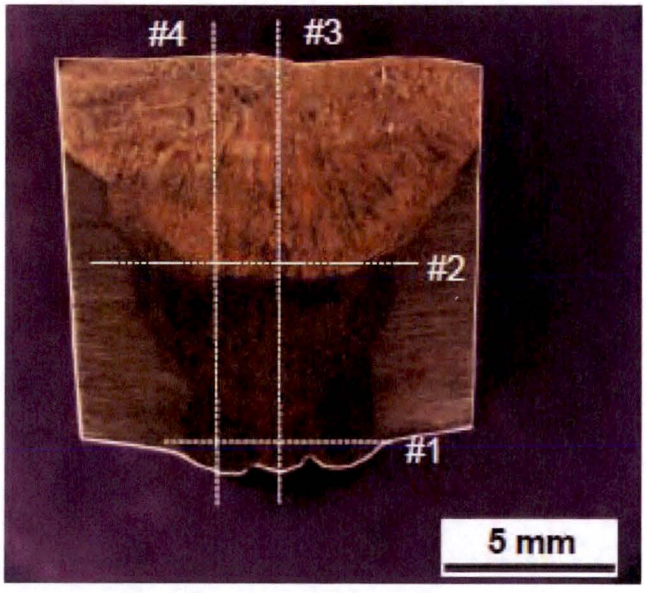

Figure 3-2 – Sample 2 – 10-inch Weld Cross-Section

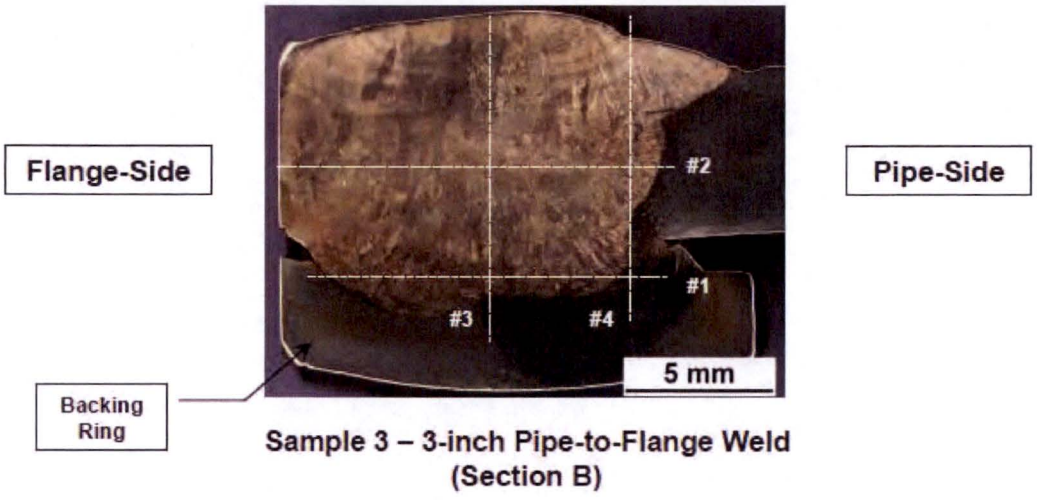

Figure 3-3 – Sample 3 – 3-inch Weld Cross-Section

a) Pipe Segment – Long View

a) Pipe Weld Cross-section – End View

Figure 3-4 – 3-inch Flange-to-Pipe Weld Showing Locations of Removed Sections

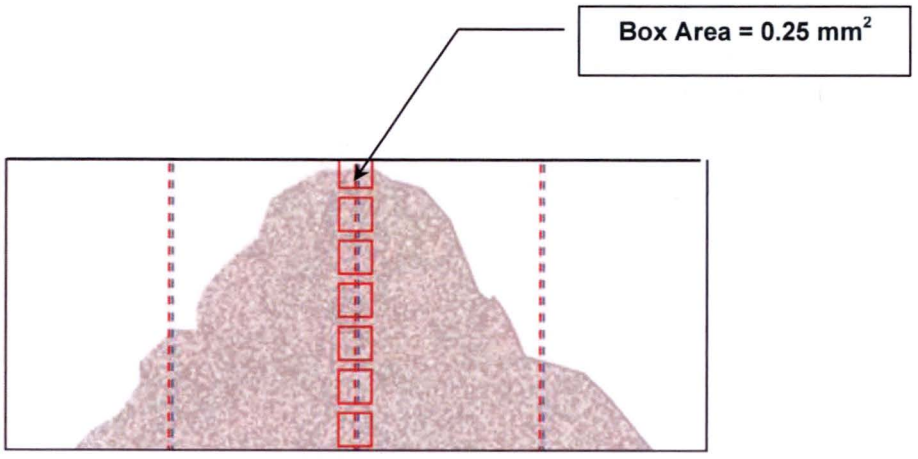

Figure 3-5 – Schematic Illustration of Area Scanning for Chemical Analysis

Section 4
CHEMICAL COMPOSITION ANALYSIS

4.1 SURFACE ANALYSIS RESULTS

The three pipe weld samples (Samples 1 through 3) were analyzed for chemical composition on the cross-section surface of the weld (Ref. 11). For each measurement location, the SEM image, EDS spectrum charts, and the reported wt% for each alloying element identified were recorded. An overall summary of the measured Al and Fe surface content of the samples in wt% is given in Table 4-1. Also listed in Table 1 are the average and one-side lower 5% and upper 95% for Al and Fe content for the weld wire used in the fabrication of the pipe welds (see Section 2.3). These values are listed to show the amount of weld metal dilution in Al during solidification. In general Al content decreases and Fe content increases in the weld pool due to mixing with the base pipe.

The summary compositions are based on averaged surface measurements in the specified region of the weld. The Al content within the weld root region is general lower than the filler (weld crown) passes. The opposite is observed for Fe content where the weld root has a higher level of Fe than in the weld crown. This is due to three conditions:

1) Dilution of the weld metal resulting in decreased Al concentration from the mixing of the lower Al content in the pipe with the weld metal during the melting process,

2) Increase in Fe content in the weld from the dilution of the higher Fe content of the pipe which mixes with the weld metal during the melting process, and

3) Smaller volume of weld metal required to make the first (root) pass compared to the larger volumes needed to complete the filler passes.

The magnitude and variation in Al and Fe content from the line scans performed transverse and through the thickness of the welds are presented in the sections that follow. The detailed results are provided in a series of plots of chemical content versus distance along each traverse for each sample. Also plotted in the composition plots are the chemical composition values for Al and Fe from the CMTR data (see Table 2-3). The lower 5% limit on Al and the upper 95% limit

for Fe are compared with the weld metal composition values to show the effect of chemical mixing in the weld pool during to the solidification process.

4.2 SAMPLE 1 - 30-INCH PIPE-TO-PIPE WELD

Surface area scans results for the 30-inch weld sample are shown in Figures 4-1 and 4-2. Also shown in these figures are the lower 5% tolerance limit on Al content and the upper 95% tolerance limit on Fe content for the as-supplied ERCrAl-A2 weld wire.

Figure 4-1 shows the variation in Al and Fe content in wt% transverse to the weld centerline (circumferential direction). The measurement data are plotted relative to the weld centerline for Traverses 1 across the root region, and Traverse 2 within the final filler pass (crown region). The Al content near the fusion line is about 7.0 wt% consistent with the nominal pipe composition and increases to about 9.0 wt% at the weld centerline, which is lower than the 5% lower limit for the Al content for weld metal based on the CMTR data. A similar trend in Al content for the final weld pass is observed for Traverse 2, where a lower Al content is detected at the fusion line of the weld. These levels reflect the dilution of Al in the deposited weld metal during melting and solidification process.

For the variation in Fe content, the opposite trend is observed where the Fe content is higher at the weld fusion line and decreases to a minimum value at or near the weld centerline. This trend reflects the dilution of Fe from the base pipe which mixes with the weld pool to increase the level of Fe in the deposited weld metal. The weld metal, which has a nominal Fe content lower than the pipe metal, has elevated above the 95% upper limit of the CMTR data.

Figure 4-2 shows the results for the variation for Al and Fe content in the through thickness direction (Traverses 3 and 4). The Al and Fe content varies in an approximate linear manner with distance from the root to the crown. The variation in Al content shows an increasing trend whereas Fe content shows a decreasing trend which is due to the increasing volume of weld metal with the subsequent weld filler passes.

4.3 SAMPLE 2 - 10-INCH PIPE-TO-PIPE WELD

In the same manner as Sample 1, surface area scan results for the 10-inch weld sample are shown in Figures 4-3 and 4-4. Figure 4-3 shows the variation in Al and Fe content in wt% transverse to the weld centerline. The measurement data are plotted relative to the weld

centerline for Traverses 1 across the root region, and Traverse 2 close to the crown region. The Al content near the fusion line is less than 7 wt% and increases to about 7.8 wt% at the weld centerline for the root and about 8.5 wt% for the final weld pass. Again this trend reflects the dilution of Al in the deposited weld metal during melting and solidification, and the higher Al level near the weld crown compared with the root pass reflects the larger weld metal volume required for the filler passes. The Al content in the weld is below the lower 5% tolerance limit of the CMTR data. This indicates that dilution of the weld metal had occurred in the root and filler passes.

For the variation in Fe content, the same trend is observed as with the 30-inch weld except that the Fe level within the root region appears more uniform without a noticeable drop in Fe content at the centerline.

Figure 4-4 shows the results for the variation for Al and Fe content in the through thickness direction for the 10-inch weld. The Al and Fe content varies in an approximate linear manner with distance from the root to the crown consistent with the measurements for the 30-inch pipe weld. In other words, the Al content decreases at the root of the weld due to dilution.

4.4 SAMPLE 3 - 3-INCH FLANGE-TO-PIPE WELD

Surface area scan results for the 3-inch weld sample are shown in Figures 4-5 and 4-6. It should be noted that the flange is a CA952 casting with a higher Al content. Therefore, there is a possibility that the as-deposited weld composition on the pipe-side will be influenced by the flange chemistry. Also, there is a backing ring for this weld joint which will influence the weld chemistry in the root pass. Pipe-to-pipe welds have been fabricated with and without backing rings.

Figure 4-5 shows the variation in Al and Fe content in wt% transverse to the weld centerline. The transverse scans were taken at the root of the weld from the backing ring, through the weld filler metal, and into the pipe. At the pipe weld side, the Al content is relatively uniform from the weld centerline to the fusion zone at about 9.5 wt%. For the root pass, the Al content is somewhat lower but following a similar trend up to the weld centerline. Based on the CMTR data, it appears that less Al dilution occurs in the flange-to-pipe welds than that observed in the pipe-to-pipe welds. For clarification, the two measurements plotted at -6.2mm and -7.5mm for the root pass are located in the backing ring HAZ and not the weld metal.

Figure 4-6 shows the results for the variation for Al and Fe content in the through-thickness direction (centerline and pipe –side weld planes) for the 3-inch weld. The Al and Fe content varies in an approximate linear manner with distance from the root to the crown, except that the first two measurements in each scan (Traverses 3 and 4) were located within the backing ring HAZ.

4.5 SUMMARY OF FINDINGS

Surface scans using SEM/EDS were completed on three field-fabricated Al-Brz pipe welds to determine the chemical composition and distribution of Al and Fe in the weldment. The following is a summary of the surface measurements for weld metal chemistry in the as-deposited condition:

1) Weld metal dilution of Al is observed resulting from the melting process involving the higher Al weld metal with the lower Al content of the wrought pipe.

2) Weld root pass shows more dilution in Al content than the subsequent filler passes (less weld metal deposited in the root pass). Al content varies roughly linearly from the root pass to the crown.

3) Fe content in the weld increases due to higher Fe present in the base pipe. Fe level is also observed to vary systematically from the root to the crown.

4) EDS results for the root pass indicates the Al content is less than ~9 wt% at the weld inside surface.

The chemical composition of the weld metal in the root pass, having generally lower Al than the weld wire composition, will have a less susceptible microstructure for general dealloying.

Table 4-1

SUMMARY OF SURFACE CHEMISTRY ANALYSIS RESULTS

Specimen (Pipe Size)[1]	Alloy Element[2]	Weld Root		Weld Crown	
		Fusion Line (wt%)	Center Line (wt%)	Fusion Line (wt%)	Center Line (wt%)
Sample 1 (30-inch)	**Aluminum** Mean = 9.48 wt% 5%/95% = 9.30/9.65 wt%	7.0	8.7	7.4	9.2
	Iron Mean = 0.907 wt% 5%/95% = 0.790/1.04 wt%	2.0	1.6	2.0	1.5
Sample 2 (10-inch)	**Aluminum** Mean = 9.48 wt% 5%/95% = 9.30/9.65 wt%	6.8	7.8	7.0	8.8
	Iron Mean = 0.907 wt% 5%/95% = 0.790/1.04 wt%	1.6	1.8	1.6	1.4
Sample 3 (3-inch)	**Aluminum** Mean = 9.48 wt% 5%/95% = 9.30/9.65 wt%	7.5	8.8	7.5	9.6
	Iron Mean = 0.907 wt% 5%/95% = 0.790/1.04 wt%	2.2	1.6	2.2	1.1

Notes:

1) 10-inch and 30-inch welds did not have a backing ring. 3-inch weld had a backing ring
2) Chemical composition for the weld wire determined from CMTR data sample. The 5% and 95% values are the lower 5th and upper 95th percentile one sided tolerance limits to the weld metal population.

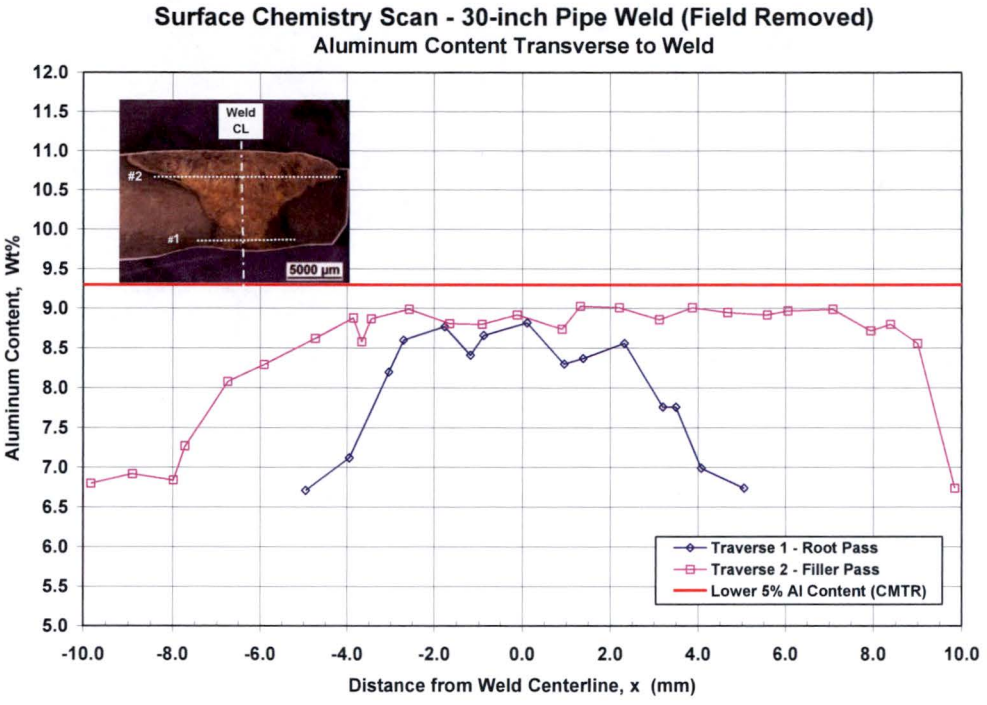

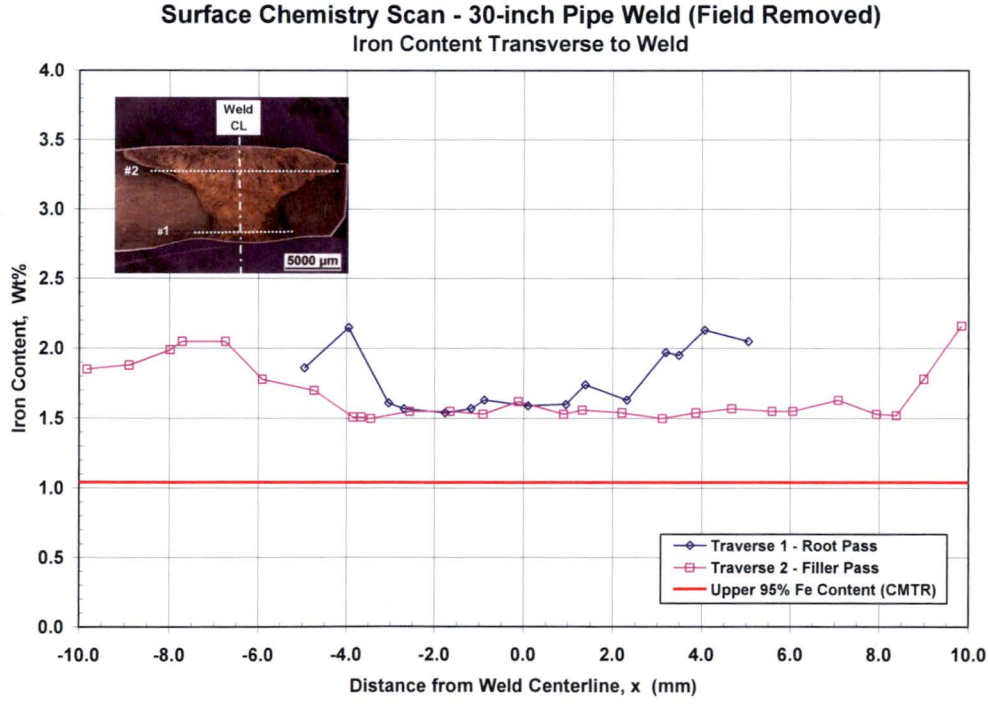

Figure 4-1 – Transverse Surface Scans for Aluminum and Iron Content (30-inch Weld Sample)

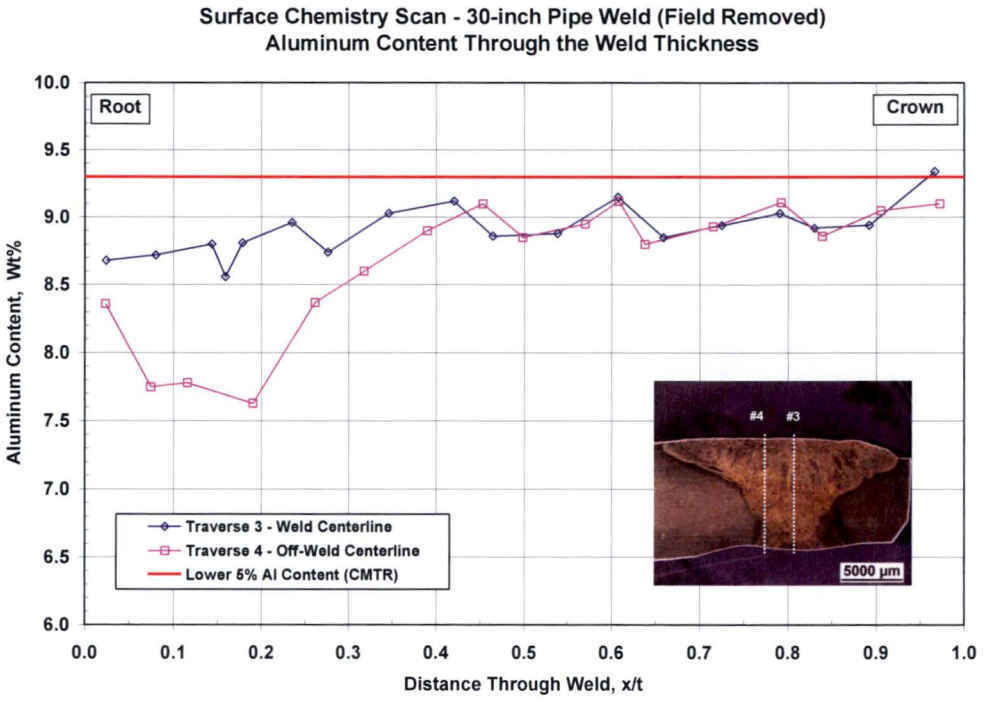

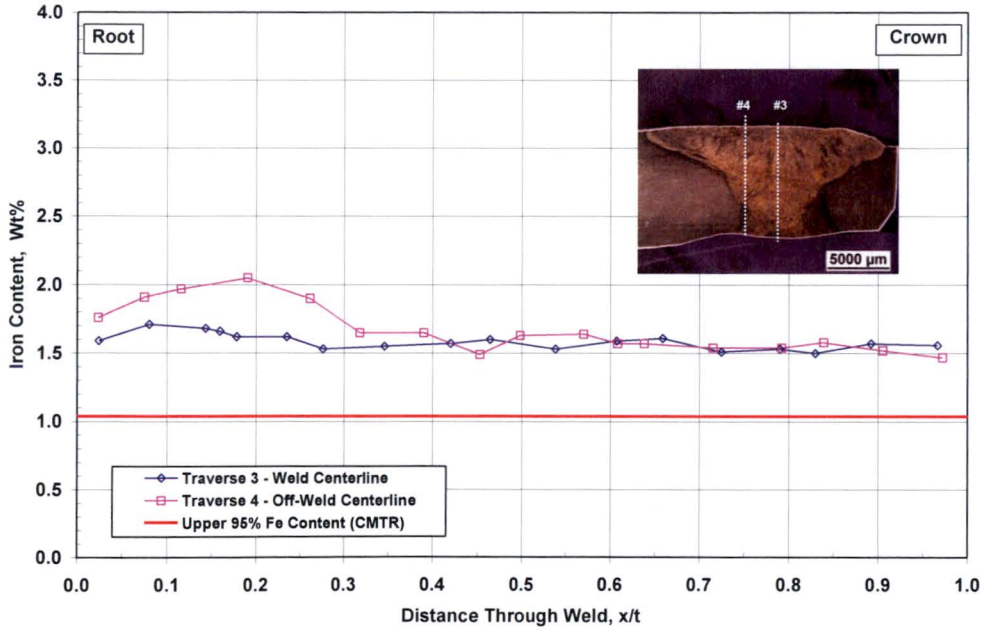

Figure 4-2 – Through-Wall Surface Scans for Aluminum and Iron Content (30-inch Weld Sample)

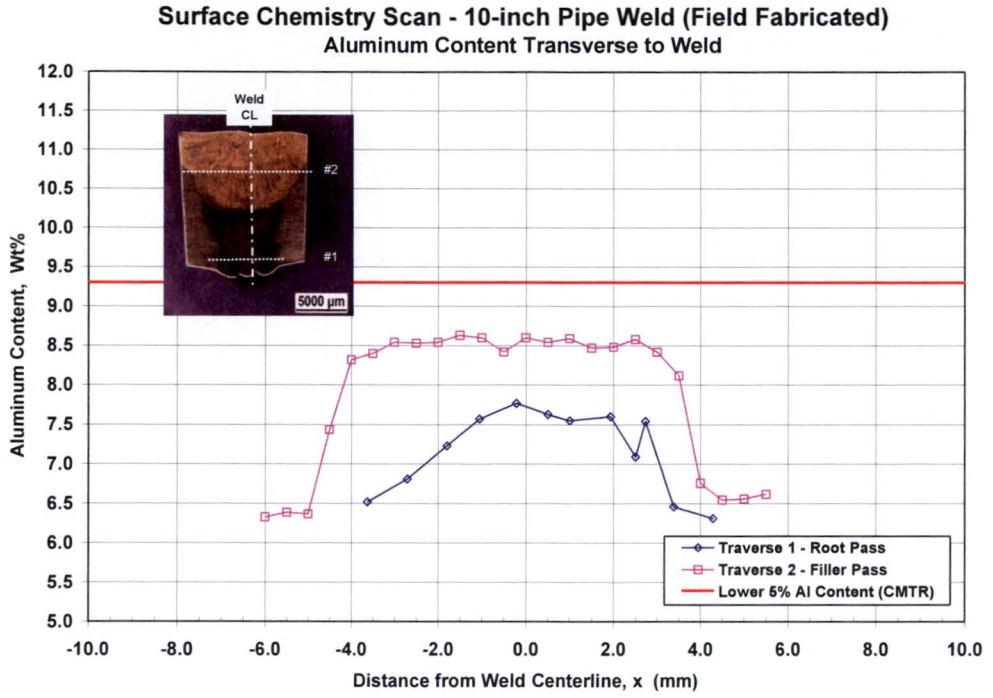

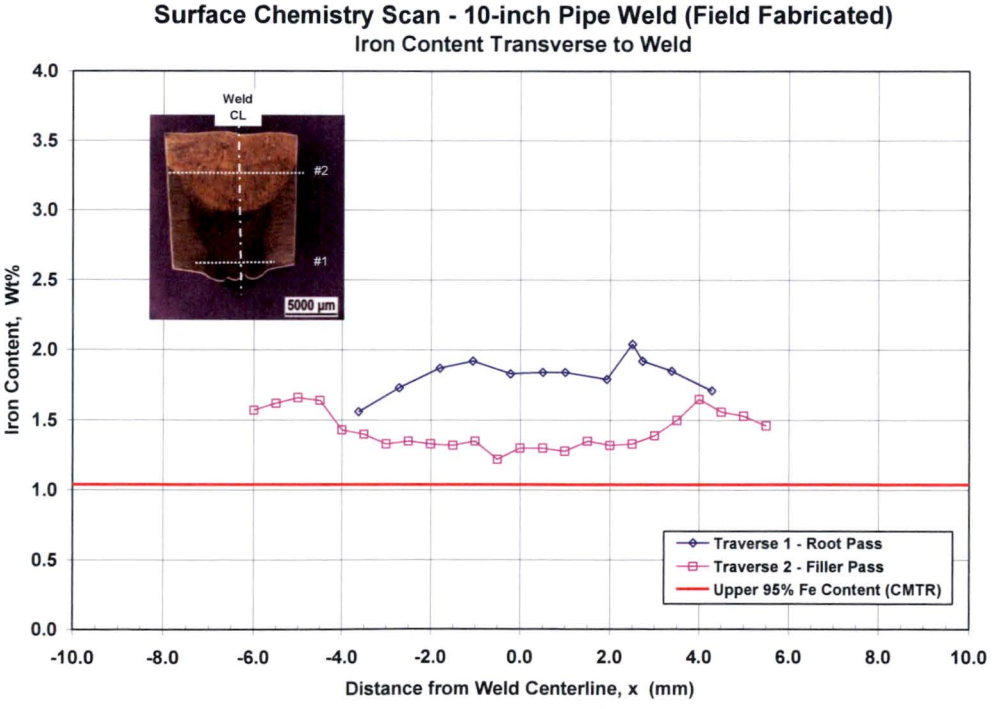

Figure 4-3 – Transverse Surface Scans for Aluminum and Iron Content (10-inch Weld Sample)

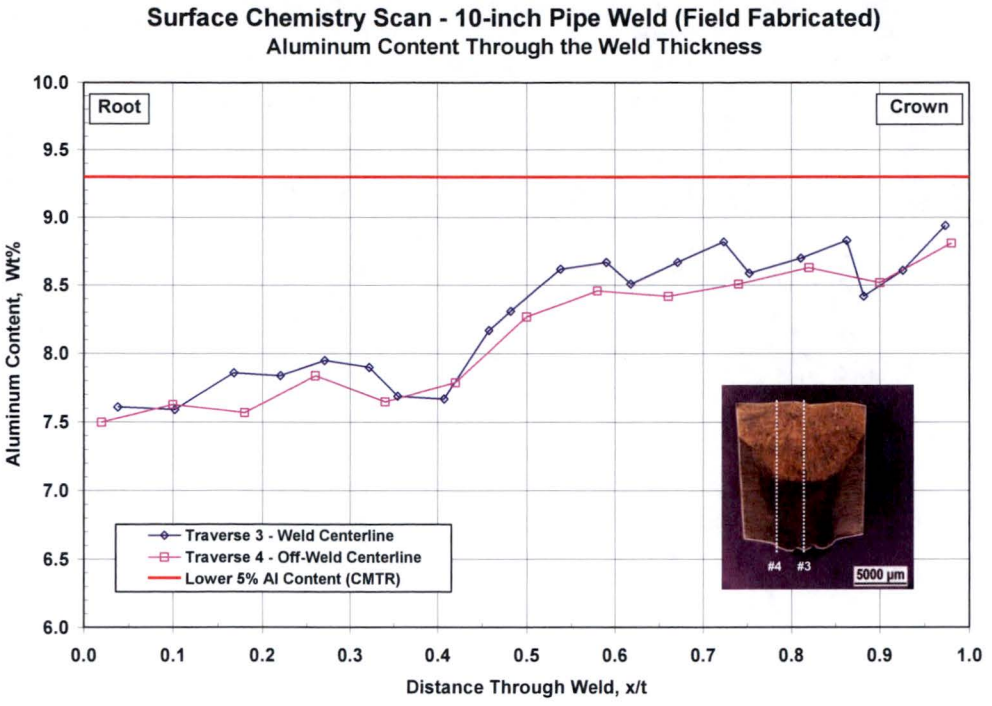

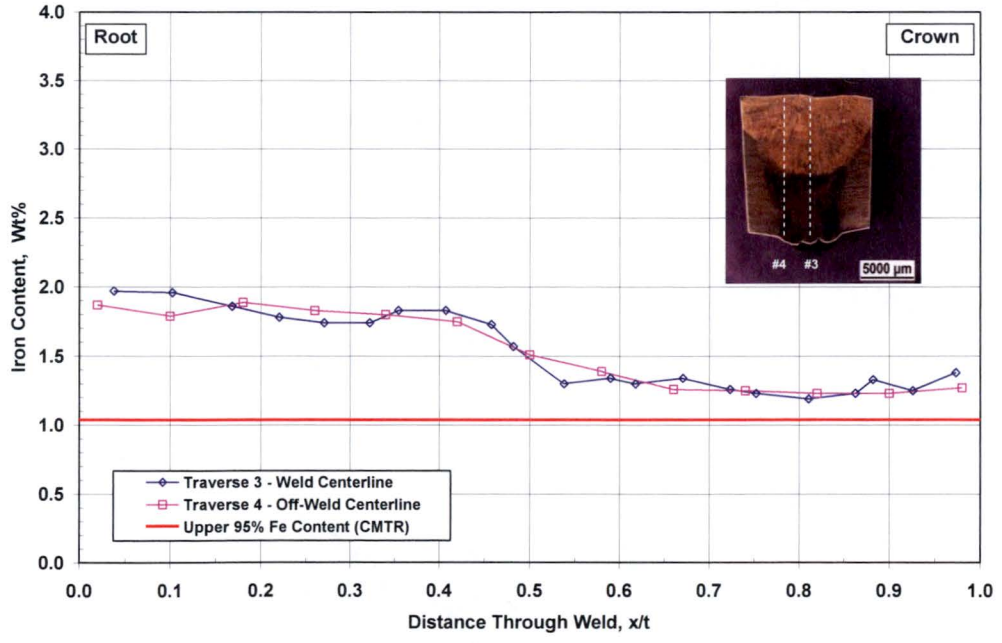

Figure 4-4 – Through-Thickness Surface Scans for Aluminum and Iron Content (10-inch Weld Sample)

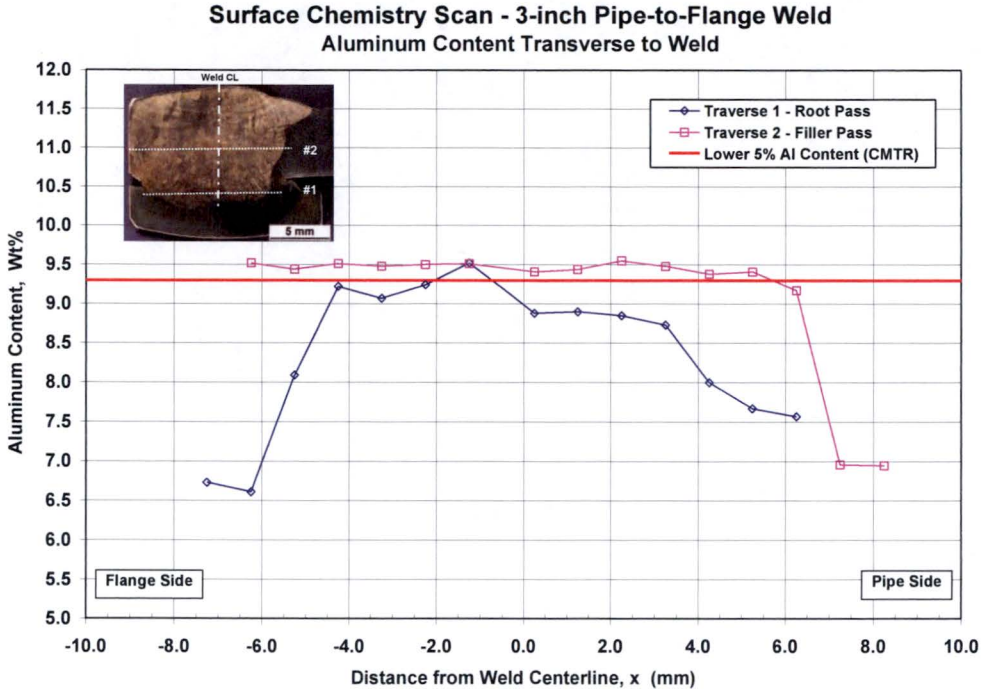

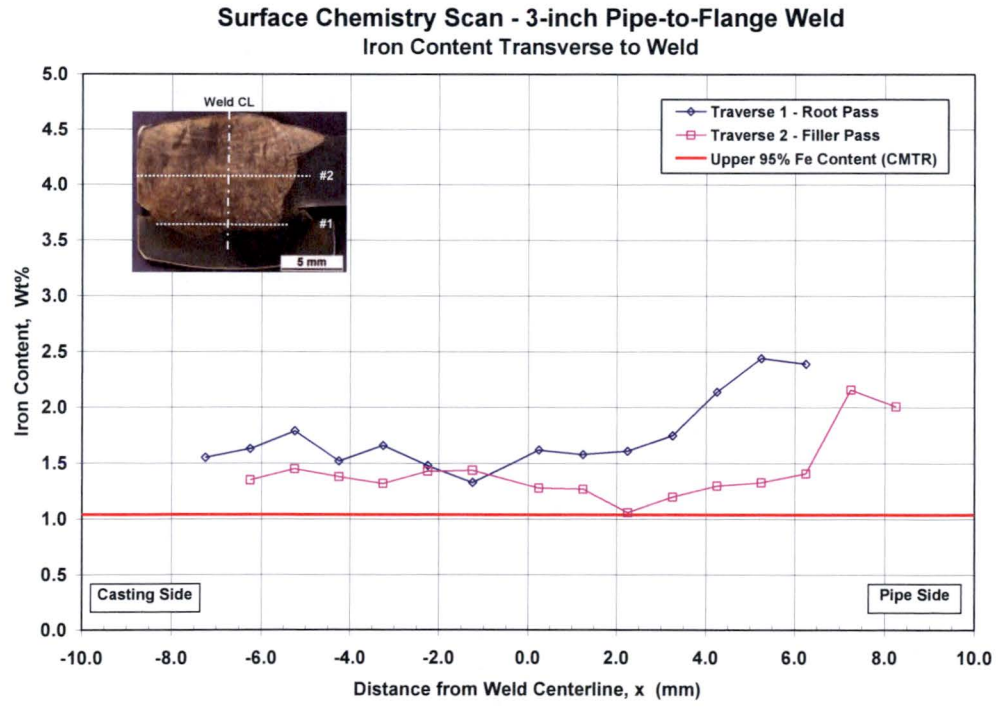

Figure 4-5 – Transverse Surface Scans for Aluminum and Iron Content (3-inch Weld Sample)

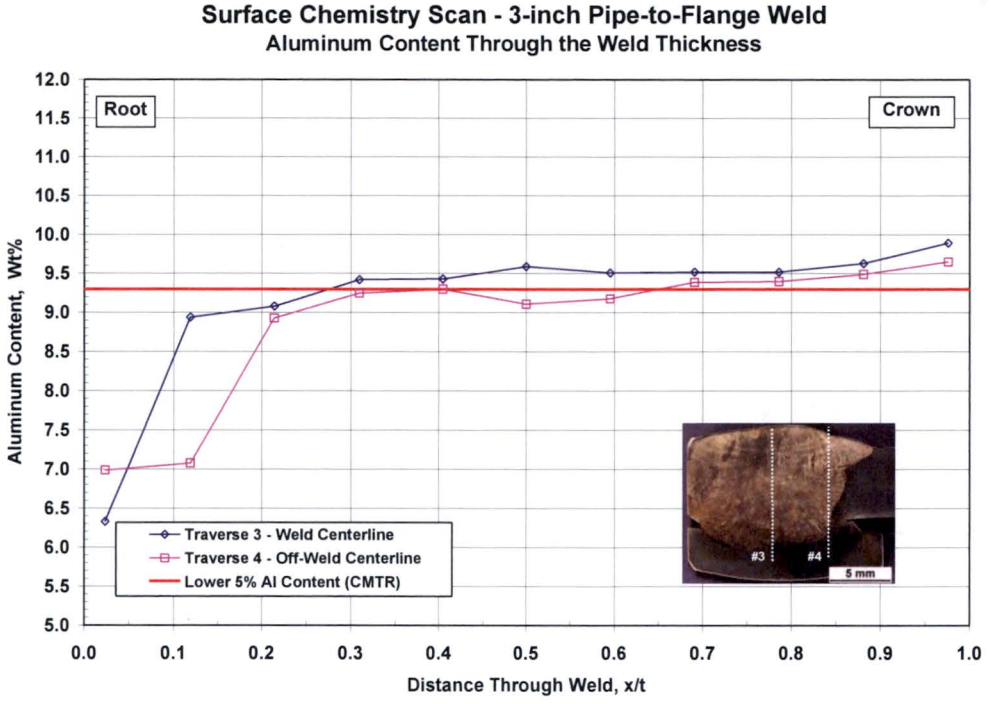

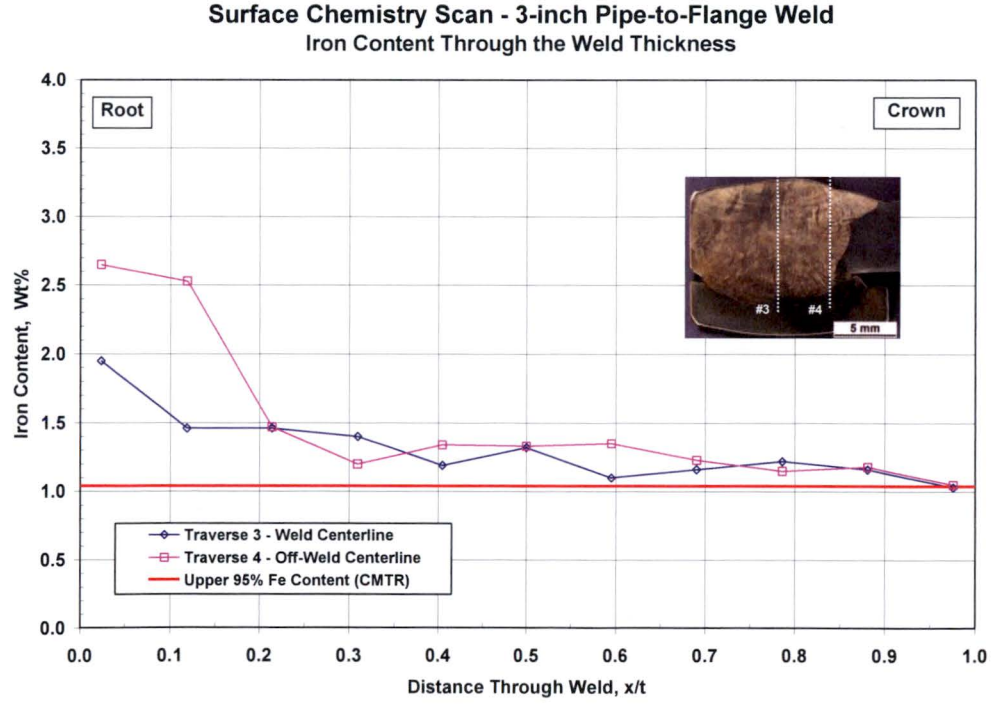

Figure 4-6 – Through-Thickness Surface Scans for Aluminum and Iron Content (3-inch Weld Sample)

Section 5
MICROSTRUCTURAL EVALUATION

5.1 METALLURCIAL ANALYSIS

The microstructure of pipe welds was studied to characterize the transformed phase composition and morphology. The susceptibility of pipe welds to dealloying is based on the distribution of the transformed phase within the weld metal. Material composition is presented in Table 5-1. The Al-Brz CA614 pipe is a single phase alloy, α phase. However, the weld metal, ERCuAl-A2, can be composed of α and transformed phases consisting of β, and/or $\beta + \gamma_2$ depending on aluminum content and cooling rate during phase formation (Figure 5-1).

The α phase is not susceptible to dealloying; whereas the transformed β and γ_2 phases within the transformed microstructure are susceptible to dealloying due to higher aluminum content. The γ_2 phase as a continuous network significantly affects the corrosion resistance causing a higher dealloying penetration through the thickness of the part. It may be possible to postulate that small isolated areas of transformed phase will result in localized superficial corrosion. However, dealloying will not penetrate into the material unless a continuous network of susceptible microstructure is present.

Cross-sections were prepared by grinding and polishing the sections. The sample microstructure was revealed using a modified potassium dichromate etchant (a solution of 1g $K_2Cr_2O_7$, 4ml H_2SO_4, 50ml H_2O, and two drops of HCl). The samples were inspected using light optical microscopy (LOM), and a scanning electron microscope (SEM) equipped with an energy dispersive x-ray spectrometer (EDS). Phase identification and semi-quantitative analysis of the phase composition was achieved with EDS.

Metallurgical evaluation was performed on weld cross-sections and CTOD test specimens listed in Table 2-2.

5.2 30-INCH FIELD WELD SAMPLES

Figure 5-2 shows a polished and etched longitudinal cross-section from a 30-inch pipe field mockup weld. Representative LOM showing the typical microstructure of the crown and root passes is also shown. The microstructure consisted of acicular α phase (light etch) and a semi-continuous network of transformed phase (dark etch), which according to the phase diagram in Figure 5-1 is likely a mixture of β, and/or $\beta + \gamma_2$; however, exact phase identification is not attainable using LOM alone. Characterization of each phase shown in the backscattered electron (BSE) image in Figure 5-3 was performed using EDS. The aluminum content of the transformed phase (Location 1) was measured at approximately 10.85 wt%, while in the α phase (Location 2) it was at 7.81 wt%. The transformed phase was isolated and dispersed between the α phase grains.

In addition, a metallographic cross-section of a 30-inch pipe field mockup weld from a bend test specimen, Sample C1, was evaluated (Figure 5-4). The sample was tested to failure as part of a previous investigation; for the purpose of assessing the weld microstructure a cross-section was taken through the ductile overload region. The cross-section, Figure 5-4 bottom, shows the microstructure of the pipe base metal, weld HAZ, and weld. As observed in previous samples, the weld crown microstructure, shown in Figure 5-5, consisted of acicular α phase with a transformed phase network. The weld root microstructure was not captured in the cross-section since fracture occurred at the HAZ; however, intergranular cracking induced by the test was observed.

5.3 10-INCH FIELD MOCKUP WELD SAMPLES

A longitudinal cross-section from the 10-inch pipe field mockup sample is shown in Figure 5-6. The weld root and crown microstructure showed distinct morphologies. The crown passes show the microstructure typically observed in the welds consisting of acicular α and transformed phase, which shows localized network surrounding the α phase. In contrast, the root weld microstructure shows isolated islands of transformed phase. The microstructure is the result of rapid cooling and high dilution of aluminum due to intermixing of the pipe. Figure 5-7 shows representative LOM of the microstructure at the weld inter-pass. The micrographs reveal that the local network of transformed phase is disrupted by the deposition of a different weld pass.

Further characterization of the weld root was undertaken using EDS. A representative BSE micrograph is shown in Figure 5-8 (top). The transformed phase had an aluminum content of 9.16 wt% as compared to the α phase with 6.82 wt%. The microstructure contained a low volume fraction of transformed phase that was discontinuous.

In addition, a cross-section was taken from a longitudinal bend test specimen (Sample B2) from a 10-inch pipe field mockup weld. The sample was tested to failure and the cross-section was taken through the ductile overload region; the pipe base metal, HAZ and weld are shown in Figure 5-9. Representative micrographs from the weld root and crown are given in Figure 5-10. The crown microstructure consisted of fine α grains and likely martensitic β (or β') in the transformed phase; this microstructure is typical of a rapidly cooled weld when the aluminum content is sufficiently high. The weld root showed acicular α phase and transformed phase showing a semi-continuous network isolated by α phase networks at the former β grain boundaries. Similar features were observed at the root of a weld from a different section of a 10-inch pipe field mockup weld (Figure 5-11). The figure shows BSE micrographs at different magnifications at the root of a weld, where the red arrows point to discontinuities in the network of transformed phase. Similarly features can be observed in the microstructure of the weld crown, Figure 5-12, where the former β grain boundaries are adorned by networks of α phase.

5.4 3-INCH FLANGE-TO-PIPE WELD REMOVED FROM SERVICE

Metallographic cross-sections were prepared at the flange-to-pipe weld from a 3-inch flange removed from service (Figure 5-13). The weld on the right side of the flange had been sectioned transversely to the long axis of the pipe for profile examination of dealloying in the cast flange; the results of the analysis are subject of a different report. In addition, the flange-to-pipe weld was previously subjected to a bend test (~59 ksi bending stress) to check for material strength and therefore some indications of bending deformation are evident in the part. Axial Sections A and B were removed for microstructural analysis.

A macroscopic visual test to check for general dealloying of the 3-inch flange-to-pipe weld was performed. The sections are polished and the surface of interest is wetted with a silver nitrate solution to exposed dealloyed regions. Locations of dealloying are stained black by the reaction between the silver nitrate from the solution and the copper rich regions of the corroded material. As shown in Figure 5-14, a small region at the root of the weld in Section A, at the location of

the backing ring showed dealloying. In addition, a small weld flaw consisting of a pore is visible in Section A; dealloying was not observed at the pore or in the vicinity of the flaw. Section B did not show indications of dealloying from the test.

Further inspection of the dealloyed region in Section A, Figure 5-15, revealed that corrosion was limited to the region adjacent to the crevice formed by the backing ring and pipe—indicated by the white arrow in the figure. A crack extending from the crevice at the backing ring into the fusion line of the weld (red arrow) is visible. Dealloying of the material is evident by the presence of copper rich regions within the transformed phase of the weld; dealloying of the α phase does not occur.

Figure 5-16 shows BSE micrographs of the dealloyed region in Section A. The relative composition of the phases was probed using EDS and reported in the figure. Aluminum content of the α phase in the weld is approximately 7.05 wt% (Location 1), while the transformed phase has an aluminum content of 10.17 wt% (Location 2). EDS analysis of the dealloyed phase (Location 3) confirmed that aluminum was leached out and nearly pure copper remained in the region. It was also noted that dealloying was confined to a small region (less than 500 μm) adjacent to the crevice at the root of the weld. Dealloying of the material necessitates a continuous network of susceptible microstructure; however, the microstructure of the welds does not show a continuous network of transformed phase. Figure 5-17 shows BSE micrographs at progressively higher magnifications at the boundary zone of the dealloyed region. Grain boundaries do not contained continuous networks of transformed phase disrupting the path for preferential corrosion.

In addition to dealloying, Figure 5-15 and Figure 5-16 for Section A and Figure 5-18 for Section B, show extensive cracking through the corroded region and into the pipe material. Cracking is most likely due to the bend test the flange-to-pipe sample was subjected to. This is evidenced by the ductility displayed in the tearing of the microstructure, in particular in Section B.

5.5 SUMMARY OF FINDINGS

Cross-sections from several field mockup welds and a flange-to-pipe weld were evaluated to assess the susceptibility of the microstructure to dealloying. Weld microstructural constituents

were composed primarily of α grains with transformed phase forming a semi-continuous or discontinuous network. Formation of γ_2 in the welds is not likely due to rapid cooling, which is supported by the formation of isolated or semi-continuous transformed phase (likely β). Aluminum dilution was measured in the root pass and resulted in lower volume fraction of transformed phases. The crown passes showed higher volume fraction of transformed phase but long-range connectivity of the susceptible microstructure was not observed.

Localized dealloying was observed in the weld region near a crevice formed by the backing ring and pipe. Dealloying was restricted to the transformed phase in the region adjacent to the crevice at the weld and it is expected to be confined and non-propagating unless a continuous network of susceptible microstructure is present.

Table 5-1

CHEMICAL COMPOSITION SPECIFICATION FOR WROUGHT AND WELD MATERIAL (WT%)

Element	Wrought Pipe SB-315 CA614	Weld Metal ERCuAl-A2
Copper, Cu	Remainder	Remainder
Aluminum, Al	6.0 – 8.0	8.5 – 11.0
Iron, Fe	1.5 – 3.5	0.5 - 1.5
Silicon. Si	-	0.10 max
Manganese, Mn	1.0	-
Nickel, Ni	-	-
Zinc, Zn	0.20 max	0.20 max
Lead, Pb	0.01 max	0.02 max
Phosphorus, P	0.015 max	-

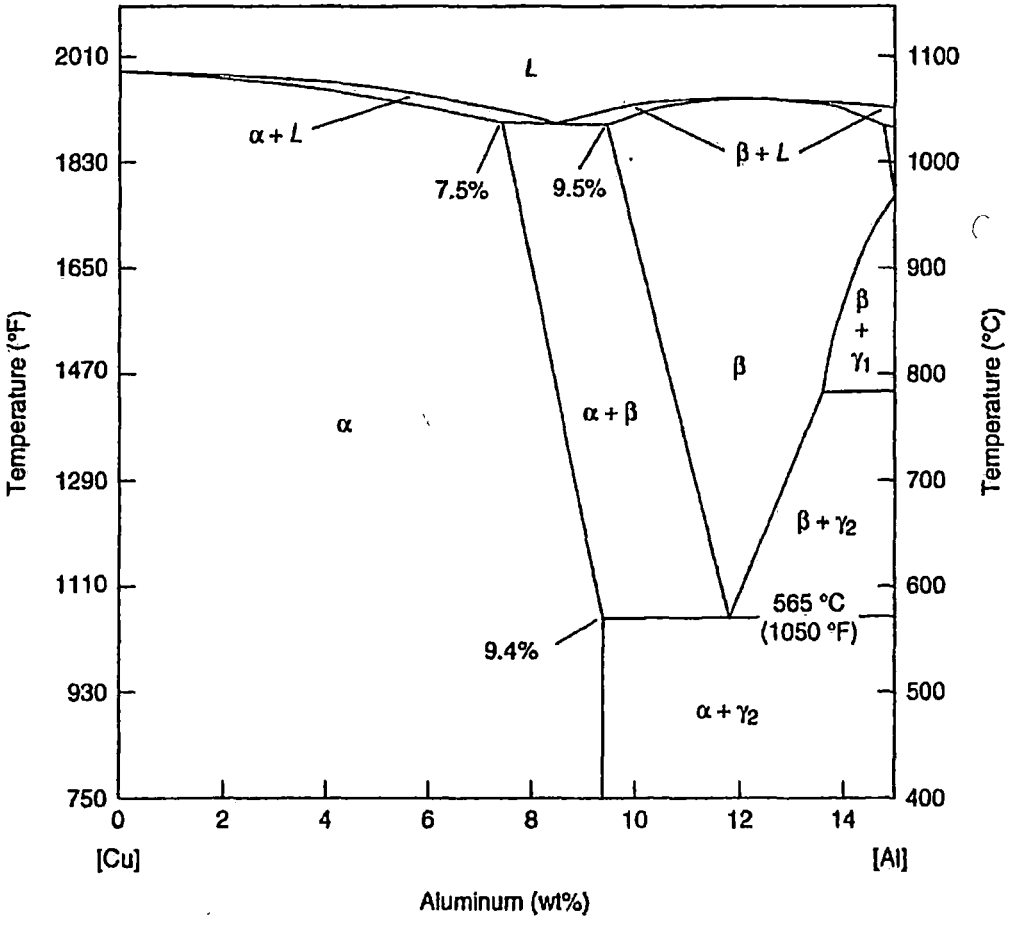

Figure 5-1 – Equilibrium Phase Diagram for a Binary Copper and Aluminum Alloy.

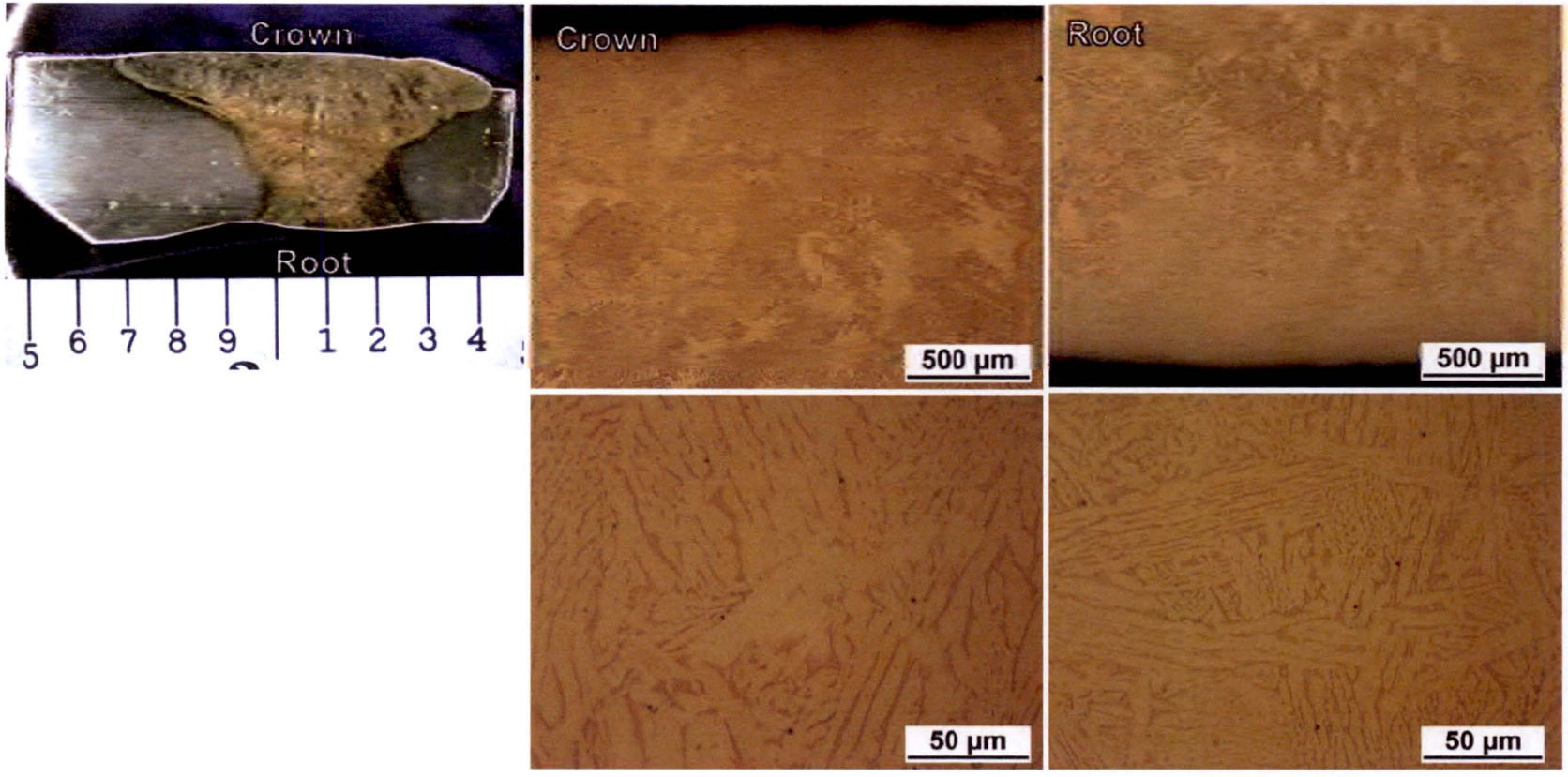

Figure 5-2 – Optical Micrograph of an Etched Cross-Section from a 30-inch Pipe Field Mockup Weld. Microstructure of the Root and Crown Passes Consists of Acicular α Phase and Transformed Phase).

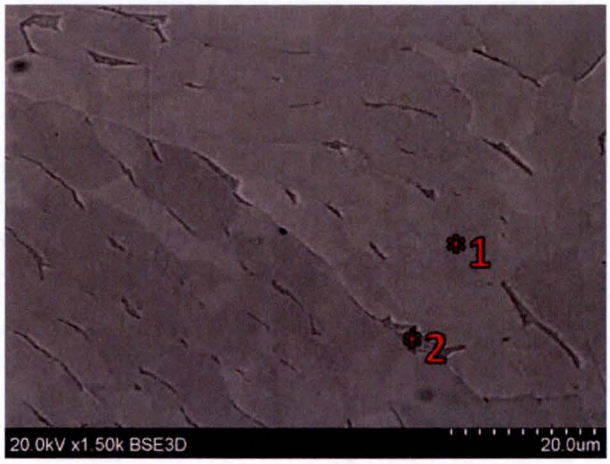

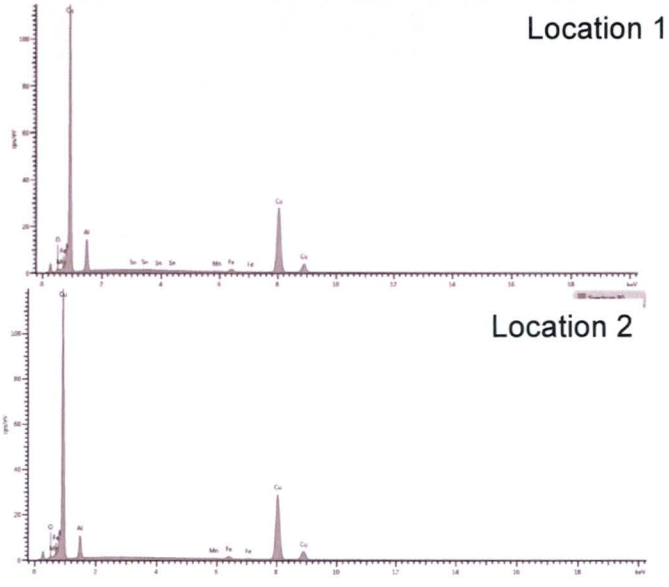

Element (wt%)		Location 1 α	Location 2 Transformed
Aluminum	Al	10.85	7.81
Silicon	Si	0.24	0.24
Iron	Fe	1.56	1.61
Copper	Cu	85.59	89.10
Other		1.77	125

Figure 5-3 – Representative BSE Micrograph (Top) of a Weld Root Microstructure from a 30-Inch Pipe Field Mockup Weld. Characterization of the Microstructural Components was Performed using EDS (Bottom Table).

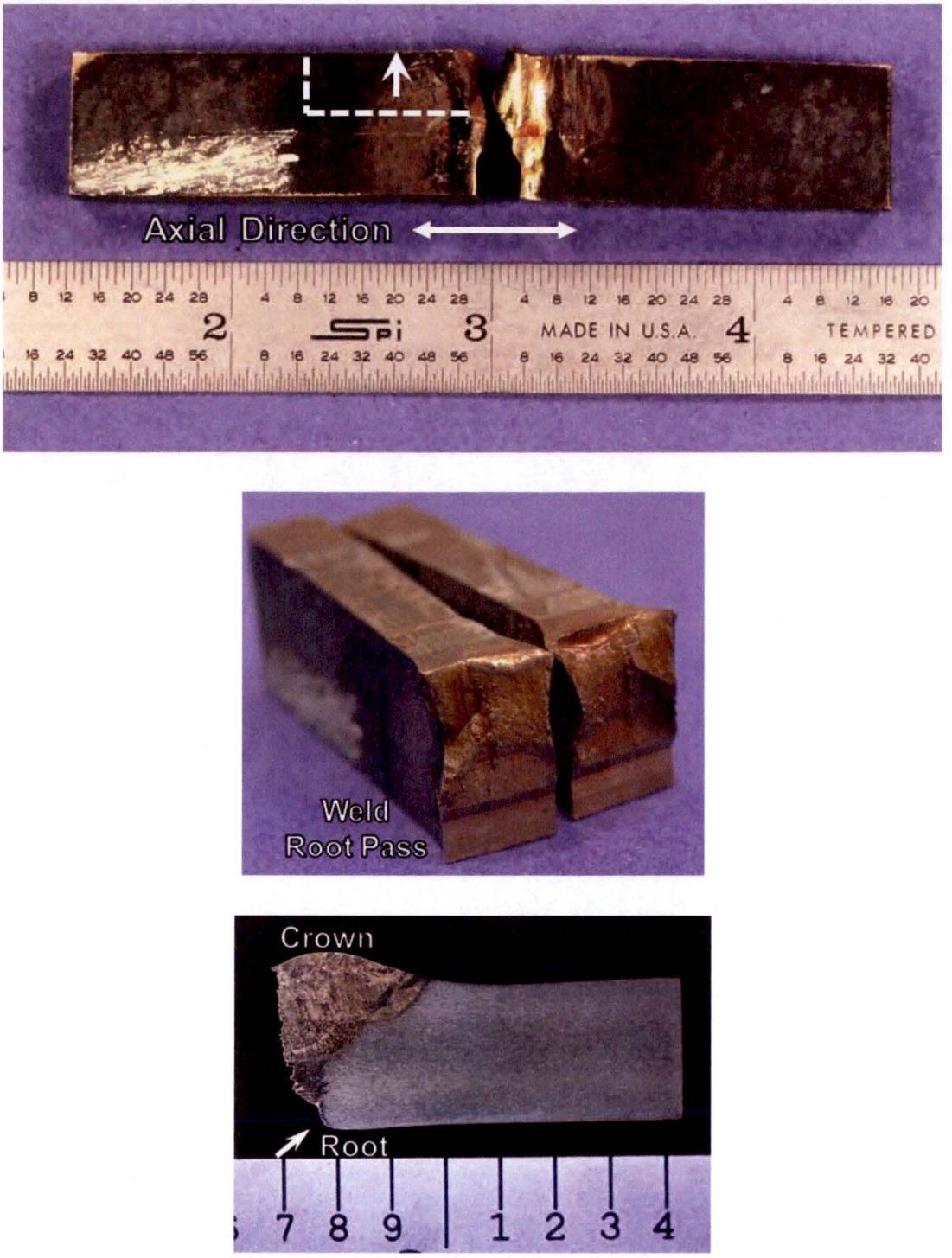

Figure 5-4 – Bend Test Specimen, Sample C1, from a 30-Inch Pipe Field Mockup Weld after Testing to Failure and Corresponding Metallographic Cross-Section Showing Weld/HAZ/Base Metal Microstructure of the Ductile Fracture Region.

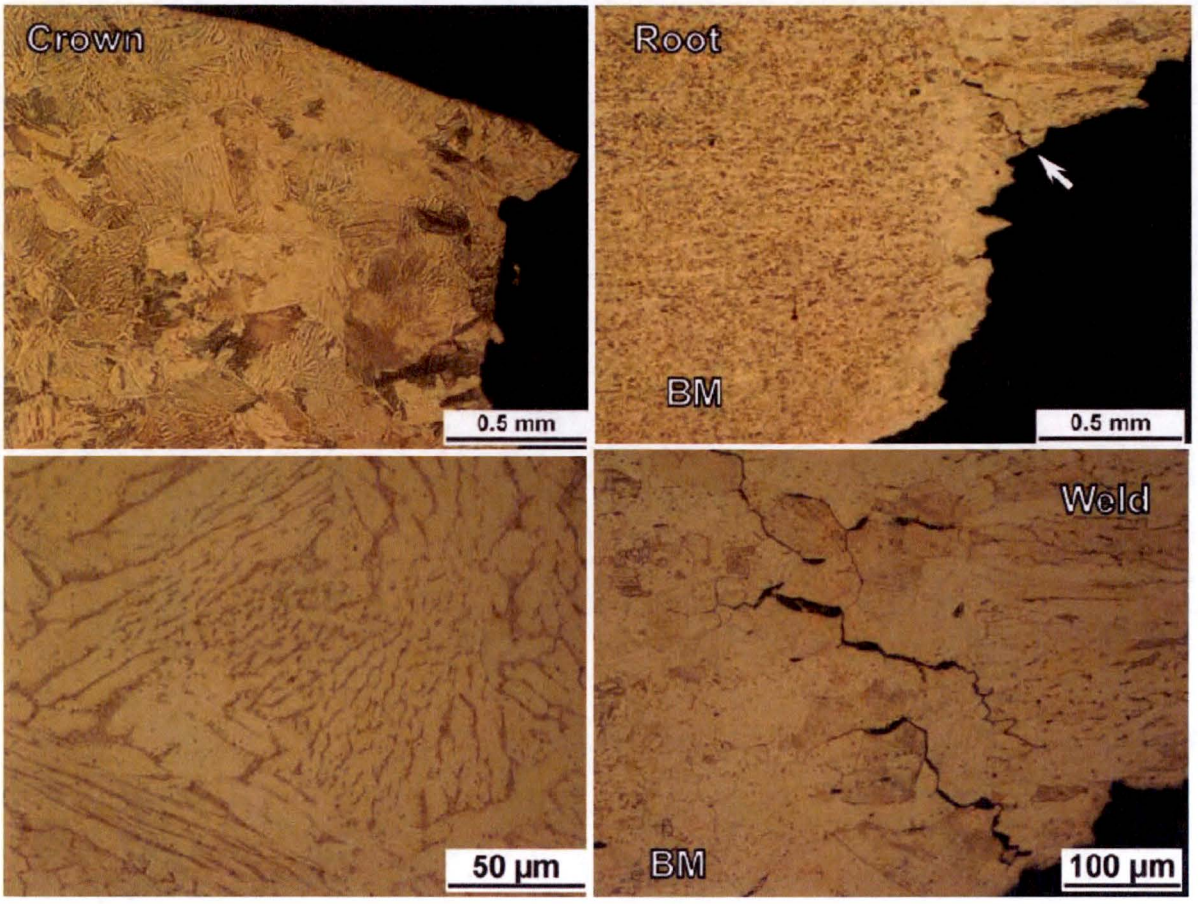

Figure 5-5 – Etched Cross-Section of a CTOD 30-Inch Pipe Field Mockup Sample Showing the Weld Microstructure at the Crown and Near Root where Ductile Fracture was Induced during Testing.

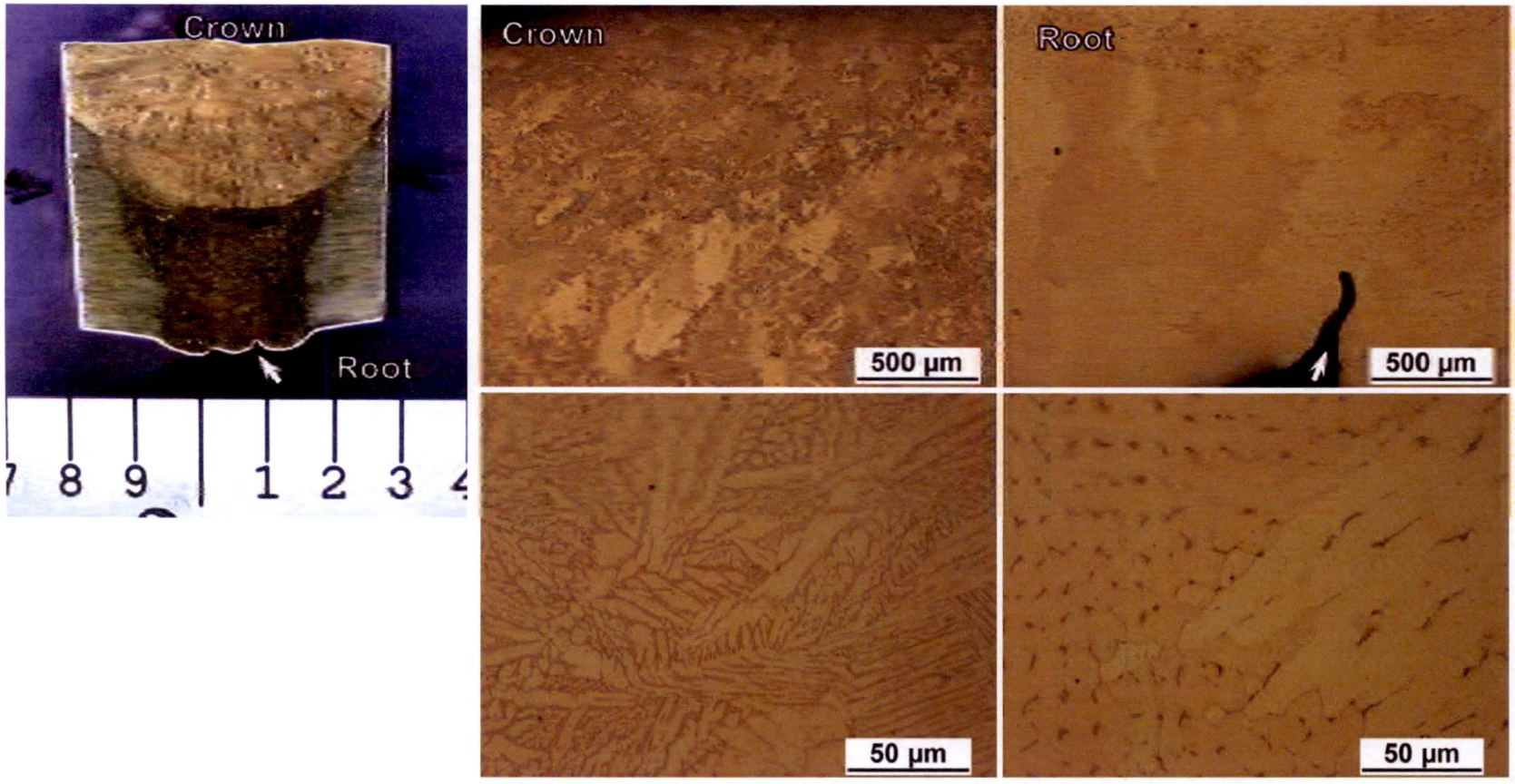

Figure 5-6 – Optical Micrograph of an Etched Cross-Section from 10-Inch Pipe Field Mockup Weld. Microstructure of the Root Shows α Grains (Light Colored Etched) and Isolated Transformed Phase (Dark Etched) and Crown Passes Consists Of Acicular α Phase and Transformed Phase.

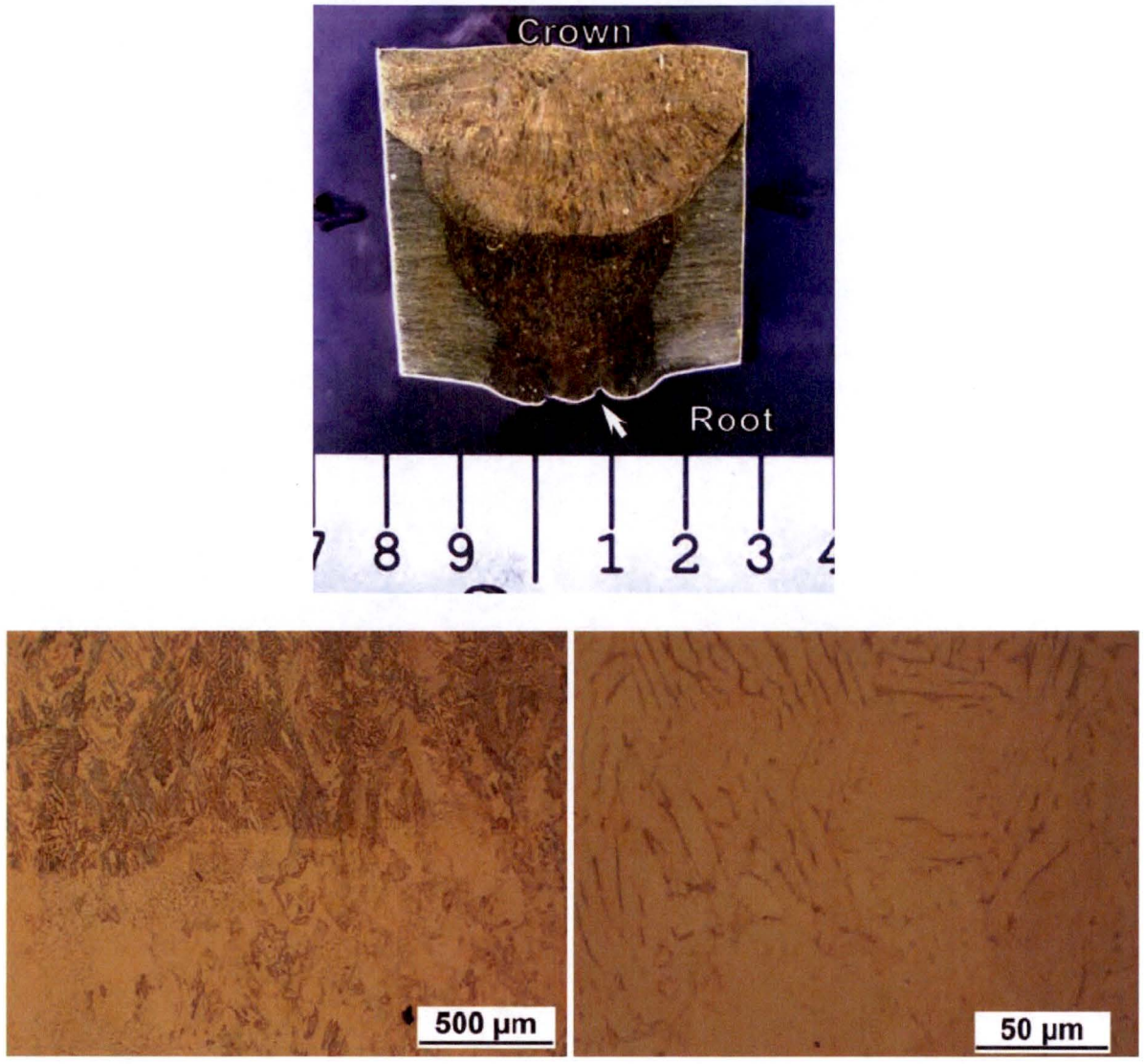

Figure 5-7 – Optical Micrograph of an Etched Cross-Section from 10-Inch Pipe Field Mockup Weld Showing the Microstructure at the Weld at Weld Inter-Pass.

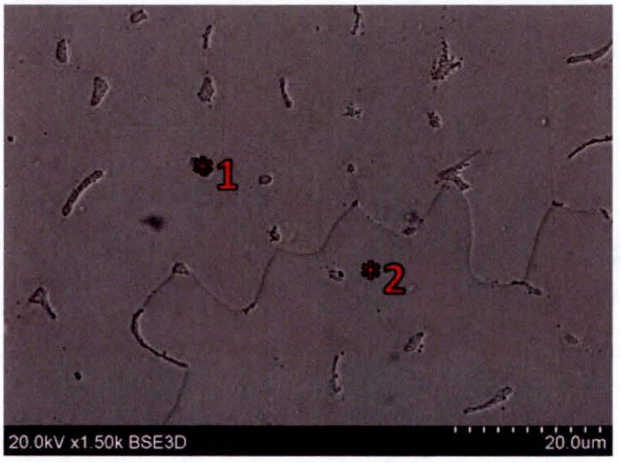

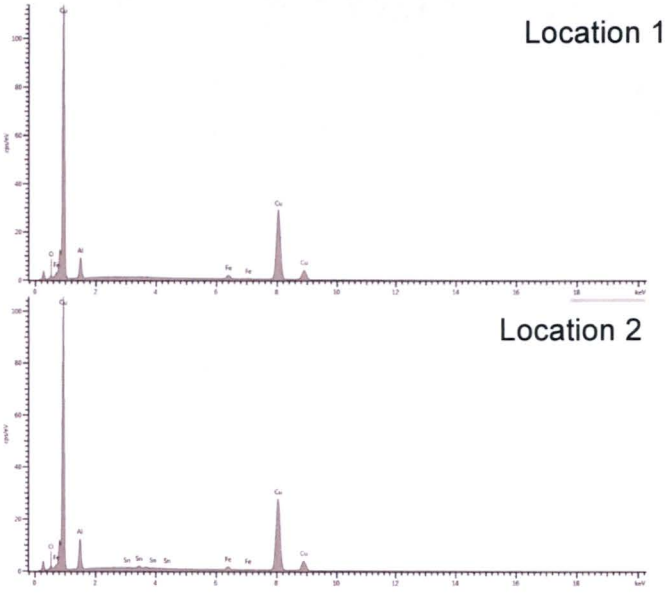

Element (wt%)		Location 1 Transformed	Location 2 α
Aluminum	Al	9.16	6.82
Iron	Fe	1.56	2.01
Copper	Cu	86.44	89.62
Other		1.27	-

Figure 5-8 – Representative BSE Micrograph (Top) of a Weld Root Microstructure from 10-Inch Pipe Field Mockup Showing Phases Present in the Microstructure. Characterization of the Phases was Performed Using EDS and Semi-Quantitative Results are Shown for the α and Transformed Phases (Bottom Table).

Figure 5-9 – Bend Test Specimen, Sample B2, from a 10-Inch Pipe Field Mockup Weld after Testing to Failure and Corresponding Metallographic Cross-Section Showing Weld/HAZ/Base Metal Microstructure of the Ductile Fracture Region

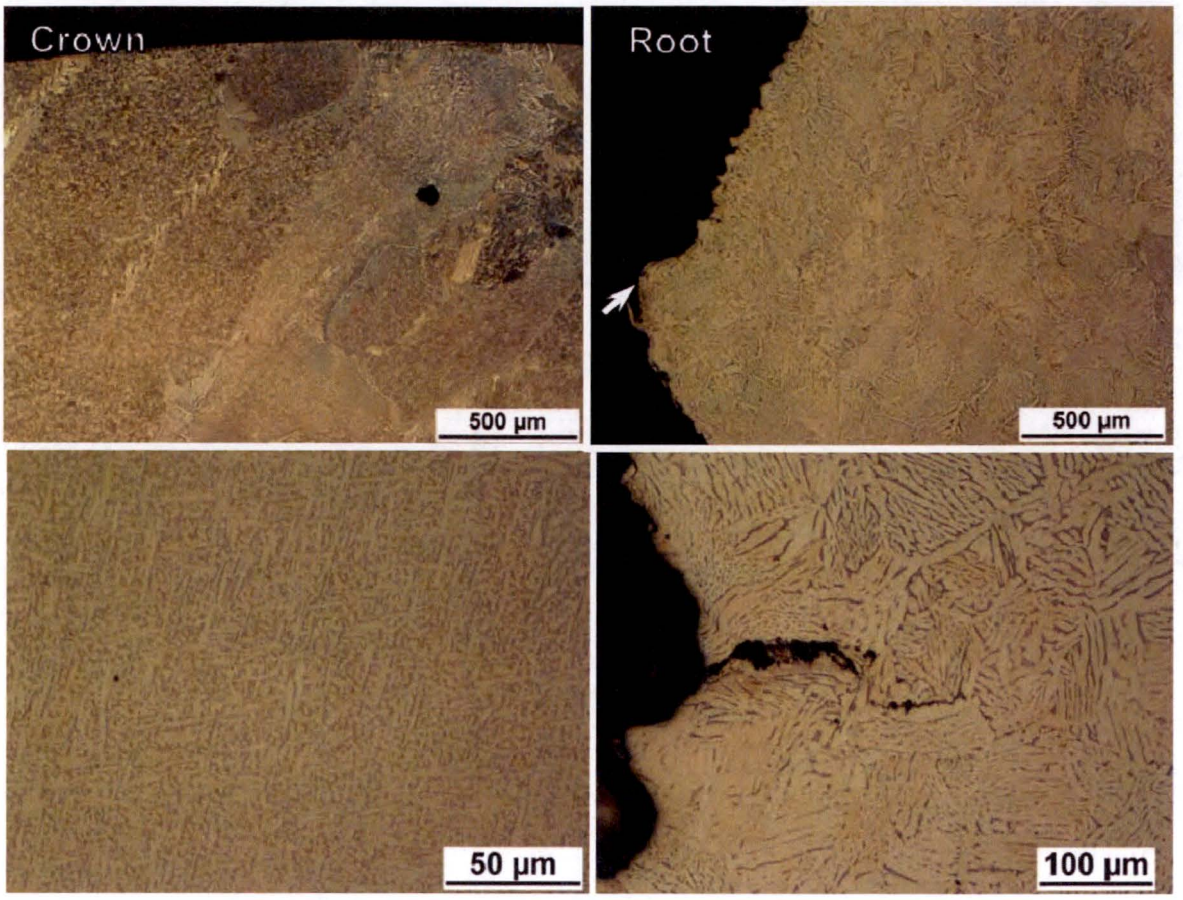

Figure 5-10 – Etched Cross-Section Showing the Weld Microstructure at the Crown and Root Near the Fusion Line where Specimen Ductile Fracture was Induced in Testing. Sample B2 is from a 10-Inch Pipe Field Mockup.

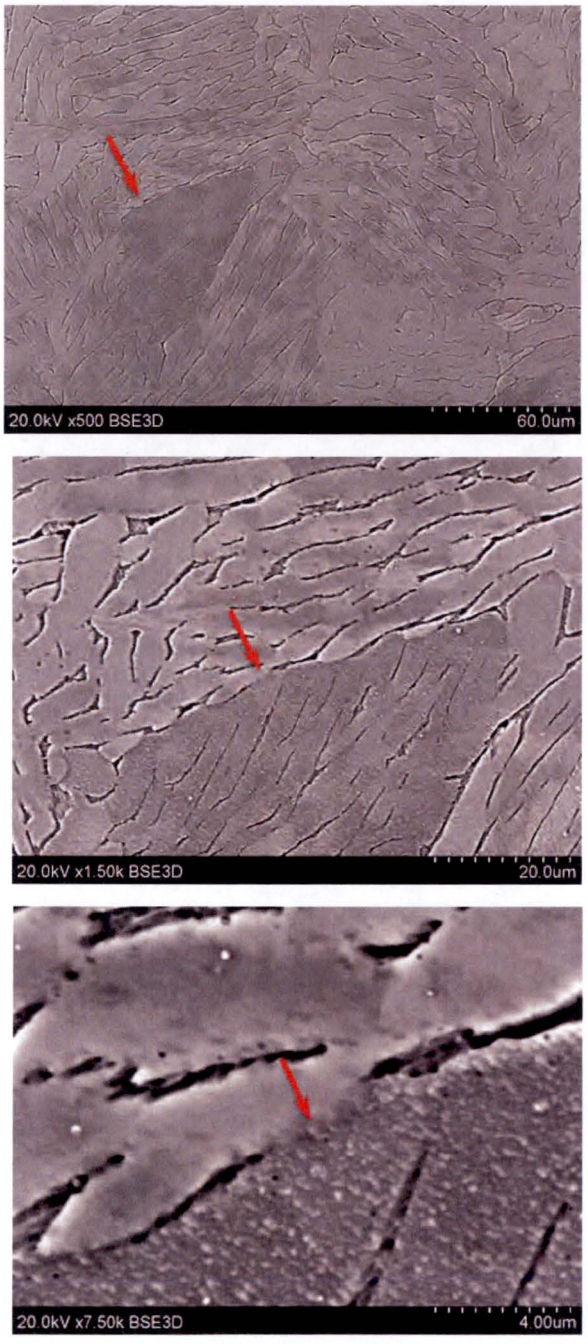

Figure 5-11 – BSE Micrographs at Progressively Higher Magnification Showing the Weld Root Microstructure for the 10-Inch Pipe Field Mockup Sample. Grain Boundaries do not Show Continuous Network of Transformed Phase.

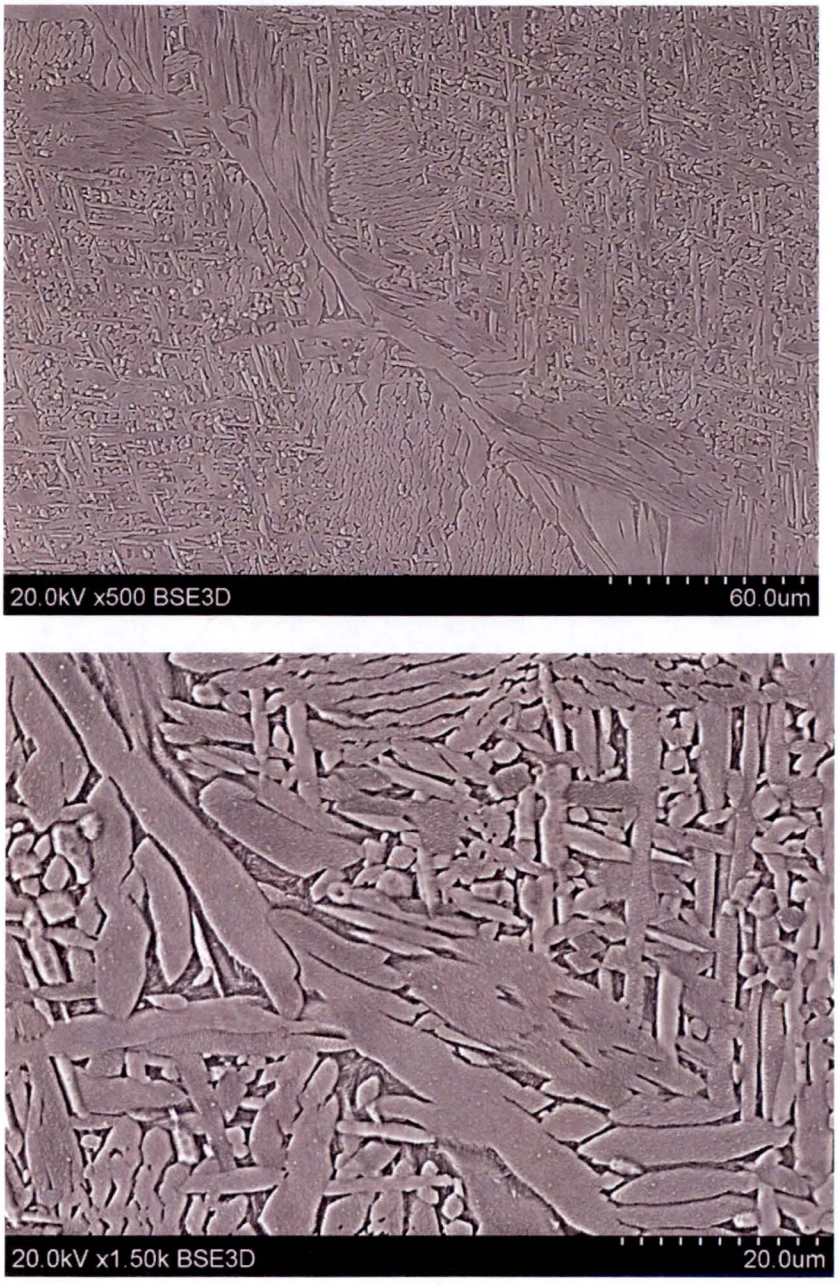

Figure 5-12 – Representative BSE Micrographs at Progressively Higher Magnification Showing the Weld Crown Microstructure 10-Inch Pipe Field Mockup Sample. Grain Boundaries Consist of α Phase Network with Interrupted Regions of Transformed Phase.

Figure 5-13 – Photograph of a 3-Inch Flange Removed from Service. Longitudinal Sections A and B were taken at the Flange-to-Pipe Weld for Microstructural Analysis.

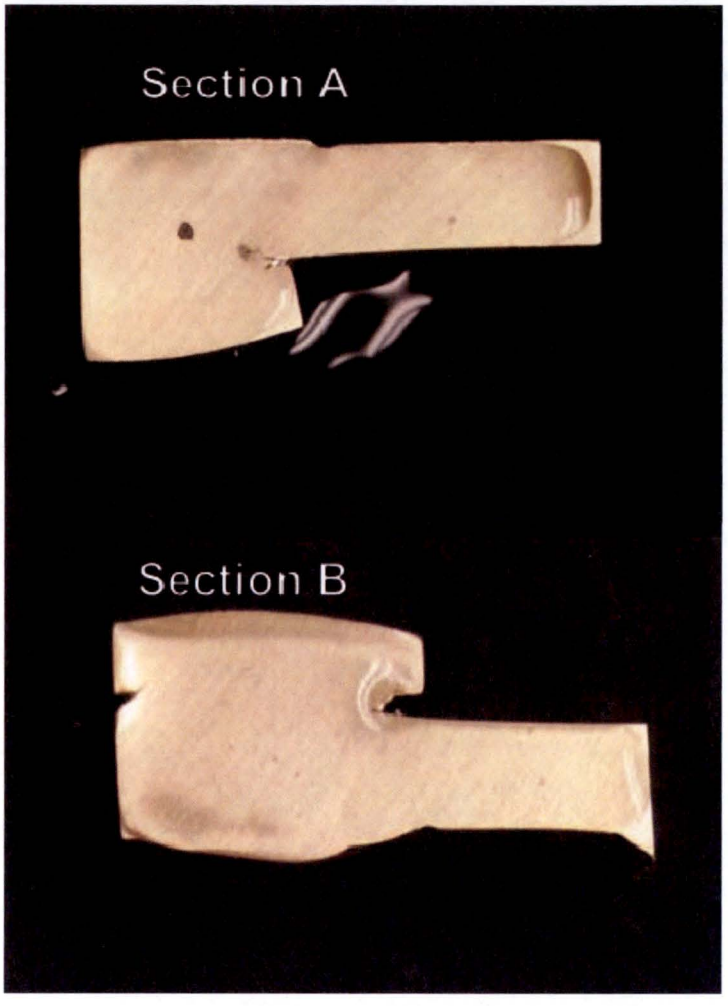

Figure 5-14 – Longitudinal Sections A and B from the 3-Inch Flange-to-Pipe Weld. Sections as Shown were Wetted with Silver Nitrate Solution to Test for the Presence of Dealloying. Indication of Dealloying (Blackish Regions) was Found In Section A at the Weld Fusion Line with Backing Ring.

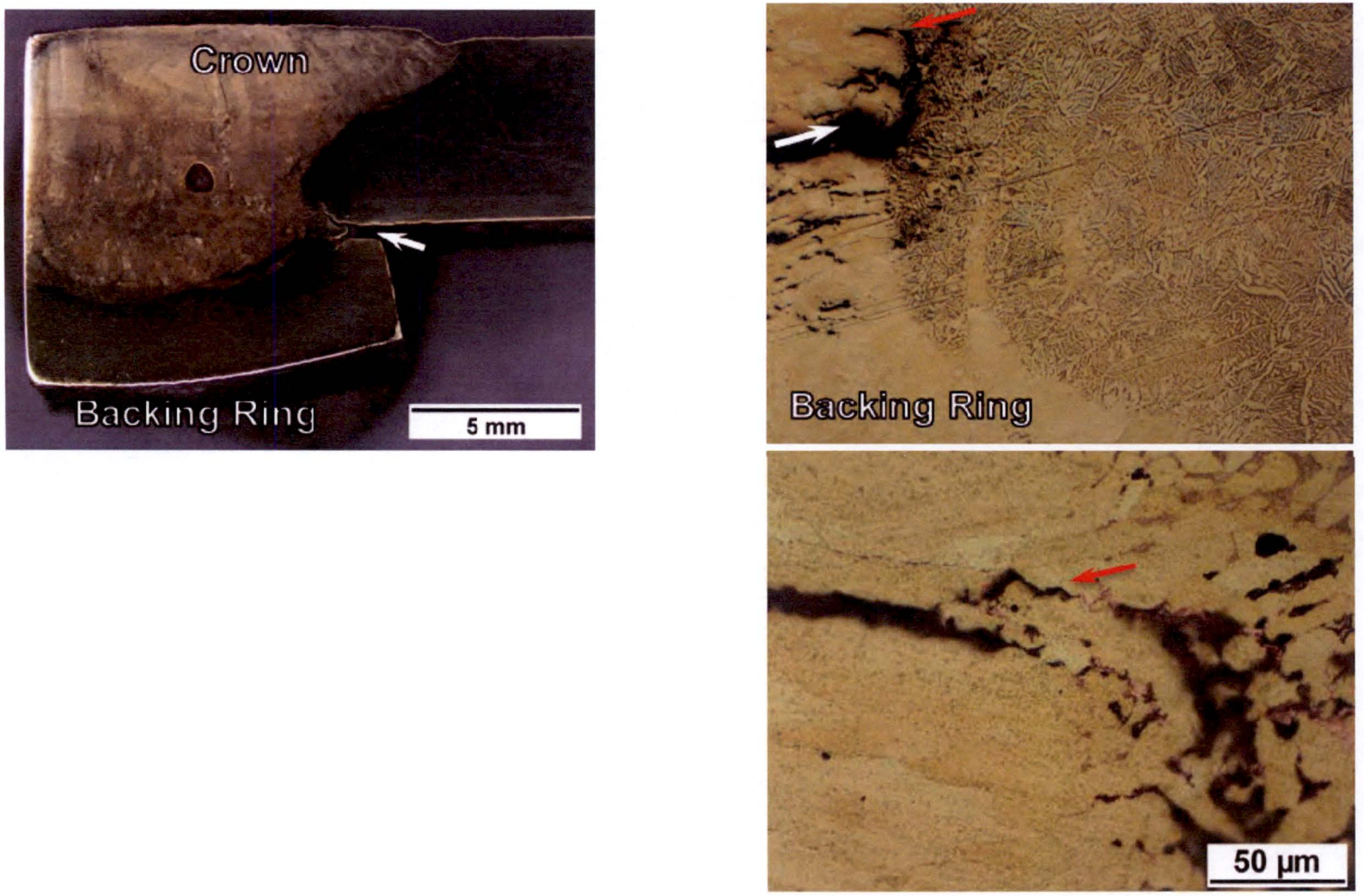

Figure 5-15 – Etched Cross-Section Showing the Weld Microstructure at the Fusion Line for Section A of the 3-Inch Flange-to-Pipe Weld. Dealloying of the Transformed Phase Region Is Evident.

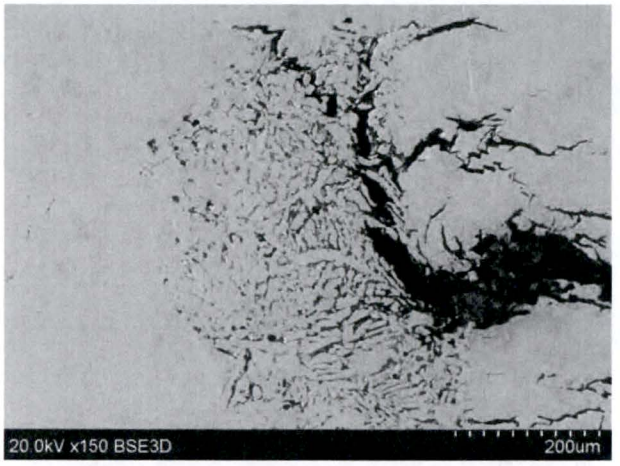

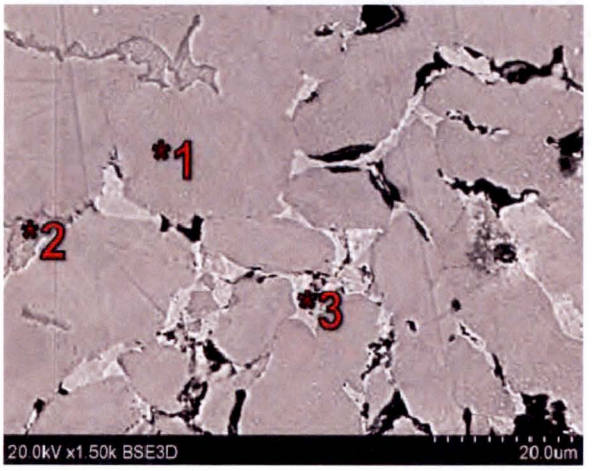

Element (wt%)		Location 1 α	Location 2 Transformed	Location 3 Dealloyed
Aluminum	Al	7.05	10.17	-
Iron	Fe	1.48	1.53	0.32
Copper	Cu	91.47	87.78	99.68
Other	-	-	0.51	-

Figure 5-16 – BSE Micrographs at Progressively Higher Magnification (Top) Showing the Weld Dealloyed Region in Section A from the 3-Inch Flange-to-Pipe Weld. Dealloying of Transformed Phase Confirmed with EDS (Semi-Quant Results in Table).

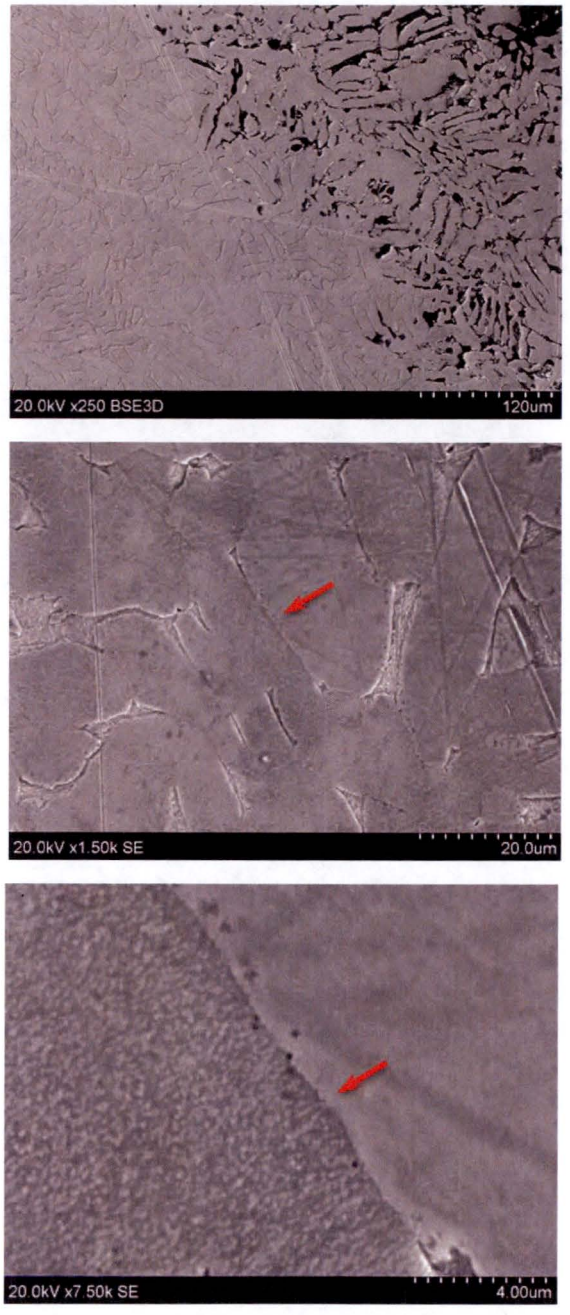

Figure 5-17 – BSE Micrographs at Progressively Higher Magnification of Section A from The 3-Inch Flange-to-Pipe Weld. Dealloying Of Weld In Semi-Continuous Network of Transformed Phase Evident (Top). Not All Grain Boundaries Contained Transformed Phase Disrupting the Network of Susceptible Phase (Arrows).

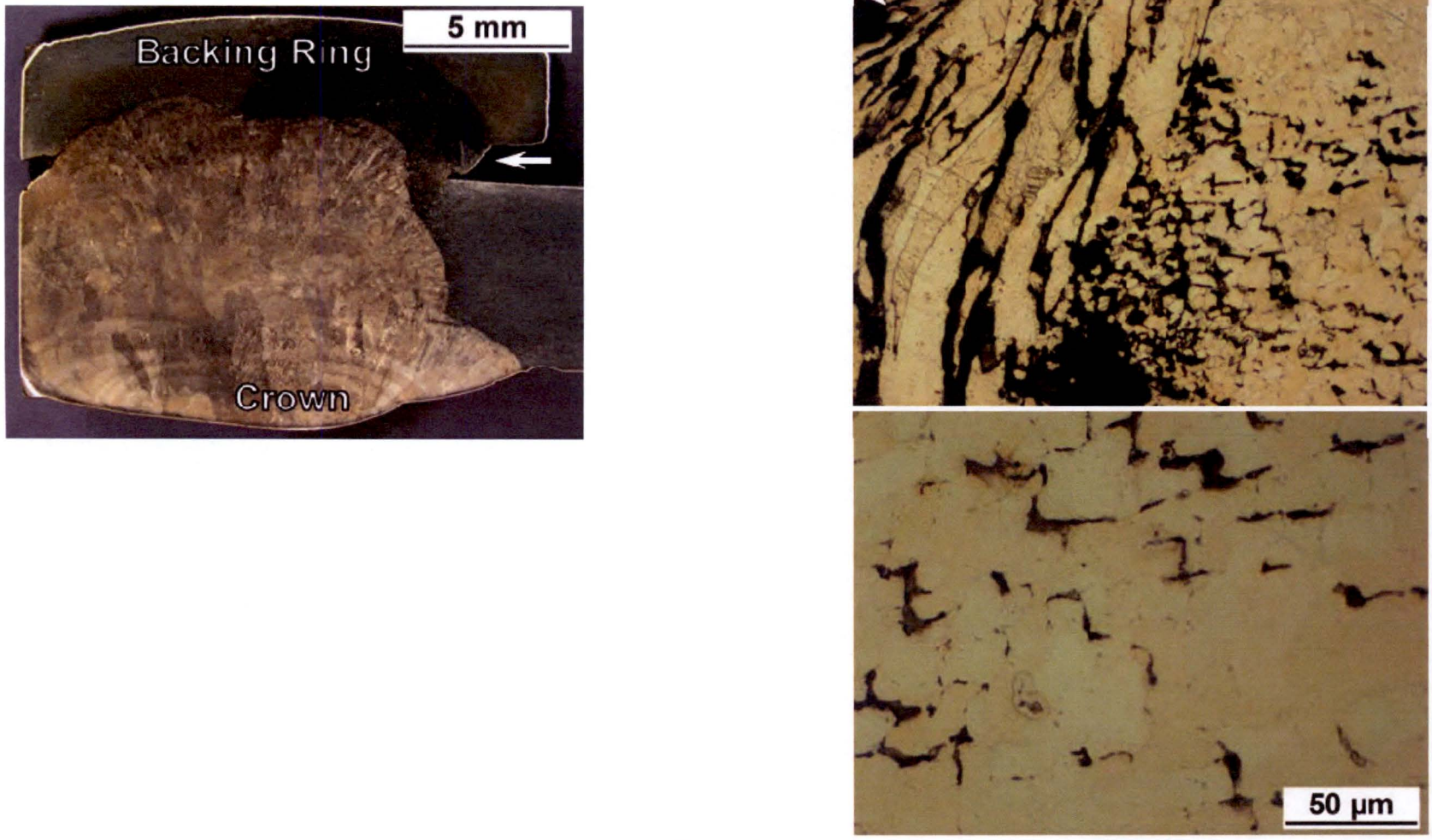

Figure 5-18 – Etched Cross-Section showing the Weld Microstructure at the Fusion Line for Section B from the 3-Inch Flange-to-Pipe Weld. Localized Area at Weld Root Displayed Ductile Tearing Consistent with Fracture Resulting from Bend Test. No Dealloying Observed.

Section 6
COMPARISON OF WELD AND CAST MICROSTRUCTURES

The susceptibility to dealloying of Al-Brz is dependent on composition and microstructure. It is known that CA952 and CA954 castings are susceptible to dealloying in ECW environment since many cast components have been replaced due to through-wall leakage. Therefore weld and casting microstructures are compared in this section. The objective is to identify clear differences in microstructural features and local chemistries within the phases.

The chemical composition of wrought pipe and castings evaluated are presented in Table 6-1. Detailed microstructural analysis of the casting was undertaken and is subject of a previous report (Ref. 8). It was concluded that dealloying in both alloys takes place only in the transformed phase, which consist of both retained β and eutectoidally transformed $\alpha + \gamma_2$ phases. A summary of the finding is presented below.

6.1 CAST MICROSTRUCTURE

Figure 6-1 shows representative optical micrographs of a cross-section taken from a cast tee made from alloy CA952. Reportedly, the cast tee was in service for 5 years in brackish water but the material did not show dealloying. Cross-sections were prepared for evaluation by polishing and etching the sample. The micrographs shows that the microstructure consists of isolated α phase (light yellow) in a matrix of transformed phase, which is likely a mixture of β and γ_2 phases (dark etching), and small iron rich precipitates (Fe_3Al) dispersed throughout.

The α phase is a Cu rich face-centered cubic with structure (α_{Cu}) that results from a solid state transformation from the β phase at temperatures below 1037°C. As a result, β is retained at grain boundaries and triple points depending on undercooling, which is the change in temperature from the equilibrium melting temperature where all phases are liquid. Retained β phase consists of a mixture of α, γ_2 and martensitic β (or β') that is metastable at room temperature. In contrast, under conditions that allow for slow cooling of the casting and

complete transformation, the β phase transforms eutectoidally to a mixture of $\alpha + \gamma_2$ at 565°C when aluminum content is greater than ~9.5 wt.%. The β and γ_2 phases are both body-centered cubic and are only distinguished by composition and lattice spacing and can only be differentiated with advanced x-ray or electron diffraction techniques. The iron precipitates form early during the casting process and are distributed in the microstructure.

Semi-quantitative composition of the phases was performed using energy dispersive x-ray spectroscopy (EDS). EDS is a technique that employs an electron microscope equipped with a spectrometer for detection of characteristic energy peaks of the elements present in the specimen. Only elements from Be to U are detectable. Semi-quantitative analysis of the amount of each element can be performed.

Distinct composition differences between α and transformed β phase are evident, as shown in Figure 6-2 for alloy CA952. Each distinct phase was probed as shown in the secondary electron micrograph in the top; corresponding characteristic energy spectra and compositions are also presented. The α phase shows Al content of 10.016 wt% (Location 1) as compared to β phase with higher Al content at 14.834 wt% (Location 2). Furthermore, retained β was found at grain boundaries forming a continuous network and potential path for dealloying of the casting.

Similarly, optical micrographs of the typical microstructure of a CA954 cast valve body are presented in Figure 6-3. The cast valve had been in service for 26 years and failed due to dealloying. The microstructure comprises isolated α (light etch) in a matrix of transformed phases (dark etched) and iron rich precipitates (grey etched). The transformed phase presents a continuous network that surrounds large α grains. Transformed phase morphology is easily distinguished in the higher magnification image (Figure 6-3, bottom) where the layered structure of the α and γ_2 mixture, and possibly martensitic β phase (β'), is obvious.

Individual phases and precipitates were characterized for composition using EDS in CA954 are shown in Figure 6-4. The top micrograph shows the locations where analysis was performed and the corresponding spectra are presented in the figure. The α phase grain shows low aluminum content of about 6.705 wt% (Location 1), while the transformed β phase (Locations 2 and 3) had an aluminum content between 9.254 wt% and 9.599 wt%. It should be noted, that

the transformed phase in CA954 also contains a large volume fraction of α phase and therefore the averaged aluminum content is lowered. Lastly, the iron rich precipitates showed an aluminum content of 7.890 wt% and iron content of 82.865 wt% (Location 4). The higher aluminum (Al) content of transformed β phases and iron rich particles renders them susceptible to dealloying.

6.2 COMPARATIVE RESULTS

X-ray diffraction (XRD) was used for partial phase identification. Acquired line patterns are shown in Figure 6-5 for a representative weld and casting specimens (Ref. 12). XRD data were collected by a coupled 2Theta scan on a Bruker D8 Vantec diffractometer equipped with a micro-focus copper x-ray tube with Montel optics, 50 μm collimator, and a Vantec 500 2-D area detector. Due to the very small areas of interest, several areas of supposed similar composition were sampled.

XRD patterns were acquired from mounted and polished cross-sections used for metallographic evaluation of a CA954 casting and a 30-inch welded pipe sample (Sample 1). An x-ray spot size of 50 μm was employed in order to sample a local area with high fraction of transformed phase and minimize the acquisition of diffracted peaks from the α phase. The results of the analysis, although not conclusive, showed distinct peaks for crystalline phases and could closely be matched to α phase in both specimens. However the CA954 specimen (Figure 6-5b) showed additional diffraction peaks between the 40° 2Theta and 50° 2Theta, which could correspond to martensitic β or γ phases (or β' and γ' correspondingly). Although conclusive phase identification was not possible due to measurement uncertainties, the XRD patterns reveal qualitative structural differences between the casting and weld samples. Most notably, the presence of transformed metastable β' and γ' in the casting, both of which are highly susceptible to dealloying.

Table 6-2 tabulates the volume fraction and morphology of transformed phase present in the weld and casting microstructures. A semi-continuous network of transformed phase is observed in the welds at the root and crown. Semi-continuous morphology is characterize by lack of long range connectivity of the transformed phase; in other words, locally the transformed phase may be connected but a long range continuous network is disrupted by α rich regions that formed at prior β grain boundaries. Furthermore, networks of α phase boundaries are observed between

filler passes in the multi-pass welds. The semi-continuous morphology is most prevalent in the filler and crown passes of the pipe welds; an example is shown in Figure 6-6 for the 30-inch field removed weld. Typical transformed phase volume fractions are between 10% and 23% at the root of the weld or 6% and 32% at the crown (Table 6-2). Under some conditions or rapid cooling and low aluminum content, the volume fraction of the transformed phase is discontinuous and discrete (Figure 6-6, 10-inch field weld). Discontinuous transformed phase is present in volume fractions ranging from 5% to 22% as reported in Table 6-2 and shown in Figure 6-6 for a representative 10-inch field fabricated weld. Continuous networks of transformed phase were not evident in the multi-pass welds.

The morphology of the welds shows stark contrast to the casting morphology. A continuous and long range network of transformed phase is observed in both casting alloys (CA952 and CA954) and was confirmed with EDS analysis of representative cross-sections. Volume fraction measurements, in Table 6-2, for CA952 determined that 10% of the material consists of transformed phase and iron rich precipitates. Microstructure morphology and phase composition for CA952 was discussed and shown in Figure 6-1, and a comparison in Figure 6-6. Alloy CA954 shows isolated α phase surrounded by transformed phase (Figure 6-3 and Figure 6-6); the volume fraction was measured at 41% (Table 6-2); therefore, the alloy shows the highest susceptibility to dealloying.

The cooling rates for Al-Brz pipe welds will be much faster than the normal cooling rates expected for the cast components. The faster cooling rate of the weld, especially the root pass, will not promote conditions to form continuous transformed phase of (α + β). Figure 6-7 shows the expected phases in Al-Brz for a range cooling times from 900°C to 400°C (start and end of phase transformation) as a function of Al content.

Appendix A discusses the numerical analysis where the cooling rates in the root pass of 10-inch and 30-inch pipe weld were estimated by heat transfer analysis. The cooling rate in the first weld pass was the main interest since the root pass is the initial barrier for resisting the initiation and propagation of dealloying though the weld thickness. The numerical results show that the time to cool through the transformation period for the alloy is about 0.6 minutes. The combination of the cooling rate and Al content indicates that the transformed phase will be α + β for Al content up to about 9.5 wt%. The γ_2 phase will not have time to form for Al contents measured in the weld samples. It is known that the absence of γ_2 improves the corrosion

resistance against general dealloying. These analytical results as shown in Figure 6-7 support the microstructure evaluation findings for the field weld samples not having a continuous phase boundaries, and the observed better performance of the pipe welds versus the cast components in ECW service.

6.3 SUMMARY OF FINDINGS

Intrinsic microstructural differences exist between weld and cast structures that are due to composition differences and solidification rates (i.e. cooling rates). It should be noted that:

1) Continuous networks of transformed phase were not evident in the multi-pass welds; moreover, due to the transformation of α phase at former β grain boundaries the networks of transformed phase are disrupted.
2) The welds are less susceptible to general dealloying than the castings due to the significantly different microstructures (isolated and lesser volume fractions of the transformed phase in the weld metal).
3) The different microstructures between the welds and castings is the result of lower (diluted) Al content in the weld metal and the faster cooling rates associated with the weld solidification process.

Table 6-1

MATERIAL CHEMICAL SPECIFICATIONS FOR WELDS AND CASTINGS

Element	Wrought Pipe SB-315 CA614	Weld Metal ERCuAl-A2	Casting SB-148 CA952	Casting SB-148 CA954
Cu	Remainder	Remainder	86.0	83.0
Al	6.0 – 8.0	8.5 – 11.0	8.5 – 9.5	10.0 – 11.5
Fe	1.5 – 3.5	0.5 - 1.5	2.5 – 4.0	3.0 – 5.0
Si	-	0.10 max	-	-
Mn	1.0	-	-	0.5 max
Ni	-	-	-	2.5 max
Zn	0.20 max	0.20 max	-	-
Pb	0.01 max	0.02 max	-	-
P	0.015 max	-	-	-

Table 6-2

VOLUMETRIC FRACTION OF MAJOR PHASES IN WELDS AND CASTINGS

Sample		Alpha Volume	Transformed Phase + Precipitates Volume %	Transformed Phase Morphology
6-inch Pipe Weld Field Mock-Up, Sample A	Root	90%	10± 2%	Semi-continuous
	Crown	85%	15± 2%	Semi-continuous
10-inch Pipe Weld Field Mock-Up, Sample C1	Root	95%	5± 2%	Discontinuous
	Crown	84%	16± 2%	Semi-continuous
10-inch Pipe Weld Field Mock-Up, CTOD Sample B2	Root	94%	6± 2%	Discontinuous
	Crown	77%	23± 2%	Semi-continuous
30-inch Field Removed	Root	77%	23± 2%	Semi-continuous
	Crown	68%	32± 2%	Semi-continuous
Cast CA952		90%	10 ± 2%	Continuous
Cast CA954		60%	40 ± 1%	Continuous

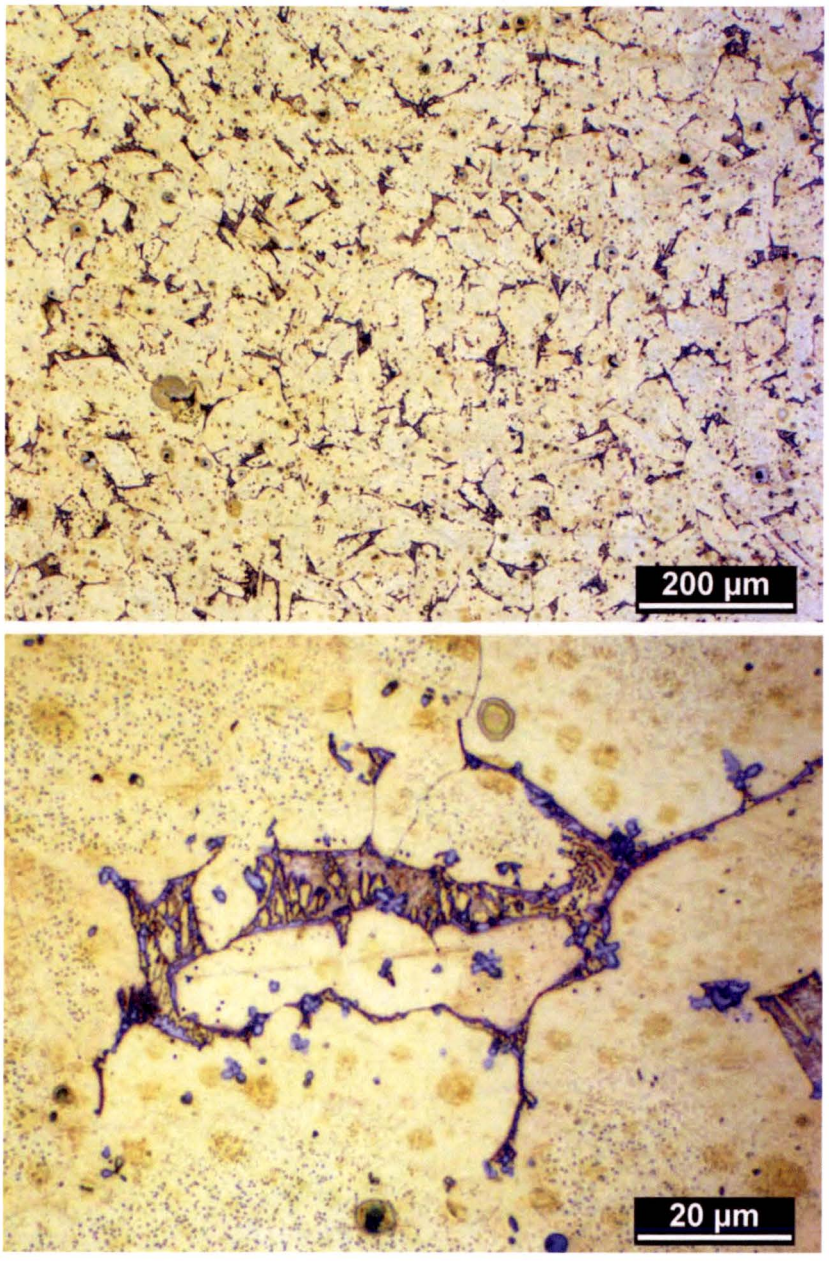

Figure 6-1 – Optical Micrographs of Virgin Cast Alloy CA952 (No Dealloying Shown).

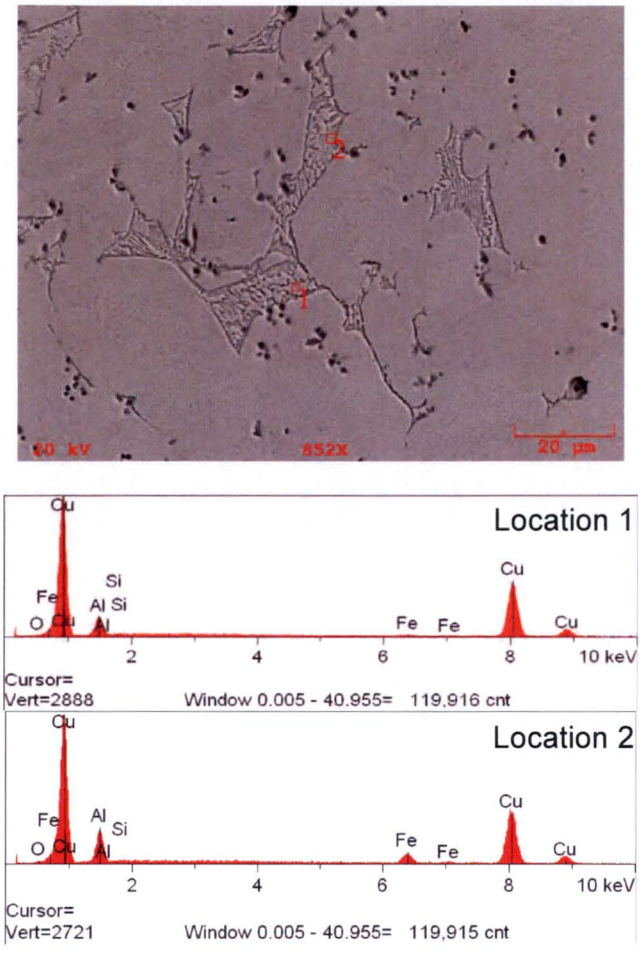

Element (wt%)		Location 1	Location 2
Aluminum	Al	10.016	14.834
Silicon	Si	0.041	0.028
Iron	Fe	0.843	5.377
Copper	Cu	89.100	79.762

Figure 6-2 – EDS Locations of Selected Phases in Non-Dealloyed CA952 Material after ~5 Years of Service in Brackish Water.

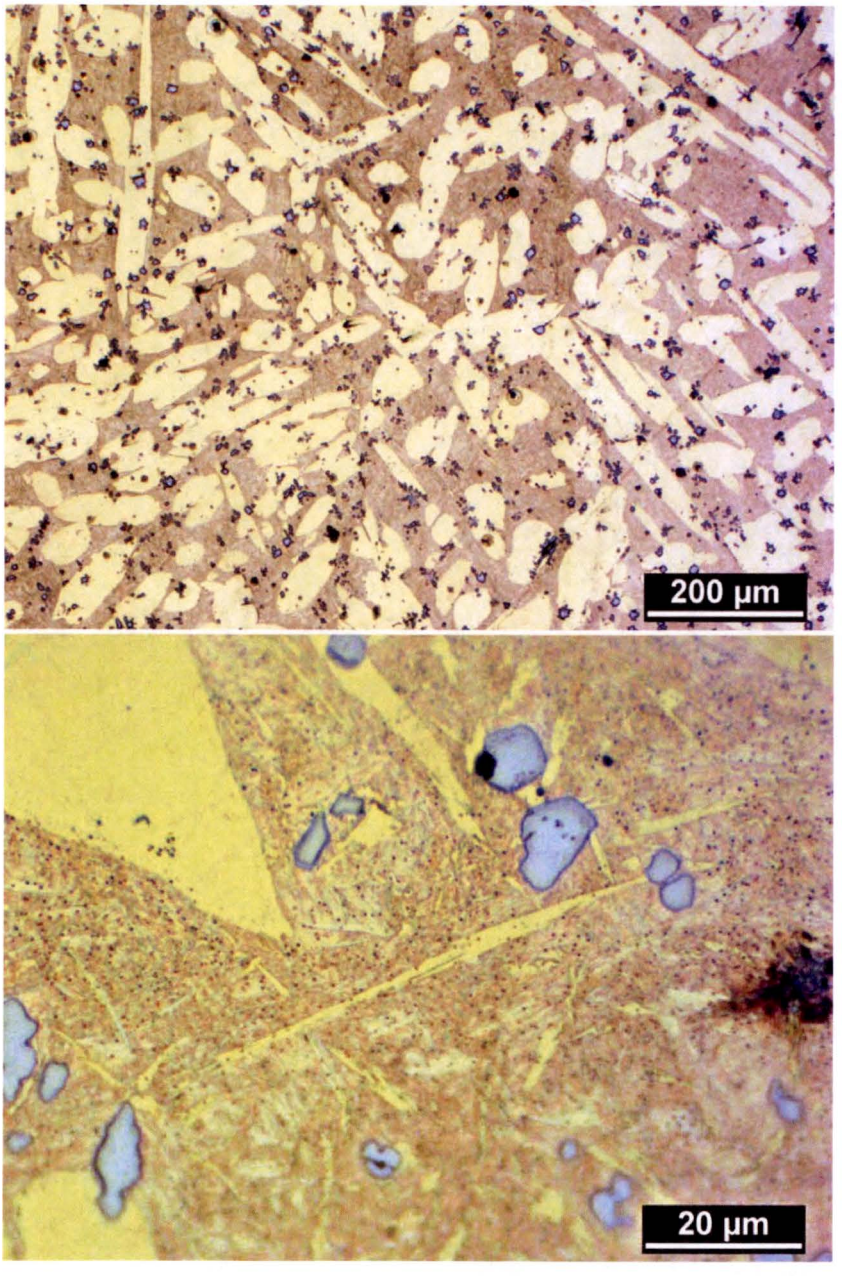

Figure 6-3 – Optical Micrographs of Virgin Cast Alloy CA954 (No Dealloying Shown).

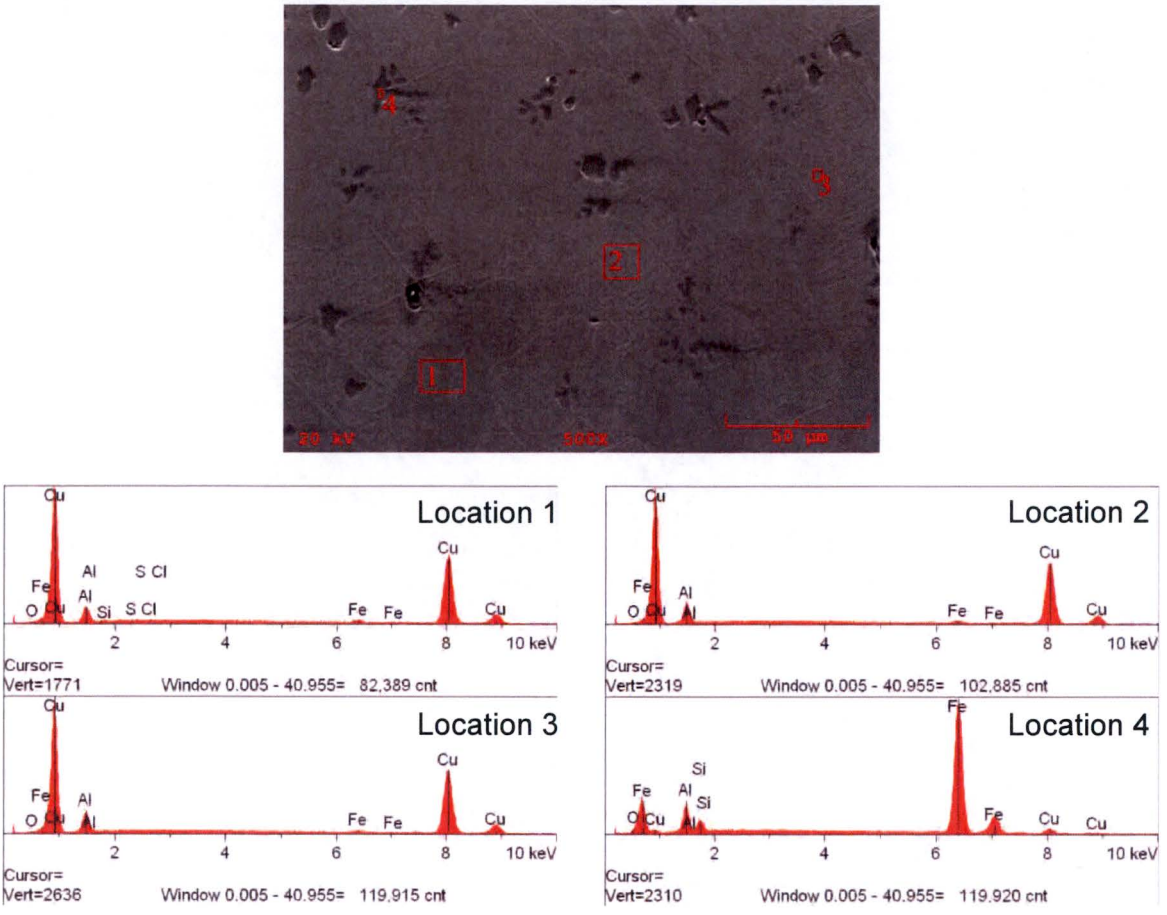

Element (wt%)		Location 1	Location 2	Location 3	Location 4
Aluminum	Al	6.705	9.254	9.599	7.890
Silicon	Si	-	-	-	2.619
Iron	Fe	1.000	0.794	0.587	82.865
Copper	Cu	92.098	89.952	89.814	5.384

Figure 6-4 – EDS Locations of Selected Phases in Dealloyed CA954 Material after ~5 Years of Service in Brackish Water.

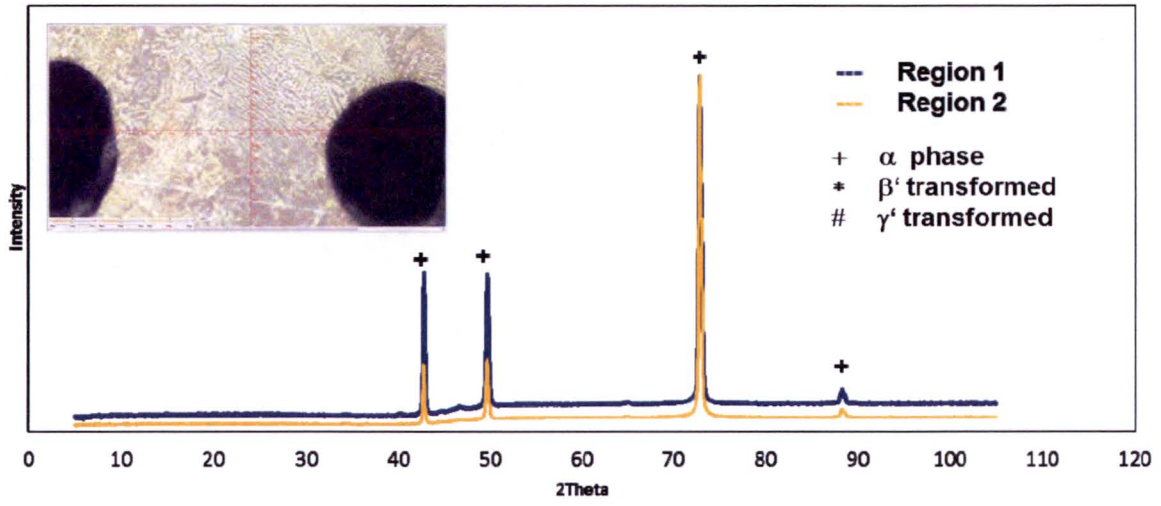

(a) Weld

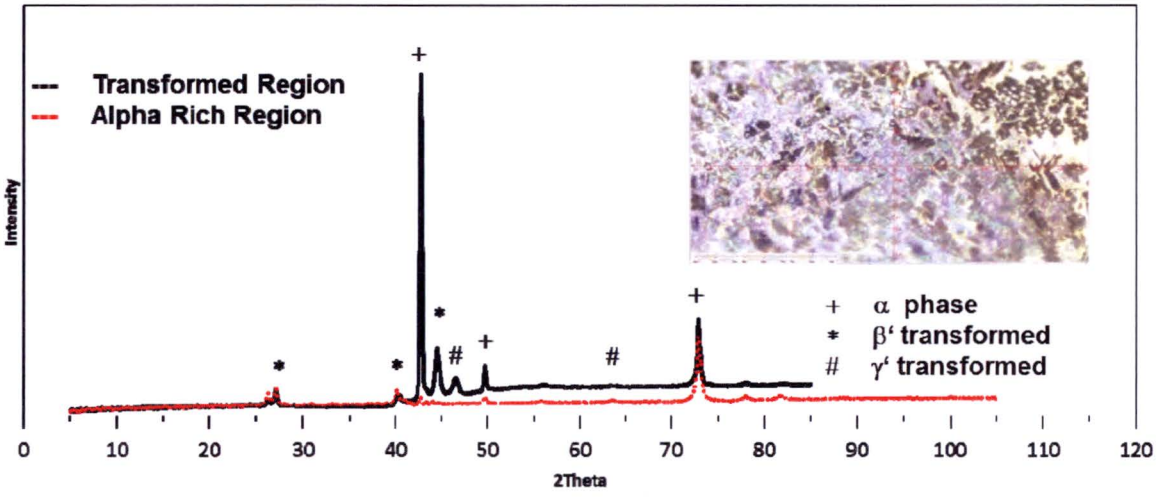

(b) Casting CA954

Figure 6-5 – XRD Line Patterns of (a) Representative Weld Microstructure, and (b) CA954 Casting. Partial Phase Identification was Performed and Peaks for α, β', and γ' were Observed for the CA954 Casting.

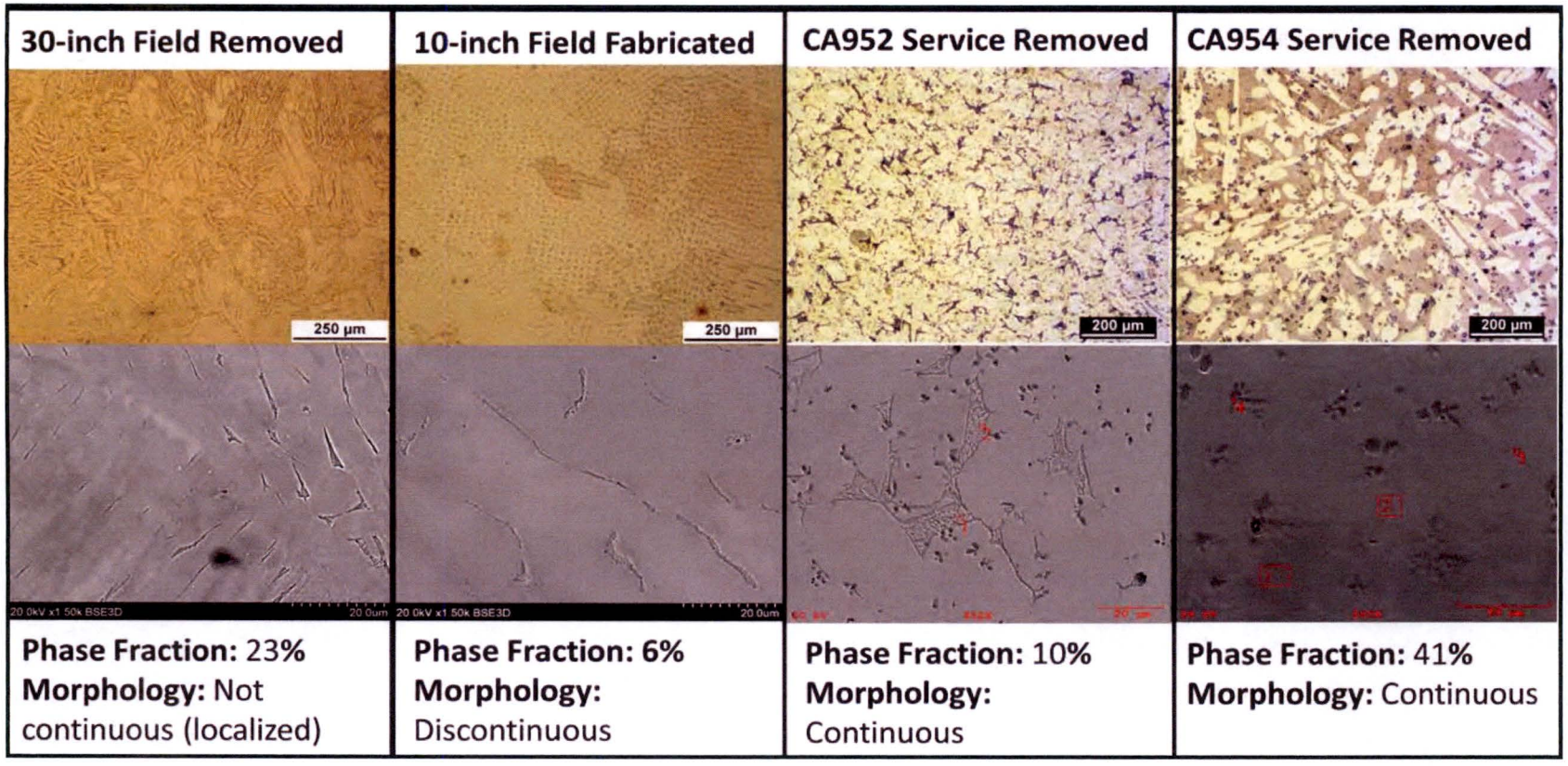

Figure 6-6 – Microstructure Comparison of Representative Sections from Welds and Casting Samples.

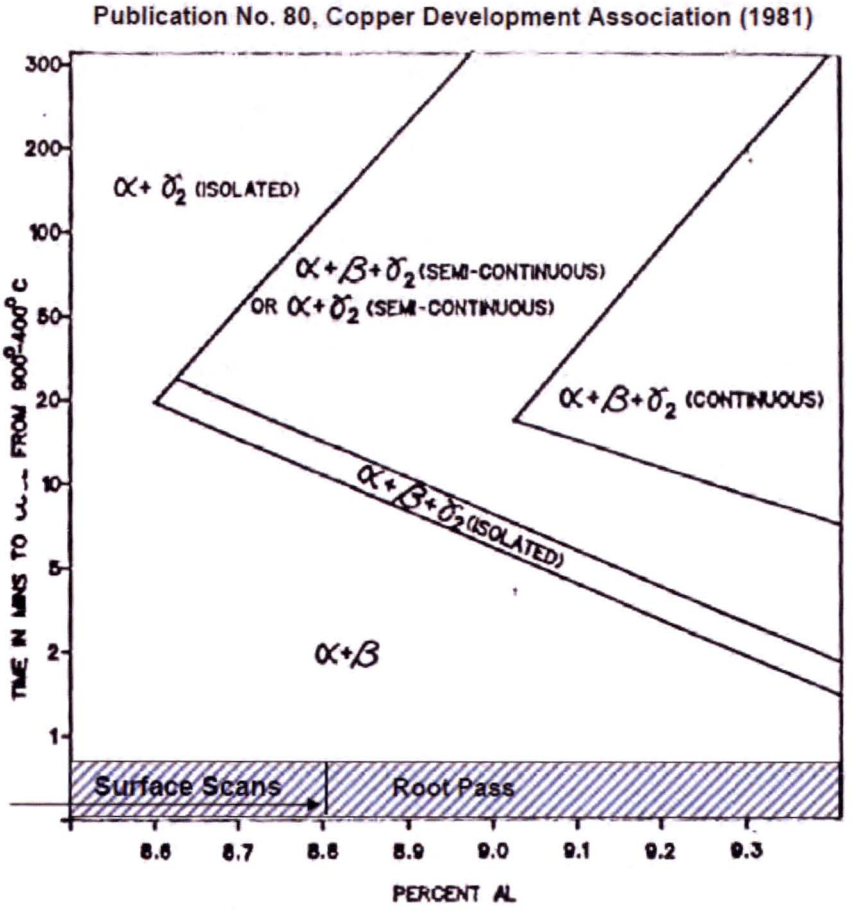

Figure 6-7 – Time-Temperature Phase Transformation Diagram for Al-Brz.

Section 7
SUMMARY AND CONCLUSIONS

A detailed metallurgical evaluation and analytical assessment of the welding process has been completed to establish the microstructural characterization of pipe-to-pipe butt welds of Al-Brz piping in the ECW system. This investigation included

1) Chemical composition measurements to determine the variation of Al and Fe content in the as-welded joint, both transverse and through-thickness directions, as determined by EDS
2) Microstructure features and characterization of transformed phases within the dendrites and at interdendritic, prior β-phase, boundaries between weld passes using light microscopy, SEM, and XRD
3) Comparative study of the microstructure of castings, which are known to be susceptible to dealloying in ECW environment, with the microstructure of the pipe-to-pipe welds that have not shown gross dealloying
4) Numerical heat transfer analysis using FEA to calculate the cooling rate to study the effect of cooling rates on the morphology and composition of the transformed phase in the root pass

Metallurgical analysis confirmed the microstructural constituents in welds consisted of primary α grains with transformed phase (eutectoid) forming a semi-continuous or discontinuous network that did not show long range connectivity in the multi-pass welds. In contrast, the castings showed a continuous morphology for the transformed material allowing for dealloying to proceed undisrupted through the thickness resulting in leakage. Preliminary XRD analysis of both cast and weld samples showed evidence that transformed phase in the castings contain β and γ_2. Evidence of γ_2 was not seen in the welds in the limited sampling performed. The presence of γ_2 is known to promote dealloying due its higher Al content making that phase more susceptible to corrosion attack.

The cooling rate in the welding process is much faster than for cast components. The isolated nature of the transformed material in the pipe welds is due to the fast cooling rate and lower bulk Al content, and therefore lower phase fraction of transformed phase, in the weld pool during solidification. Aluminum dilution was measured in the weld metal where a lower volume fraction of eutectoid phase was observed. The aluminum dilution is due to the joining of the lower aluminum wrought pipe with the higher aluminum weld wire. The dilution is more pronounced in the root pass compared to the subsequent filler passes which makes the first pass the most resistant region of the weld to general dealloying corrosion.

Localized dealloying was observed in the weld region near a crevice from a 3-inch flange-to-pipe weld (with backing ring) which was removed from service. The dealloying was restricted to the transformed phase within a localized area where the transformed phase formed a semi-continuous network but did not extend beyond. The eutectoid phase within the weld, being segregated and contained within the former β-boundaries (e.g., dendrites) that were created during solidification, did not exhibit a continuous network of transformed material from root to crown was not observed.

Based on the metallurgical findings and analytical calculations to establish cooling rates during phase formation, the following conclusions are reached:

1) The pipe-to-pipe welds are less susceptible to general dealloying than the castings due to significantly different microstructures. The transformed phases are isolated and exhibit smaller volume fractions of the eutectoid in the weld metal compared with the more susceptible castings. Therefore, dealloying through the component thickness is not expected in pipe-to-pipe welds
2) The weld metal, specifically the root pass, has a more resistant microstructure and chemical composition to dealloying compared to the filler passes
3) Formation of γ_2 in the welds is not likely due to rapid cooling during phase transformation.
4) Local dealloying at wetted crevices, if it occurs, is expected to be contained within the former dendrites and non-propagating

REFERENCES

1. STP Relief Request, ST-HL-AE-3984 (January 17, 1992).
2. "Structural Integrity Analysis of Essential Cooling Water Lines (South Texas Project)," Aptech Engineering Services, AES 8303381 Final Report, Rev. 0 (June 1983) and Rev. 1 (July 1983).
3. "Structural Testing of 3-inch, 8-inch, and 10-inch Aluminum-Bronze Flanges Removed from the Essential Cooling Water System," Intertek AIM Report AES 13078445-2Q-1, (December 2013).
4. "Profile Examination of 3-inch, 8-inch, and 10-inch Aluminum-Bronze Flanges Removed from the Essential Cooling Water System," Intertek AIM Report AES 13078445-2Q-2, Rev. 0, (May 2014).
5. Specification B-315 (SB-315), "Specification for Seamless Copper Alloy Pipe and Tube," ASTM, (1980).
6. ERCuAl-A2, Aluminum Bronze Bare Wire, Midalloy Technical Bulletin.
7. ASME SB-148, "Specification for Aluminum Bronze Sand Castings," ASME Section II, Part B, (1983 Edition).
8. "Surface Chemical Analysis of Dealloyed Aluminum-Bronze Material Removed from the Essential Cooling Water System," AES 13078445-2Q-4, Revision 1 (November 2015).
9. Email to R. Cipolla (Intertek) from A. Aldridge (STP), "Weld Wire CMTRs," and "Dravo VDP with CMTRs" (February 29, 2016).
10. Email to R. Cipolla (Intertek) from M. Hiatt (STP), "Group 2 Flange Information," (7/25/2013).
11. "Procedure for Determining Surface Composition on Dealloyed Al-Brz Samples," Intertek AES 13078445-2Q, (WP8445-1), Rev. 1 (May 2015).
12. Goldstein, J. I., et al., Scanning Electron Microscopy and X-ray Microanalysis, 3rd Edition, Plenum Press, New York (2003).
13. Anamet EDS and SEM Results, Project 5005-2698 (February 2016).
14. "X-Ray Diffraction (XRD) Analysis Report," Evans Analytical Group, (March 21, 2016).

Appendix A
WELD ROOT PASS COOLING RATE

A.1 INTRODUCTION

The characterization of the microstructure in AL-Brz pipe-to-pipe weldments will depend on chemical content (aluminum and iron content in the alloy) and the cooling rate during the phase transformation process. The cooling rate during welding will depend on the arc energy, travel speed, pre-heat conditions, and interpass temperature controls. The microstructure of the root pass is critical since the root will be in contact with the raw water and its corrosion performance will have a direct benefit on the resistance to dealloying during service.

Figure A-1 shows the typical weld profiles of a 10-inch and 30-inch pipe butt weld. After the root pass is completed, the remainder of the weld is generally completed in two to four filler passes, dependent on pipe wall thickness. For the root pass weld, the main variables are the melting temperature of the weld metal and the travel speed so that a simple conductive heat transfer analysis will be sufficient to estimate the cooling rate in the first pass. It is not necessary to perform a complete weld simulation.

The purpose of this appendix is to describe the heat transfer analysis that was performed to calculate the cooling rate of the first (root) weld pass in Al-Brz pipe welds. The main focus was the 10-inch and 30-inch pipe sizes which constitute the underground piping runs as well as the large diameter above-ground piping. The cooling rate of interest is the time it takes to pass from 900°C (1650°F) to 400°C (750°F).

A.2 ANALYSIS ASSUMPTIONS

The following are the major assumptions used in the analysis:

1) The initial weld temperature is taken as 2000°F. The melting point of Al-Brz melting point is ~1900°F.

2) The effective arc coverage during welding is taken as 1/2 inch. This assumption coupled with the travel speed defines the time the weld pool is receiving heat flux. This assumption was studied parametrically to determine the sensitivity on the results.
3) A minimum weld travel speed was assumed. This is conservative since it permits the high heat input from the arc to the pipe.
4) Weld backing rings were not included in the model. This is conservative since the backing ring would serve as a heat sink to the root pass promoting a faster cooling rate.
5) A weld pre-heat condition was assumed
6) Pipe ID It was conservatively assumed that there is no heat loss by convection from the inside surface of the pipe. Heat loss from the outside surfaces was assumed to be from natural convection only.
7) Thermal conductivity and specific heat properties of low carbon steel were assumed for the Al-Brz weld metal and base pipe. Specific physical property data for Al-Brz were not readily available. However, low carbon steel thermal properties at room temperature are similar to Al-Brz.

Additional analysis assumptions are discussed in the various sections that follow.

A.2 FINITE ELEMENT MODEL

A.2.1 Model Geometry

The pipe-to-pipe weld was modeled by the finite element analysis (FEA) method using the ANSYS computer program (Ref. A1). Figure A-2 shows the FEA axisymmetric model constructed of 8-noded higher-order elements. Half the pipe weld was modeled due to axial symmetry plane at the weld centerline. The single-V weld prep of 37.5° represented the bevel angle as specified in the welding procedure. The weld root geometry included the 1/8-inch gap tolerance between mating pipes and a portion of the pipe that would be melted during the welding. The height of the first pass was assumed to be 1/3 of the pipe wall thickness, based on the weld cross-sections shown in Figure A-1. Because the 10-inch pipe is thicker than the 30-inch pipe, the size of the root pass is larger and the cooling rate will be different

A.2.2 Initial and Surface Boundary Conditions

The welding procedure specification (WPS) from the time period of plant construction was reviewed to obtain relevant welding process parameters (Ref. A2). These are:

1) Specified minimum pre-heat of 115°F
2) Weld prep angle = 37.5 degrees
3) Minimum weld travel speed 2.88 in/min (ipm). (WPS gives range of 2.875 to 8.5 ipm)

The initial weld metal temperature equal to 2000°F for all elements defining the weld root geometry. The elements defining the adjoining pipe had an initial temperature of 68°F. The hold time for the initial weld temperature was approximated by an effective arc coverage length taken as 0.5 inch with the minimum weld travel speed of 2.88 ipm. This defines the time the weld pool is receiving heat flux for ~10s. The effect of hold time on was evaluated parametrically over a range from 1s to 15s with no significant impact on the results for cooling rate within the temperature of interest.

For surface boundary conditions, heat loss at the pipe inside surface was assumed to be negligible and natural convection at the pipe outside surface with heat transfer coefficient (h) equal to 2.0 BTU per hr-ft^2-°F. Radiation heat loss was conservatively ignored.

A.2.3 Thermal Properties

Thermal properties for conductivity and specific heat for Al-Brz were obtained from the literature for room temperature (68°F). Elevated temperature properties were not available and physical properties for pure Cu or Al were judged to be not representative of Al-Brz. The room temperature properties for Al-Brz were similar for low carbon steel (Ref. A3). The elevated temperature behavior for low carbon steel was used for Al-Brz pipe and weld properties in this study. Figure A-3 shows the thermal conductivity and specific heat properties as a function of temperature used in the analysis.

A.3 DISCUSSION OF RESULTS

A thermal transient analysis was performed for both pipe sizes. The temperature output data at the weld centerline was stored and the temperature for the corner node at the inside surface plotted as a function time. The two plots (10-inch and 30-inch) are given in Figure A-4.

The cooling rate within the temperature range where phase transformation begins and ends is 900°C (1650°F) to 400°C (750°F). The cooling rate is relatively fast compare to that expected for cast components. From Figure A-4, the time spent within the transformation process is no longer than about 35s (~0.6 minutes).

A.4 REFERENCES

A1 ANSYS Finite Element Analysis Software, Version 15.

A2 Welding Procedure Specification P35-ArHe-1, HL&P, (6/26/92).

A3 ASME Boiler and Pressure Vessel Code, Section II, Part D, Material Properties," (2015 Edition).

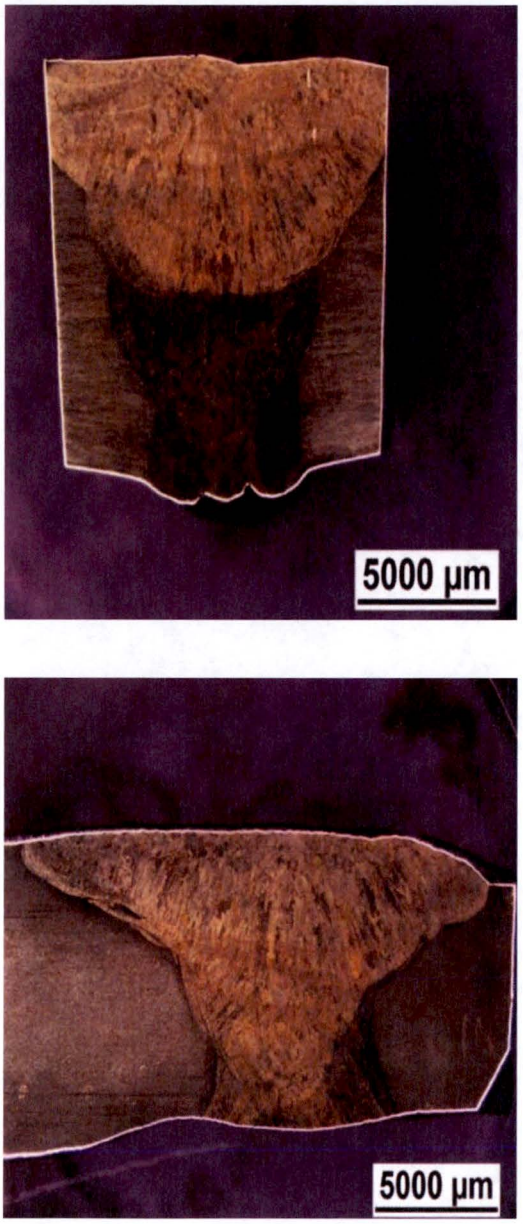

Figure A-1 – Typical Field Mockup Weld Cross-Sections
10-inch (Top) and 30-inch (Bottom)

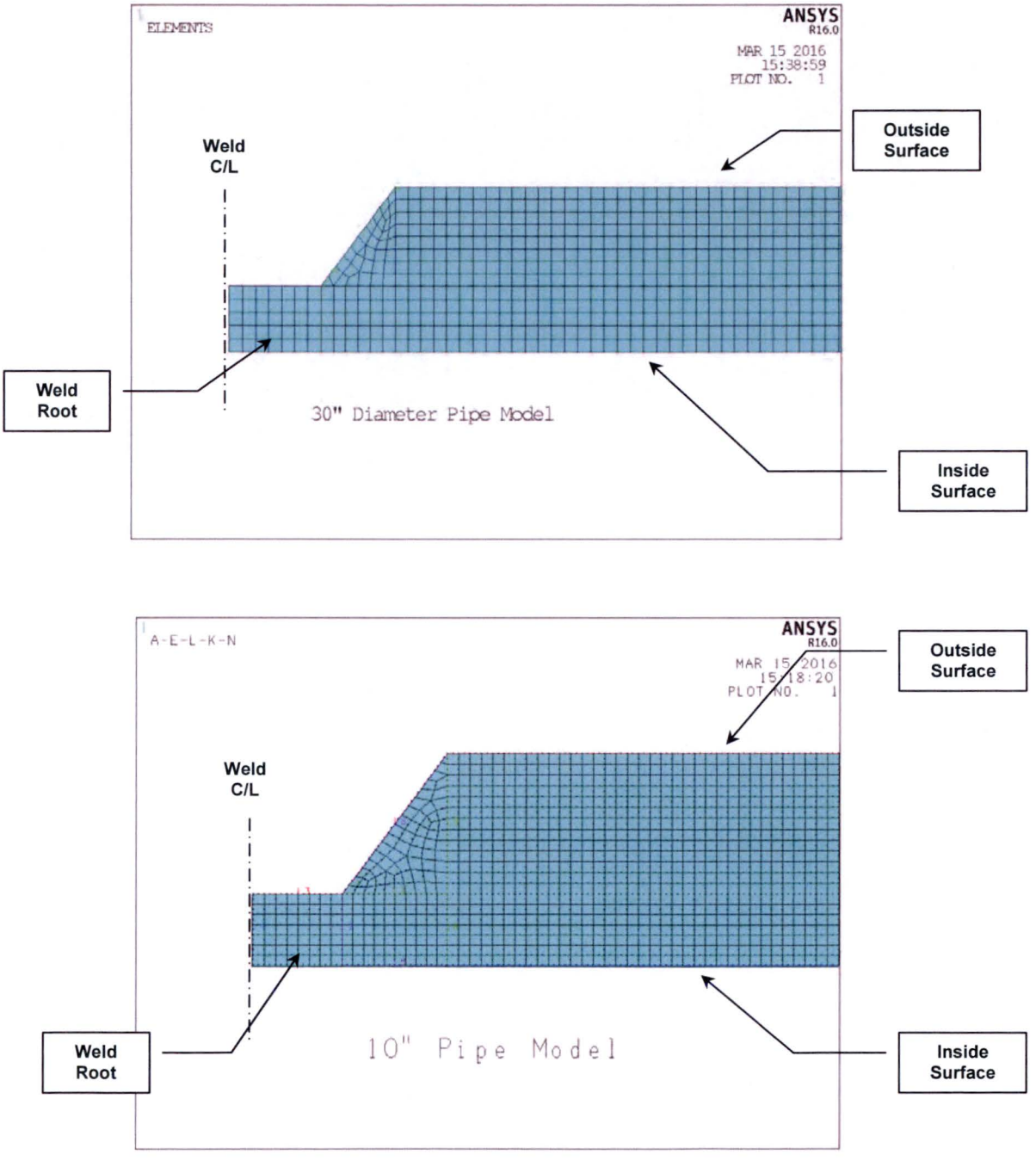

Figure A-2 - Finite Element Analysis of Pipe-to-Pipe Weld Root Pass

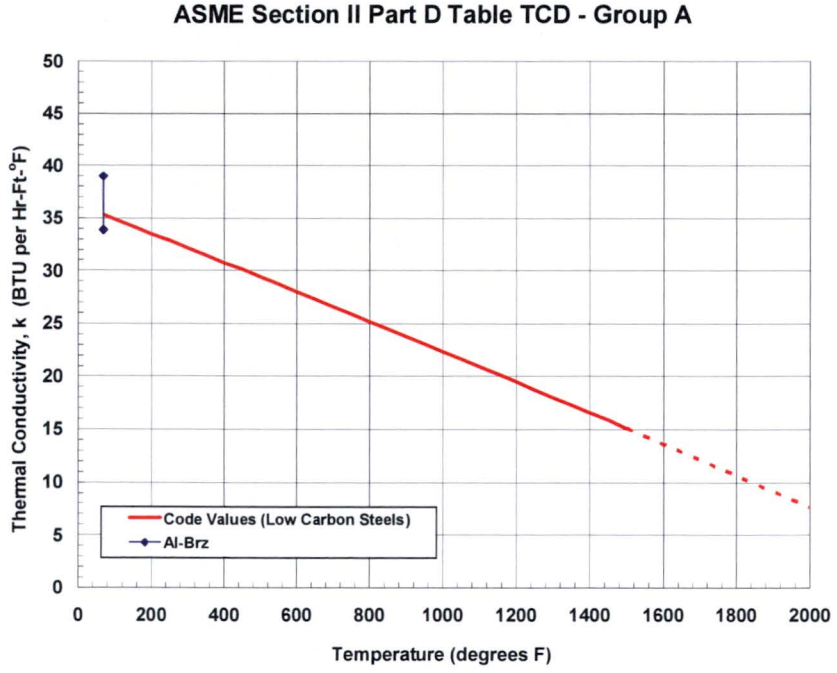

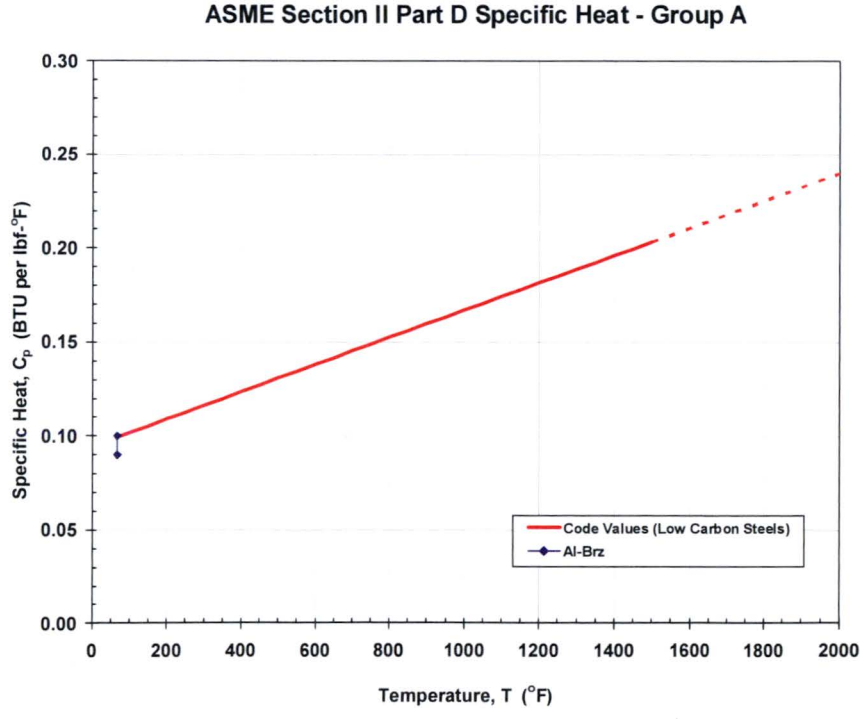

Figure A-3 – Thermal Properties Assumed for the Al-Brz Pipe and Weld Metal

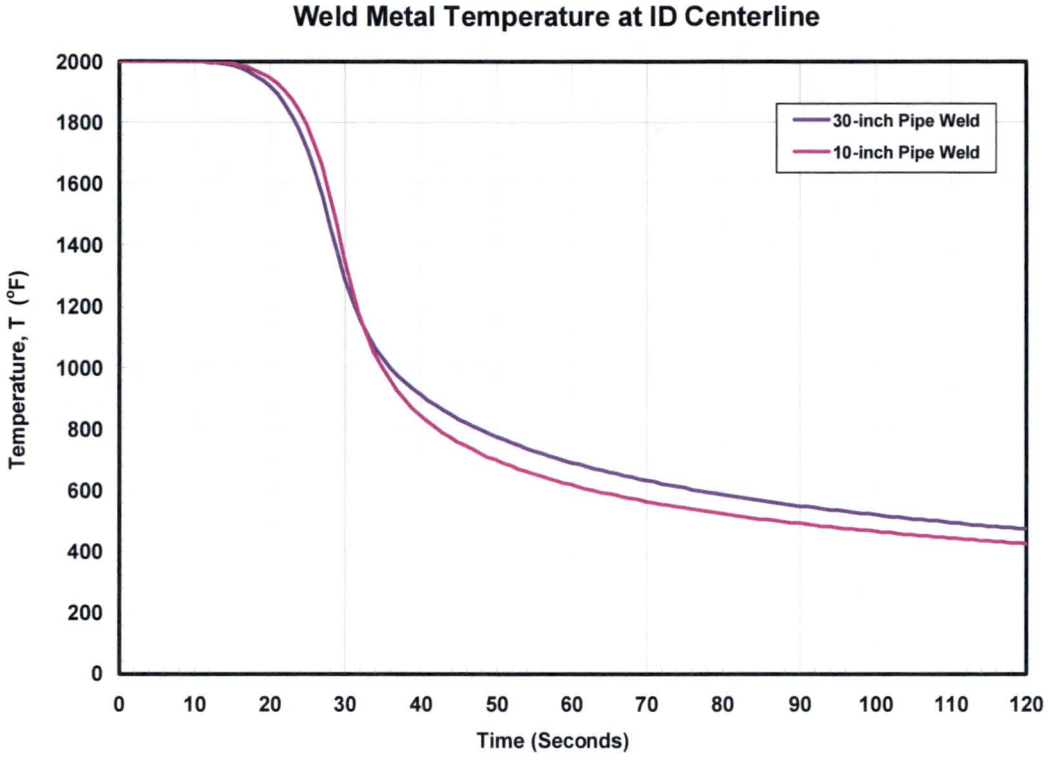

Figure A-4 – Thermal Properties Assumed for the Al-Brz Pipe and Weld Metal